

DRILLING OF MICRO-SCALE HIGH ASPECT RATIO HOLES WITH ULTRA- SHORT LASERS

by

Vahid Nasrollahi

**A thesis submitted to the University of Birmingham for the degree of
DOCTOR OF PHILOSOPHY**

Department of Mechanical Engineering

School of Engineering

University of Birmingham

May 2019

University of Birmingham Research Archive
e-theses repository

This unpublished thesis/dissertation is copyright of the author and/or third parties. The intellectual property rights of the author or third parties in respect of this work are as defined by The Copyright Designs and Patents Act 1988 or as modified by any successor legislation.

Any use made of information contained in this thesis/dissertation must be in accordance with that legislation and must be properly acknowledged. Further distribution or reproduction in any format is prohibited without the permission of the copyright holder.

ABSTRACT

Laser micro drilling is a very attractive option for a growing number of industrial applications due to its intrinsic characteristics, such as high flexibility and process control and also capabilities for non-contact processing of a wide range of materials. However, there are some constraints that limit the applications of this technology, i.e. taper angles on side walls, edge quality, geometrical accuracy and achievable aspect ratios of produced structures. To address these process limitations and control the morphology and quality of the holes that are important factors in broadening the application areas of this technology, three different approaches have been proposed and developed in this research:

(i) A novel method for two-side laser processing is proposed. The capabilities of this method are investigated with a special focus on its key enabling technologies for achieving high accuracy and repeatability in two-side laser drilling. The pilot implementation of the proposed processing configuration and technologies is discussed together with an in-situ, on-machine inspection procedure to verify the achievable positional and geometrical accuracy. It is demonstrated that acceptable alignment accuracy is achievable using this pilot two-side laser processing platform. In addition, the morphology of holes with circular and square cross-sections produced with one-side laser drilling and the proposed method was compared in regard to achievable aspect ratios and holes' dimensional and geometrical accuracy and thus to make conclusions about its capabilities.

(ii) Effects of a wide fluence spectrum associated with the use of femto-second lasers on achievable aspect ratios were investigated by employing lenses with different focal distances. It was demonstrated that the achievable aspect ratio can be increased substantially just by

varying the lenses' focal distances. In addition, the quality of produced holes in terms of taper angle and cylindricity was investigated and the results showed that the quality would be improved by increasing the fluence and/or decreasing the focal distance. At the same time, the limitations in drilling holes with low focal distance lenses were discussed, i.e. sensitivity to defocusing, risks of recast formations inside the holes and bending effects, that should be considered in designing processes for high aspect ratio percussion drilling.

(iii) A beam shaping solution for laser micro drilling has been designed and implemented to achieve a top-hat spatial profile. The morphology of the high aspect ratio holes in terms of cylindricity, circularity, tapering angle, heat affected zone (HAZ) and penetration depth was investigated. The capabilities and limitations of the proposed beam shaping solution for producing micro-scale high aspect ratio holes are discussed, i.e. its sensitivity to defocusing, and the resulting hole morphology compared with that achievable with a Gaussian beam spatial distribution. It's been shown that the penetration depth and aspect ratios achievable with a Gaussian beam are higher, but the use of a top-hat beam improves the holes geometrical accuracy, especially the deviations of the holes from cylindricity are less and also the holes are with a lower tapering angle. The top-hat spatial distribution minimises not only HAZ but also fluence at the beam spot area can be tailored accurately in respect to the ablation threshold.

To assess the holes' morphology, depth and quality in all these approaches, a non-destructive method i.e. a high-resolution X-ray tomography (XCT) with a minimised measurement uncertainty was employed.

DEDICATION AND ACKNOWLEDGEMENTS

I gratefully acknowledge the support of my supervisor, Prof. Stefan Dimov for his consistent support, motivation, encouragement and direction to conduct this research.

My sincere thank goes to Dr Pavel Penchev for his assistance and constructive advice during my research.

I would like to thank my friends in laser manufacturing group. It was a pleasure to work with you all and share the laser laboratory with you during these four years.

Finally, I extend my deepest thank to my amazing family and in particular my parents, for the love, support, and constant encouragement I have gotten over the years. I would especially like to express my gratitude to my precious love **Moloud**, for all the inspiration and extraordinary support during this research. Without you I could have never accomplished my goals.

TABLE OF CONTENTS

CHAPTER 1: INTRODUCTION	1
1.1. Motivation	1
1.2. Research aims and objectives	4
1.3. Thesis organization	5
References	7
CHAPTER 2: LITERATURE REVIEW	8
2.1. Introduction	8
2.2. Laser beam drilling	9
2.3. Laser drilling characterisation	10
2.4. Techniques for addressing limitations of laser drilling	11
2.4.1. Optimising process parameter and drilling strategy	11
2.4.2. Integrating optical elements in the beam delivery system	12
2.4.3. Other Complementary Processes	13
2.5. Two-sides laser drilling	14
2.6. Investigating a wide fluence spectrum with different focal distance lenses	18
2.7. Shaping the spatial profile of the beam	20
2.8. Summary of open research issues	26
References	28
CHAPTER 3: Two-side Laser Processing Method for Producing High-Aspect Ratio	
Micro Holes	32
Abstract	3-1
3.1. Introduction	3-2
3.2. Process characteristics and literature review	3-5
3.3. Process design	3-8
3.3.1. Background and sources of errors	3-8
3.3.2. Design and requirements	3-12
3.3.2.1. Rotary mechanical stages	3-13
3.3.2.2. Linear mechanical stages	3-14
3.3.2.3. Modular workpiece holding device	3-15
3.3.2.4. System level tools.....	3-16

3.3.3. Fully automated process setting procedure	3-18
3.3.4. In-situ, on-machine inspection methodology	3-22
3.3.5. In-situ measurement uncertainty	3-24
3.4. Experimental validation	3-25
3.4.1. Material	3-25
3.4.2. Equipment	3-26
3.4.3. Percussion drilling.....	3-27
3.4.4. Design of experiments	3-29
3.4.4.1. In-situ, on-machine measurement uncertainty	3-29
3.4.4.2. Hole alignment accuracy.....	3-31
3.4.4.3. Hole morphology.....	3-31
3.5. Results and discussion	3-33
3.5.1. In-situ, on-machine measurement uncertainty	3-33
3.5.2. Hole alignment accuracy	3-34
3.5.3. Hole morphology	3-35
3.6. Conclusion	3-41
Acknowledgments	3-43
References	3-44

CHAPTER 4: Drilling of micron-scale high aspect ratio holes with ultra-short pulsed lasers: critical effects of focusing lenses and fluence on the resulting holes' morphology

.....	33
Abstract	4-1
4.1. Introduction	4-2
4.2. Materials and Methods	4-4
4.2.1. Experimental and measurement setups	4-4
4.2.2. Design of experiments	4-6
4.2.3. Depth of focus analysis	4-7
4.3. Results and Discussion	4-8
4.3.1. Saturation point	4-8
4.3.2. Fluence effects	4-10
4.3.3. Depth of focus analysis	4-12
4.3.4. Hole morphology	4-17

4.4. Conclusions	4-18
Acknowledgment	4-19
References	4-20
CHAPTER 5: Laser drilling with a top-hat beam of micro-scale high aspect ratio holes in silicon nitride	34
Abstract	5-1
5.1. Introduction	5-2
5.2. Refractive field mapping beam shapers	5-4
5.3. Experimental	5-9
5.3.1. Experimental setup and measurement procedure	5-9
5.3.2. Design of experiments	5-12
5.4. Results and Discussion	5-13
5.4.1. Effects of beam shape on holes' morphology	5-13
5.4.1.1. Penetration depth	5-13
5.4.1.2. Heat Affected Zone (HAZ)	5-16
5.4.1.3. Circularity and cylindricity	5-18
5.4.2. Sensitivity of beam shaper to defocusing	5-20
5.5. Conclusion	5-21
Acknowledgment	5-22
References.....	5-23
CHAPTER 6: CONTRIBUTIONS, CONCLUSIONS AND FUTURE WORK.....	35
6.1. Contributions	35
6.2. Conclusions	37
6.3. Future research.....	40

LIST OF FIGURES

CHAPTER 1

Figure 1.1. Probe card and arrays of micro pins supported by a perforated ceramic wafer (from: www.technoprobe.com)	3
---	---

CHAPTER 2

Figure 2.1. Schematic of laser beam drilling techniques [5]	9
Figure 2.2. Features of the laser drilled holes [4]	10
Figure 2.3. Profile images of fabricated hole by the ECM from two sides with different machining times: (a) 60 s, (b) 120 s, (c) 150 s, (d) 180 s, (e) 240 s, (f) 300 s [36]	15
Figure 2.4. Benefits of two side laser processing [37]	16
Figure 2.5. Experimental setup for micro hole drilling from two sides [38]	17
Figure 2.6. The schematic of (a) side view, (b) cross section and micrographs of (c) cross section (d), hole opening and (e) is the SEM image of a part of hole [38]	17
Figure 2.7. Rectangular through hole produced with one-side machining strategy: top view at its entrance (a) and at (b) the exit side [35]	18
Figure 2.8. Rectangular through hole produced with two-side machining strategy: top view at its entrance (a) and at (b) the exit side [35]	18
Figure 2.9. Beam radius near the focal distance for lenses with focal length of 60 and 20 mm [39]	19
Figure 2.10. The maximum achievable hole depth for lenses with different focal distance [40]	20
Figure 2.11. Side effects of using a Gaussian beam distribution compared to a flat-top [42]	20
Figure 2.12. The dependency of the hole shape on the Gaussian beam distribution [44]	21
Figure 2.13. Cross sectional SEM image of drilling in 50 μ m thickness by (a) Gaussian (b) Conventional Bessel beam (c) Tailored Bessel beam- and in 100 μ m by Tailored Bessel beam (d) Cross section (e) front (f) rear view [45]	22
Figure 2.14. The variation of the distance between workpiece and DOE leads to different hole diameters [20]	23

Figure 2.15. SEM image of the produced hole by (a) circular top-hat, (b) square top-hat, (c) doughnut [55]	24
Figure 2.16. Hole drilled by a Gaussian (Left) and Top-hat (Right) after 1s.....	25
Figure 2.17. A three-lens beam shaping system to transform a Gaussian beam into a pitchfork beam [58].....	26

CHAPTER 3

Figure 3.1. Angular displacements of incident beam and: (a) workpiece normal in regards to the A axis, $\Delta\alpha^\circ$; (b) workpiece normal in regards to the B axis, $\Delta\beta^\circ$ (c) A axis, $\Delta\psi^\circ$	3-11
Figure 3.2. Required adjustments in X and Y directions (dx, dy) due to: (a) displacement of holes' positions in respect to the A axis; and (b) the A axis not being parallel to the X axis, $\Delta\gamma^\circ$	3-12
Figure 3.3. Required compensational movements in Z direction due to displacements between A axis and the centre plane of the workpiece, ΔZ	3-12
Figure 3.4. The setting up procedure for determining initial coordinates of two through holes centres (Points 5, 6) and their corresponding coordinates (points 7, 8 respectively) after a rotation by 1800.....	3-21
Figure 3.5. In-situ, on-machine inspection method with a 3D metrology sensor: (a) the first side field of view and (b) the second side field of view	3-23
Figure 3.6. Three views of the used laser processing setup: (a) confocal sensor; (b) the focusing lens together with the stack of mechanical stages; (c) the R25 sensor.....	3-26
Figure 3.7. The specially designed modular work holding device.....	3-27
Figure 3.8. Determining the optimum numbers of pulses with two different lenses	3-29
Figure 3.9. The array of holes used to evaluate uncertainty in correlating SCSs on the sample two sides	3-31
Figure 3.10. The test sample designed to compare one- and two-side drilling methods	3-32
Figure 3.11. Holes' cross-sections generated using the XCT system: (a) section G-G of holes' array B produced by two-side drilling with 2500 pulses; (b) section H-H of holes' array B produced by two-side drilling with pulse numbers of 200, 400, 800, 1600, 2500, 5000 and 7500; (c) section I-I of holes' array A produced by one-side drilling with pulse numbers of 200, 400, 800, 1600, 2500, 5000 and 7500.	3-36

Figure 3.12. Morphology analysis of holes produced employing one-side percussion drilling with different pulse numbers	3-37
Figure 3.13. Morphology analysis of holes produced employing two-side percussion drilling with different pulse numbers	3-37
Figure 3.14. Holes' cross-sections generated using the XCT system: (a) section J-J of 60 μ m square holes (Array D) produced by two-side drilling; (b) section K-K of square and circular holes with different dimensions (Array D) produced by two-side drilling; (c) section L-L of square and circular holes with different dimensions (Array C) produced by one-side drilling	3-39
Figure 3.15. Morphology analysis of circular holes (arrays C and D) produced employing one- and two-side drilling.....	3-40
Figure 3.16. Morphology analysis of square holes (Arrays C and D) produced employing one- and two-side drilling.....	3-40
Figure 3.17. Roundness and tapering angles of 75 μ m circular holes (arrays C and D) produced by one- and two-side drilling.....	3-41

CHAPTER 4

Figure 4.1. The XCT cross sections of the holes produced with the three lenses by delivering 500, 1000, 5000 and 10000 pulses. Note: all measurements are in micrometers and were taken employing VG studio 3.0	4-9
Figure 4.2. Percussion drilling saturation points for the three lenses.....	4-10
Figure 4.3. The penetration depths achieved with the different fluence levels for the three lenses when 1,000 and 10,000 pulses were used.....	4-11
Figure 4.4. The achievable aspect ratios with the different fluence levels for the three lenses when 1,000 and 10,000 pulses were used.....	4-12
Figure 4.5. The achieved penetration depth with three lenses when a defocusing is applied, (a) 500 pulses and (b) 5,000 pulses.....	4-13
Figure 4.6. Rate of the fluence change for 3 different lenses.....	4-14
Figure 4.7. Beam spatial profiles of the three lenses at the substrate surface when different levels of defocusing are applied	4-16
Figure 4.8. The filtered out portions of beam intensity: (a) a focused beam and (b) a negative defocused beam	4-16
Figure 4.9. Issues with high aspect ratio holes, (a) recasts and (b) bending	4-18

CHAPTER 5

Figure 5.1. The beam propagation after the focusing lens: (a) Gaussian (b) Top-hat and (c) Sinc entrance beams	5-8
Figure 5.2. Laser drilling setup with beam profiles at different positions along the beam path	5-10
Figure 5.3. XCT results of Gaussian and Top-hat distribution for different NoP. Note: S is the surface area inside the hole and is in μm^2 . All other measurements are in micrometers	5-14
Figure 5.4. The penetration depths achievable with Gaussian and top-hat beams with an increasing number of pulses	5-15
Figure 5.5. Irradiated surface areas inside the holes together with respective effective fluence for Gaussian and top-hat beams.....	5-16
Figure 5.6. HAZ around the holes produced with Gaussian and top-hat beams	5-17
Figure 5.7. The effects of (a) Gaussian and (b) top-hat beams on HAZ and the holes' shape	5-18
Figure 5.8. The changes of holes' diameters at different depths for the Gaussian and top-hat beams after 5000 NoP	5-19
Figure 5.9. Sensitivity of holes' depth after 5000 NoP to defocusing of top-hat and Gaussian beams	5-20

LIST OF TABLES

CHAPTER 2

Table 2.1. Spot size and maximum achievable fluence for each lens [40]..... 19

CHAPTER 3

Table 3.1. The uncertainty budgets allocated to different error sources in performing in-situ, on-machine alignment measurements3-34

CHAPTER 4

Table 4.1. Design of experiments for assessing the fluence effects, employing three focusing lenses4-7

ABBREVIATIONS

AJM	Abrasive Jet Machining
BCS	Laser Beam coordinate System
CAD	Computer Aided Design
CAM	Computer Aided Manufacturing
CNC	Computer Numerical Control
DoE	Design of Experiment
DOE	Diffraction Optical Elements
DoF	Degree of Freedom
DOF	Depth Of Focus
EBM	Electron Beam Machining
ECM	Electrochemical Machining
EDM	Electrical Discharge Machining
GUM	Guide For Expression Of Uncertainty In Measurements
HAZ	Heat Affected Zone
ISO	International Organization For Standardization
LIPSS	Laser Induced Periodic Surface Structures
LMP	Laser Micro Processing
MCS	Machine Tool Coordinate System
MEMS	Microelectromechanical System
MRR	Material Removal Rate
NoP	Number of Pulses
PAM	Plasma Arc Machining
SCS	Sensor Coordinate System
SEM	Scanning Electron Microscopy
SLM	Spatial Light Modulators
USM	Ultrasonic Machining
WCS	Workpiece Coordinate System
XCT	X-Ray Computed Tomography

NOMENCLATURES

$\Delta\alpha$	Angular displacements of the incident beam from the workpiece surface normal in regards to the A axis.
$\Delta\beta$	Angular displacements of the incident beam from the workpiece surface normal in regards to the B axis.
$\Delta\psi$	Perpendicularity displacement of incident beam and the A axis.
$\Delta\emptyset$	Angular displacement between A_{MCS} and X_{SCS} .
$\Delta\gamma$	Angular displacements of X_{MCS} and A_{MCS} .
ΔX_A	Axial displacements of the stage in X direction after executing a rotation by 180°.
$\Delta\theta$	Angular displacement of the stage after a rotation by 180° with the A stage.
α	Absorption coefficient
λ	Wavelength of the laser beam
ω_0	beam radius in focus
$\omega(z)$	beam radius in z position
a	The slope of A_{MCS} in $X_{MCS}Y_{MCS}$ plane.
b	Y intercept of A_{MCS} axis in $X_{MCS}Y_{MCS}$ plane.
d	Beam diameter in focus
D	input beam diameter at the lens.
DOF	depth of focus
DoF	Degree of freedom.
E_x, E_y	Misalignment of a hole in X_{SCS} and Y_{SCS} directions.
E_{xy}	Total misalignment of a hole.
E	Pulse energy
f	Focal distance of lens
F_{th}	Ablation threshold of material
F	Fluence
$F(z)$	Fluence in z position
k	K-factor for estimating expanded uncertainty.
M^2	Beam quality factor.
n	Number of samples used to estimate standard uncertainty.
U	Expanded uncertainty.
U_c	Combined uncertainty.
X, Y	Hole's coordinates in MCS on first side.
X_{new}, Y_{new}	Hole's coordinates in MCS on second side.
z	Position of substrate in respect of focal plane

LIST OF PUBLICATIONS

Journal Publications

1. **Nasrollahi, V.**, Penchev, P., Dimov, S., Korner, L., Leach, R. and Kim, K., (2017), Two-Side Laser Processing Method for Producing High Aspect Ratio Microholes. *Journal of Micro and Nano-Manufacturing*, 5(4), 041006 doi.org/10.1115/1.4037645
2. **Nasrollahi, V.**, Penchev, P., Jwad, T., Dimov, S., Kim, K. and Im, C. (2018). Drilling of micron-scale high aspect ratio holes with ultra-short pulsed lasers: Critical effects of focusing lenses and fluence on the resulting holes' morphology. *Optics and Lasers in Engineering*, 110, 315-322 doi.org/10.1016/j.optlaseng.2018.04.024
3. **Nasrollahi, V.**, Penchev, P., Batal, A., Dimov, S., Kim, K., (2019), Laser drilling with a top-hat beam of micro-scale high aspect ratio holes in silicon nitride' morphology. **(Submitted in journal of materials processing technology)**

Other Journal Publications

4. Jwad, T., Penchev, P., **Nasrollahi, V.**, Dimov, S., (2018) Laser induced ripples' gratings with angular periodicity for fabrication of diffraction holograms. *Applied Surface Science*. 30;453:449-56 doi.org/10.1016/j.apsusc.2018.04.277
5. Batal, A., Michalek, A., Garcia-Giron, A., **Nasrollahi, V.**, Penchev, P., Sammons, R., Dimov, S., (2019), Effects of laser processing conditions on wettability and proliferation of Saos-2 cells on CoCrMo alloy surfaces. **(Submitted in Journal of Advanced Optical Technologies)**.

Conference Publications

6. Penchev, P., **Nasrollahi, V.** and Dimov, S., (2016) Laser micro-machining method for producing high aspect ratio features, ICOMM 2016, 29-31 March 2016, Orange County, California, USA.
7. **Nasrollahi, V.**, Penchev, P. and Dimov, S., (2016) A new laser drilling method for producing high aspect ratio micro through holes, 4M/IWMF 2016 Conference, 13-15 Sep 2016, Copenhagen, Denmark doi.org/10.3850/978-981-11-0749-8_741
8. Jwad, T., Penchev, P., **Nasrollahi, V.**, Dimov, S., (2018) Laser Induced Ripples' Gratings for Fabrication Periodic Pattern of Diffraction Holograms, WCMNM2018 Conference, 18-20 Sep 2018, Portoroz, Slovenia doi.org/10.3850/978-981-11-2728-1_41

9. **Nasrollahi, V.**, Penchev, P., Dimov, S. and Kim, K., (2018) Effects of focusing lens and laser fluence on drilling of high aspect ratio microholes, WCMNM2018 Conference, 18-20 Sep 2018, Portoroz, Slovenia doi.org/10.3850/978-981-11-2728-1_15
10. **Nasrollahi, V.**, Penchev, P., Batal, A., Dimov, S. and Kim, K., (2019) Top-hat laser drilling of micro-scale holes in SiN substrates: morphological effects, WCMNM2019, 10-12 Sep 2019, Raleigh, North Carolina, USA.
11. Batal, A., Garcia-Giron, A., **Nasrollahi, V.**, Penchev, P. and Dimov, S., (2019) Effect of laser processing conditions on wettability and proliferation of Saos-2 cells on CoCrMo alloy surfaces, WCMNM2019, 10-12 Sep 2019, Raleigh, North Carolina, USA.

CHAPTER 1 : INTRODUCTION

1.1 Motivation

The trend toward product miniaturization and thus the growing needs for manufacturing micro scale functional features and components especially in biomedical, optical, aerospace, electronics and automotive industries demand new tools, methods and also a better understanding of materials' behaviour at such scales [1, 2]. Both, conventional, e.g. micro milling or micro drilling, and non-conventional micromachining technologies are developed but there are still many open issues related to their scalability while achieving the required level of predictability, reproducibility, productivity and cost effectiveness in producing complex geometries in a variety of materials [3]. The non-conventional technologies used to produce micro-scale structures fall into three main categories [4]:

- Chemical and electrochemical, e.g. photochemical machining;
- Mechanical, e.g. ultrasonic and abrasive water jet machining;
- Thermal energy, e.g. electron beam, electric discharge and laser ablation.

A suitable process or processes can be selected by considering the material removal rate (MRR), the process reliability and capital investment required for cost-effective manufacture, together with components' technical requirements and batch sizes. In some cases, especially for difficult-to-cut materials, hybrid machining solutions have been developed that combine

the capabilities of two or more machining processes and thus to benefit from their complementarity in achieving an acceptable manufacturing performance [5-7].

The focus of this research is on producing high aspect ratio (depth to diameter ratio) micro holes on ceramics by adopting and developing appropriate manufacturing approaches. Micro-scale holes are common features in products, e.g. the channels for delivering media in micro-electromechanical systems (MEMS), nozzles for diesel fuel injection, cooling channels for turbine blades, drug delivery orifices, interconnecting vias of printed circuit boards, etc. [8-10]. Another important and growing application area for such holes is in electronic industry, in particular for guide blocks of interface vertical probe cards [11-14]. Probe cards as a tester of semiconductor wafers, provide an electrical path into the circuits on the wafer and maintain an appropriate contact between micro pins of the probe card and the circuit. In Figure 1.1 an array of pins are depicted and it is shown how a perforated wafer is required as a support for the pins and also to keep them in place without inclination. The quality and precise positioning of the drilled holes directly affect the probe card performance. Hence, such arrays of holes should fulfil stringent requirements in regards to their quality, size and pitch accuracy and repeatability. In particular, it is necessary in such applications to produce arrays of holes usually in ceramic substrates with aspect ratios more than 5 while their diameters and pitches are less than 60 μm and taper angle does not exceed 10° . The positional accuracy needs to be better than 5 μm and the deviations in hole shape less than 5%.

Different methods have been used for producing such holes, in particular photo-etching, electro-chemical machining, electro-discharge machining, mechanical machining and laser drilling, and their capabilities and limitations have been investigated by researchers [9, 15].

In this context, one option is the use of photolithography to produce such through holes. However, photolithography requires multi-step processing in clean room environment that make this fabrication route capital intensive and thus potentially viable only for relatively high batch sizes [16]. Another manufacturing technology that could be employed is micro EDM drilling but this process has shortcomings too, i.e. material low conductivity, high electrode wear and low MRR [17]. Electro-chemical machining and mechanical drilling can also be considered however the throughput required for cost-effective processing of such arrays of holes and considering the growing demand for drilling micro holes with diameters down to 10 μm , makes laser micro drilling an attractive option that potentially can fulfil all requirements. Laser micro drilling by its non-contact nature and efficiency in ablating almost any material offers a wide range of application. However, it has some limitations in drilling micro-scale holes too, such as tapered sidewalls, achievable geometrical accuracy and edge definition due to the heat affected zone (HAZ) and material spatters, and some penetration depth constraints. Different research groups have investigated laser parameter domains, different process setups and drilling strategies to reduce and even eliminate these shortcomings. This research is another attempt to address the limitation of laser micro drilling technology and thus to broaden its application areas.

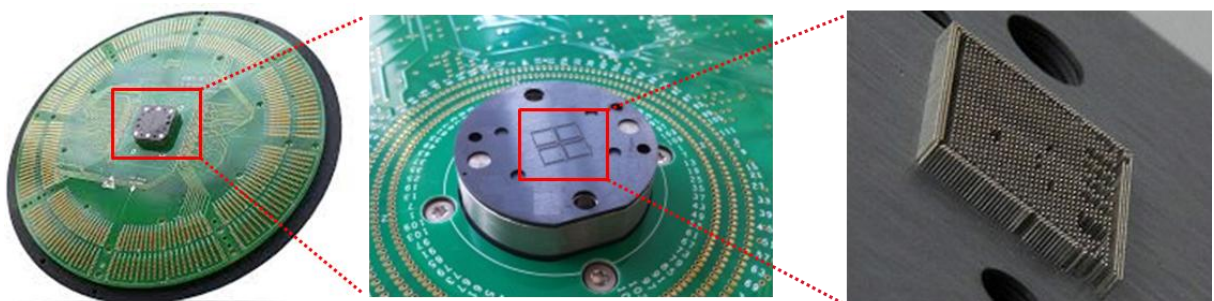


Figure 1.1. Probe card and arrays of micro pins supported by a perforated ceramic wafer (from: www.technoprobe.com)

1.2. Research aims and objectives

The research reported in this thesis aims to address some key limitations of laser micro drilling technology and thus to broaden its manufacturing capabilities, flexibility and reliability. The overarching aim of this research is to develop new capabilities for laser micro drilling of high aspect ratio holes on ceramics substrates and thus to overcome some key constraints that restrict the application area of this technology. The main focus is on improving the processing efficiency, aspect ratio and quality of micro-scale holes in terms of geometrical accuracy and edge definition while considering their dimensional accuracy, repeatability and reproducibility.

To achieve this aim, the following main objectives are addressed in this research:

Objective 1: *To design, implement and validate a novel method for two side laser drilling that can lead to a step change in process efficiency and achievable aspect ratios in comparison to one-side drilling methods while improving the holes' dimensional and geometrical accuracy.* The capabilities of a pilot implementation of this method will be investigated in regards to achievable accuracy and repeatability. System level tools will be proposed and implemented for automating the process setting up and thus to compensate and minimize the impact of various error sources on achievable accuracy and repeatability. In addition, an inspection method should be developed for monitoring the drilling process, especially the alignment accuracy and quality of the holes/structures produced from two sides.

Objective 2: *To investigate the effect of a wide fluence spectrum on the morphology of the resulting holes by employing lenses with different focal distance.* The research will involve quantifying the improvements achievable in regards to aspect ratio, diameters

and geometrical accuracy of the resulting holes and also to analyse the limitations associated with the use of lenses with different focal distances.

Objective 3: *To design and implement a beam shaping solution for top-hat laser processing and investigate its capabilities in drilling micro holes.* The capabilities of laser beams with top-hat intensity profiles will be investigated in regards to achievable holes' quality, edge definition and holes' aspect ratios while analysing the constraints associated with using such solutions on flexibility and efficiency of the drilling process.

1.3. Thesis organisation

This thesis consists of six chapters, the motivation and research objectives are introduced in this chapter and the literature review is covered in Chapter 2. The carried out research to achieve the three main objectives is reported in Chapters 3 to 5, respectively. The main contributions to knowledge, general conclusions and future research directions are summarised in Chapter 6. The contents of these chapters are outlined below:

- **Chapter 2** presents a general introduction of laser drilling technology and different drilling methods and strategies with their respective limitations. A review of the relevant research on laser drilling is conducted with a special focus on laser micro drilling and the specific objectives of this research to develop and validate technologies for improving the processing efficiency, aspect ratio and quality of micro-scale holes.
- **Chapter 3** presents a new method for two-side processing to address some of the limitations associated with the laser micro drilling process. First, the distinguishing characteristics of the proposed method are described and the relevant research is

reviewed. Then, the process design is discussed with a special focus on key enabling methods and technologies for achieving high accuracy and repeatability in two-side laser drilling. Next, a pilot implementation of the proposed method is described that is then used to validate the proposed two-side laser processing method. An in-situ, on-machine inspection method for verifying the alignment accuracy achievable with the proposed two-side laser processing method is also proposed. Finally, conclusions are made about the capabilities of the proposed method together with its enabling technologies based on the obtained experimental results.

- **Chapter 4** investigates the effects of a wide fluence spectrum in ultra-short percussion drilling by employing different focal distance lenses. Especially, the effects on achievable aspect ratios and morphologies of micro holes produced on silicon nitride substrates were investigated experimentally. The constraints associated with the use of different lenses on achievable geometrical accuracy, processing efficiency and flexibility in producing high aspect ratio holes are discussed.
- **Chapter 5** reports the development of a beam shaping solution for drilling holes with top-hat spatial profile beams at the focal plane. The capabilities of the proposed solution was investigated and compared with the drilling results achievable with a Gaussian beam. The morphology of high aspect ratio holes was analysed to understand the effects of uniform beam spatial profiles on their geometrical accuracy, processing efficiency and quality in general.
- **Chapter 6** summarizes the main contributions to knowledge and conclusions of the research. The thesis concludes with a discussion of some future research directions.

References

- [1] Y. Qin, A. Brockett, Y. Ma, A. Razali, J. Zhao, C. Harrison, W. Pan, X. Dai, D. Loziak, Micro-manufacturing: research, technology outcomes and development issues, *The International Journal of Advanced Manufacturing Technology*, 47 (2010) 821-837.
- [2] T. Özel, Editorial: Special section on micromanufacturing processes and applications, *Materials and Manufacturing Processes*, 24 (2009) 1235-1235.
- [3] X. Luo, K. Cheng, D. Webb, F. Wardle, Design of ultraprecision machine tools with applications to manufacture of miniature and micro components, *Journal of Materials Processing Technology*, 167 (2005) 515-528.
- [4] S.P. Leo Kumar, J. Jerald, S. Kumanan, R. Prabakaran, A review on current research aspects in tool-based micromachining processes, *Materials and Manufacturing Processes*, 29 (2014) 1291-1337.
- [5] A.M.A. Al-Ahmari, M.S. Rasheed, M.K. Mohammed, T. Saleh, A Hybrid Machining Process Combining Micro-EDM and Laser Beam Machining of Nickel-Titanium-Based Shape Memory Alloy, *Materials and Manufacturing Processes*, 31 (2016) 447-455.
- [6] S.Z. Chavoshi, X. Luo, Hybrid micro-machining processes: A review, *Precision Engineering*, 41 (2015) 1-23.
- [7] C.R. Dandekar, Y.C. Shin, J. Barnes, Machinability improvement of titanium alloy (Ti-6Al-4V) via LAM and hybrid machining, *International Journal of Machine Tools and Manufacture*, 50 (2010) 174-182.
- [8] E. Ferraris, V. Castiglioni, F. Ceyskens, M. Annoni, B. Lauwers, D. Reynaerts, EDM drilling of ultra-high aspect ratio micro holes with insulated tools, *CIRP Annals - Manufacturing Technology*, 62 (2013) 191-194.
- [9] Z.Y. Yu, Y. Zhang, J. Li, J. Luan, F. Zhao, D. Guo, High aspect ratio micro-hole drilling aided with ultrasonic vibration and planetary movement of electrode by micro-EDM, *CIRP Annals - Manufacturing Technology*, 58 (2009) 213-216.
- [10] C. Diver, J. Atkinson, H.J. Helml, L. Li, Micro-EDM drilling of tapered holes for industrial applications, *Journal of Materials Processing Technology*, 149 (2004) 296-303.
- [11] B. Adelman, R. Hellmann, Rapid micro hole laser drilling in ceramic substrates using single mode fiber laser, *Journal of Materials Processing Technology*, 221 (2015) 80-86.
- [12] W.C. Choi, J.Y. Ryu, Fabrication of a guide block for measuring a device with fine pitch area-arrayed solder bumps, *Microsyst Technol*, 18 (2012) 333-339.
- [13] N. Watanabe, M. Suzuki, K. Kawano, M. Eto, M. Aoyagi, Fabrication of a membrane probe card using transparent film for three-dimensional integrated circuit testing, *Jpn. J. Appl. Phys.*, 53 (2014) 06JM06.
- [14] W.C. Choi, J.Y. Ryu, A MEMS guide plate for a high temperature testing of a wafer level packaged die wafer, *Microsyst Technol*, 17 (2011) 143-148.
- [15] T. Masuzawa, State of the Art of Micromachining, *CIRP Annals - Manufacturing Technology*, 49 (2000) 473-488.
- [16] H. Huang, L.-M. Yang, J. Liu, Micro-hole drilling and cutting using femtosecond fiber laser, *Optical Engineering*, 53 (2014) 051513.
- [17] H.S. Lim, Y.S. Wong, M. Rahman, M.K. Edwin Lee, A study on the machining of high-aspect ratio micro-structures using micro-EDM, *Journal of Materials Processing Technology*, 140 (2003) 318-325.

CHAPTER 2 : LITERATURE REVIEW

2.1. Introduction

Lasers work based on the principle of stimulated emission, delivering photons in the same phase, frequency and polarisation. The outcome beam will be coherent and monochromatic with low divergence and high brightness [1]. These unique characteristics explain their wide range of application for different purposes such as alignment, length and velocity measurement, printing, heat source, communications and etc. The main components of a laser source are active medium, pumping source and optical resonator. The active medium which can be found in all four states of matter i.e. solid, liquid, gas and plasma, defines the wavelength of the outcome beam. The importance of the wavelength is evident in material processing, where it defines the portion of absorbed, reflected or transmitted beam energy through material. Other parameters such as material composition, surface roughness, temperature of the sample, polarisation of the light and incidence angle are also effective on absorption of the light [2]. Another important parameter which mainly effects on the mechanism of ablation is pulse duration or temporal shape of the beam. Short pulses are in the range of nano second and the mechanism of ablation is mainly thermal with a considerable heat affected zone. On the other hand, ultra-short pulses as an athermal process provide an improved quality, edge definition and repeatability. Different technologies including Q-Switching, Cavity Dumping, Mode Locking or Chirping are developed to deliver short pulses and ultra-short pulses [1, 3].

2.2. Laser beam drilling

There is a wide range of unconventional drilling methods, in particular abrasive jet machining (AJM), electrochemical machining (ECM), chemical machining (CM), ultrasonic machining (USM), electron beam machining (EBM), plasma arc machining (PAM) and electro discharge machining (EDM). Laser beam drilling as a contactless process, is gaining popularity due to its capabilities of processing a wide range of materials, high production rate, high flexibility and accuracy, high repeatability and possibility of achieving beam size of less than 10 μm [4].

Different laser drilling techniques are introduced to achieve a variety of hole diameters, precision, quality and throughput [2] as it is shown in Figure 2.1:

- Single pulse drilling: Drilling by a single pulse with high energy
- Percussion drilling: Delivering a successive number of pulses onto the same spot
- Trepanning: Cutting the hole by moving the beam around its contour
- Helical: Spiral movement of the laser beam into the substrate at several steps

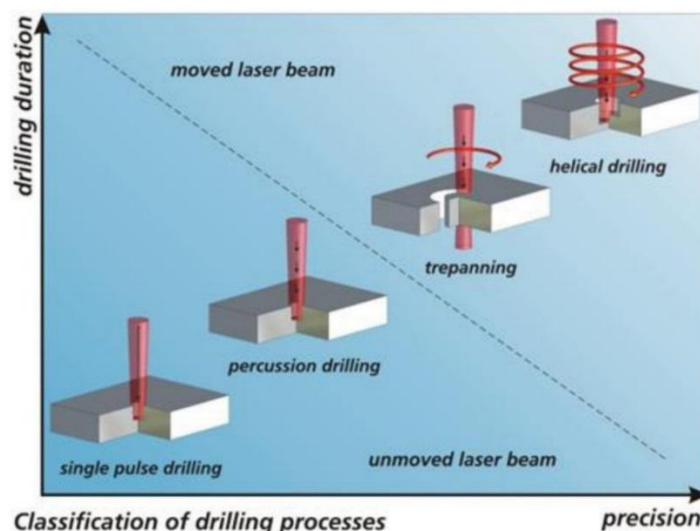


Figure 2.1. Schematic of laser beam drilling techniques [5]

When the targeted diameter of the hole is in order of the beam waist diameter, percussion approach which is the fastest method with a low precision has to be adopted.

2.3. Laser drilling characterisation

While the preference of drilling is to achieve a cylindrical hole with well-defined edges, in practice there is a range of deficiencies in the process as it is illustrated in Figure 2.2 which limits the achievable hole quality and throughput:

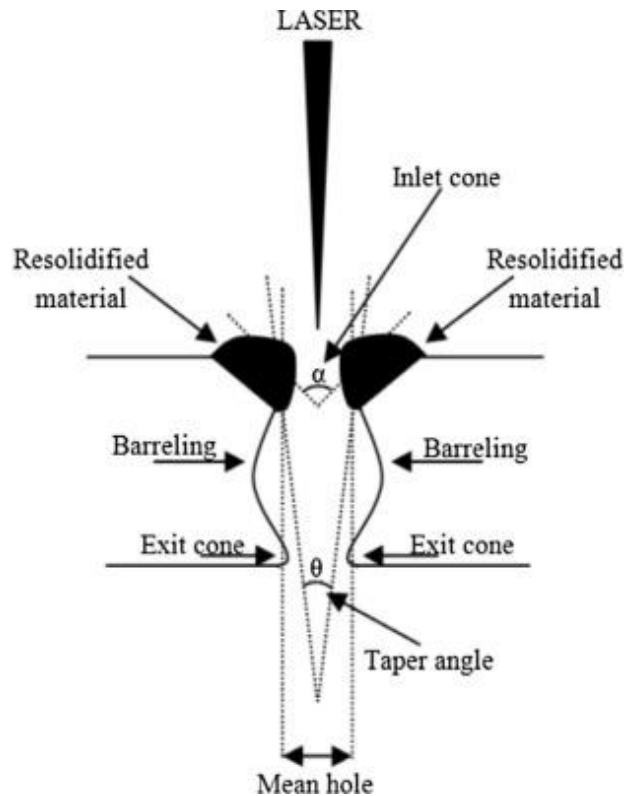


Figure 2.2. Features of the laser drilled holes [4]

They can be broadly divided into the following three subcategories [4]:

- Metallurgical characteristics: Including Heat affected zone (HAZ), Recast layer, Spatters and Micro cracks.
- Geometrical characteristics: Including Hole taper, Hole circularity, Hole diameter and overcut, Depth and aspect ratio, Bending effect, Edge definition and Cylindricity
- Others: Including Removal rate, Repeatability, Reproducibility and Surface roughness

2.4. Techniques for addressing limitations of laser drilling

2.4.1. Optimising process parameter and drilling strategy

Pulse energy, frequency, pulse duration, number of pulses, wavelength, pulse overlap, beam quality, peak power and focusing position are the most important controllable parameters in laser drilling and have a direct impact on the characteristics of a drilled hole. Hence, different approaches have been developed to optimise these effective parameters. For instance Zhang et al [6] investigated helical drilling of TiC and showed how laser fluence and repetition rate had an impact on hole depth and circularity. In another attempt Ghoreishi et al [7] did a comprehensive study on percussion drilling of stainless steel. They investigated the number of pulses, frequency and focus position on hole taper, hole diameter and hole circularity by performing a proper design of experiments and analysis of variance. They also utilized a neural network to develop a model of percussion drilling and after combining it with the genetic algorithm, implemented it as an optimisation tool to control the process in offline mode [8]. Another empirical neural network model has been proposed by Casalino et al [9] to minimise the micro-cracks, recast layer and the variance of inlet and outlet diameter. The input parameters in their study was frequency, pulse duration and pulse energy. These parameters have been considered also by Jackson et al [10] to investigate the effect of laser intensity at three different wavelengths on the drilling rate.

Pulse duration as another effective parameter is examined by Schoonderbeek et al [11] who concluded that the melt expulsion is the dominant material removal mechanism in nano-second regime. Pulse duration [12] and focusing position [13, 14] have been shown to have an impact on hole diameter as well.

The evolution of shallow craters' diameter and depth in regards to number of pulses (NoP) and fluence [15] and the effect of different average power on circularity, HAZ and taper angle [16] has also been investigated.

Apart from optimizing laser parameters, choosing the right drilling strategy for improving the quality and throughput of the process is also well studied. In particular Romoli et. al. [17] proposed a novel cycle to obtain taper less cylindrical holes on stainless steel in total absence of burrs and debris. It includes three cycles of pilot-hole, enlargement and finishing. Wang et. al. [14] proposed a drilling strategy of multiple concentric circles with certain pause times to have sufficient time to dissipate generated heat effectively and minimize the risk of cracks.

2.4.2. Integrating optical elements in the beam delivery system

A range of optical elements have been introduced by researchers to control laser beam characteristics including, beam quality, beam shape, beam spatial distribution, beam size and polarisation to overcome the drilling limitations. Polarisation of the beam is known to have an effect on the final shape of the hole. For instance in percussion drilling by linearly polarized pulse, the shape of the hole usually cannot be maintained at the rear surface of the workpiece. This problem arises due to the different reflectivity for s- and p-polarized light at the walls of the hole [18]. So, non-circular holes and tapered walls are inevitable phenomena in drilling high aspect ratio holes and minimising these effects demand implementing circular polarisation [18, 19]. However, it has been shown that special attention has to be paid to the adjustment of the quarter wave plate and a slight elliptical polarization leads to undesired deformations of the hole geometry [20]. Thus, rotating a half waveplate mechanically by a stage for percussion drilling [20] or a quarter-wave plate synchronised with the rotating

wedges of the trepanning optics are the solutions for this issue [21]. Using fast-response liquid-crystal provides more flexibility in controlling the polarization direction including rotating the polarization direction or different polarization synchronized with the optical scanner [22].

Another optical solution to avoid tapered wall, is changing the inclination angle of the beam. In most of the cases it has been suggested to adopt wedges with misalignment to incline the beam with respect to the optical axis. This misalignment can be adjusted as a controlling parameter of the process, and it is capable of producing holes with positive taper, negative taper or cylindrical walls [17, 23, 24].

Other optical solutions including lenses with different focal distance and tailoring the spatial beam distribution will be addressed in sections 2.6 and 2.7 respectively.

2.4.3. Other Complementary Processes

There are a variety of complementary approaches to overcome limitations associated with laser drilling. For instance using assisted gases for improving the material ejection rate and to prevent contamination of the focusing optics from the ejected material [25]. Different parameters are controllable and need to be optimized, hence Khan et al [26] studied the effects of different nozzle diameters and gases on achievable drilling rates and hole diameter. Some investigations focused on the strategy of delivering assisted gas. Hsu et al [27] employed an intermittent gas delivery system to minimize spatter and holes' taper, while Ho et al [28] compared the effects of swirling and straight gas system on holes' depth. Also drilling in a chamber and investigating the influence of different surrounding gas, in particular Helium, Argon, Air and vacuum on the surface integrity of the holes has been investigated [29].

Drilling under water is considered to be effective in improving drilling rate and quality of the holes in terms of HAZ and micro cracks. This method introduces other assistant mechanisms like the plasma shielding, water-cooling, and dissolving effects [30, 31].

There are more complementary approaches like preheating the sample (which proved to be helpful in decreasing the spatter area [32]) which going through all of them demands a comprehensive study and a proper experimental plan. In the next section, literature review of another complementary approach i.e. two side drilling is covered.

2.5. Two-sides laser drilling

The concept of two-side laser drilling is simple. The operation requires first processing from one side until the saturation point is reached, i.e. when the penetration rate decreases substantially, and then to continue from the opposite side. The main advantages of this approach compared with one-side laser processing are [33, 34]:

- 1- The achievable aspect ratios can be doubled at least and thus to drill holes that cannot be produced due to their high aspect ratio.
- 2- The effect of taper angle that leads to considerable differences between the entry and exit holes' diameters can be eliminated.
- 3- The achievable processing efficiency is higher as drilling is performed only in its optimum processing window, i.e. the drilling process stops when the saturation point is reached.
- 4- Through holes with higher geometrical and dimensional accuracy can be produced as the number of pulses required is minimised and hence also the side effects associated with the laser drilling process.

5- The method is not limited to drilling only circular holes but can also be used for producing any structures, both through and blind, as high positional accuracy can be achieved in producing functional features from the two opposite sides of the workpiece [35].

Two-side holes' drilling has been implemented in other processes like ECM as illustrated in Figure 2.3 [36]. It is used to produce a 2 mm diameter holes employing electrochemical machining through a mask. The hole formation was studied step by step and then the method was applied to fabricate hole arrays with a lower taper angle.

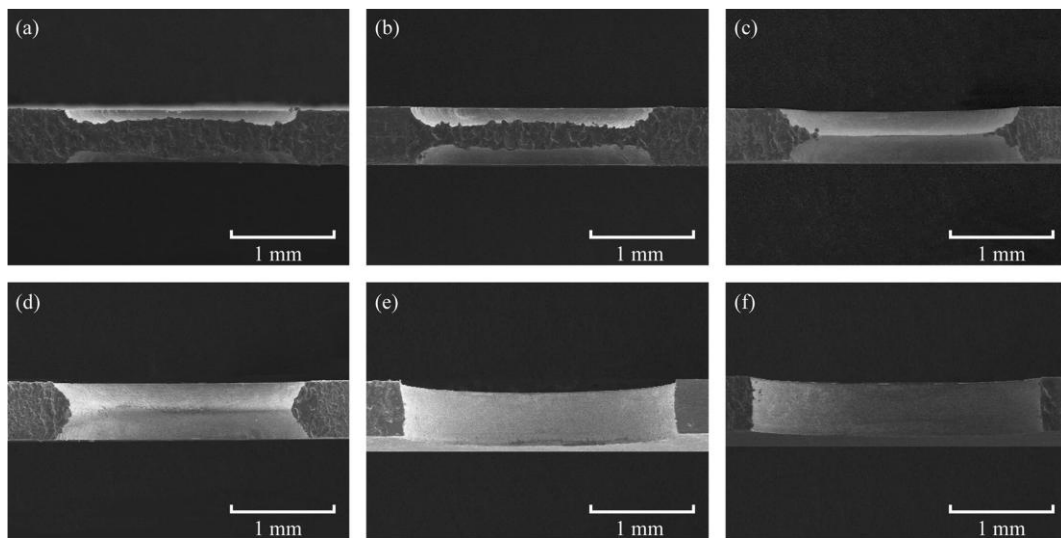


Figure 2.3. Profile images of fabricated hole by the ECM from two sides with different machining times: (a) 60 s, (b) 120 s, (c) 150 s, (d) 180 s, (e) 240 s, (f) 300 s [36].

In laser processing, two-side laser drilling can be implemented in three configurations:

- Adopting two laser sources and aligning them in a way to process the material from opposite sides.
- Using one laser source and deflecting the beam by a beam splitter and a series of mirrors onto the other side of workpiece.

- Using one laser source and a rotary stage to rotate the sample by 180° after processing one side and start processing the opposite side.

A limited number of reports have been published using two side laser drilling. For instance Bovatsek et al [37] used two laser source and one laser source approach without rotating the sample for trepanning 5 mm hole diameters in glass with various thicknesses. They commented that compared to one side drilling, throughput has been improved by 1.75 and 3.5 times when using one and two laser sources respectively. Also as it is illustrated in Figure 2.4 only one-quarter of the volume need to be removed.

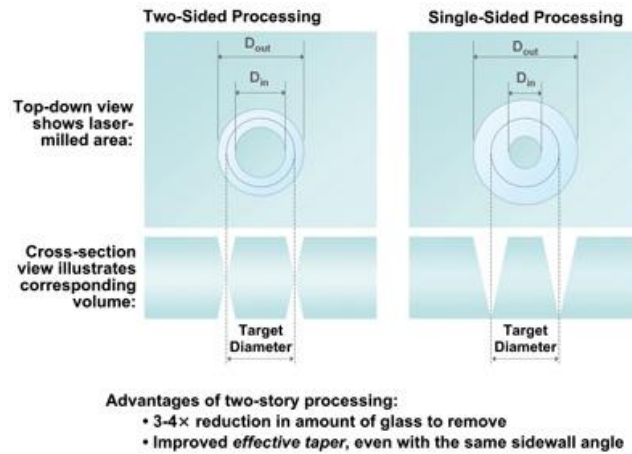


Figure 2.4. Benefits of two side laser processing [37]

In another attempt, Goya et al [38] used this method to drill a hole into a 62.5 μm glass optical fibre with a femtosecond laser and thus to fabricate a micro probe for spectroscopic measurements. It can be seen in Figure 2.5 that their method is based on rotating the sample and the main focus of this research was on the performance of a sensor produced with the proposed drilling method. It was reported that the micro holes produced from the two opposite sides connected successfully and thus it was possible to produce a through hole. As it is shown in Figure 2.6, the diameter of the holes were found to be approximately 10 and 18 μm at the waist and at the fibre surface, respectively.

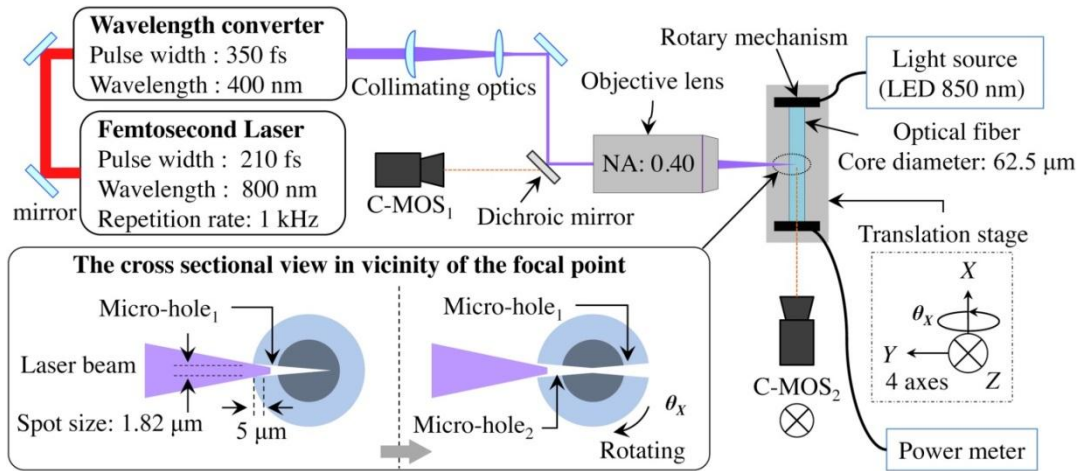


Figure 2.5. Experimental setup for micro hole drilling from two sides [38]

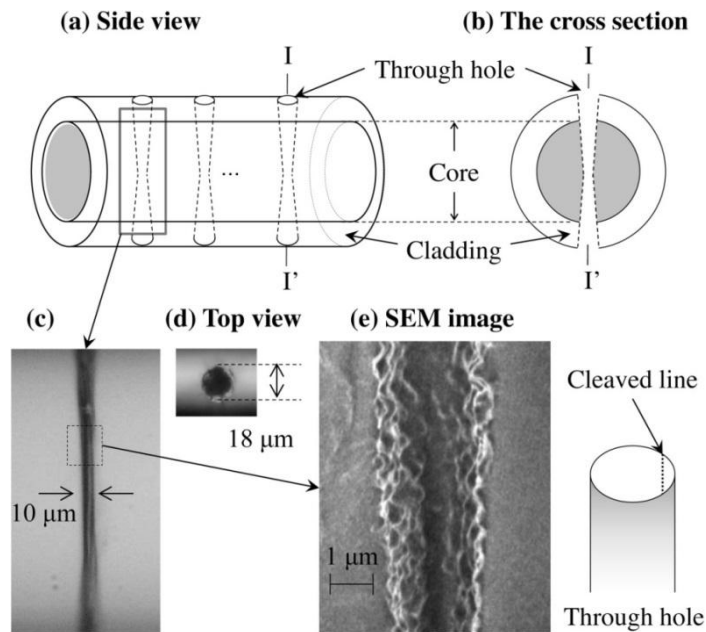


Figure 2.6. The schematic of (a) side view, (b) cross section and micrographs of (c) cross section (d), hole opening and (e) is the SEM image of a part of hole [38].

Pavel et. al. [35] used this method to produce sub millimetre features of waveguide of Terahertz Device. Their results for one side and two sides processing are shown in Figure 2.7 and Figure 2.8 respectively and confirms the dimensional improvements in particular in the exit side of the feature.

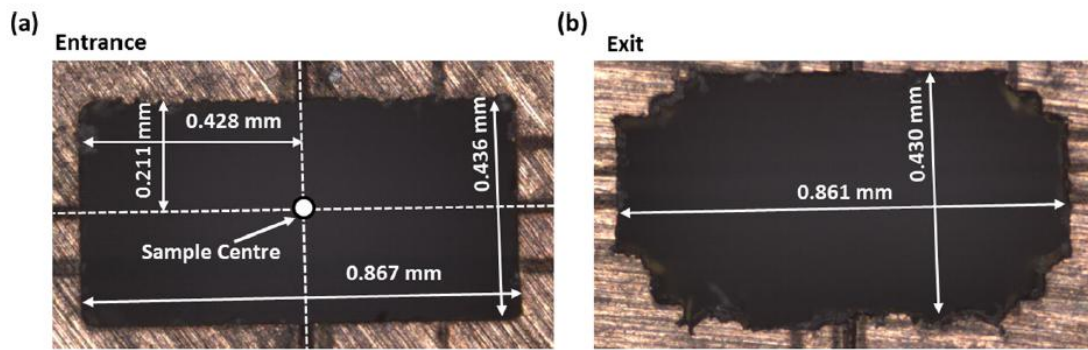


Figure 2.7. Rectangular through hole produced with one-side machining strategy: top view at its entrance (a) and at (b) the exit side [35].

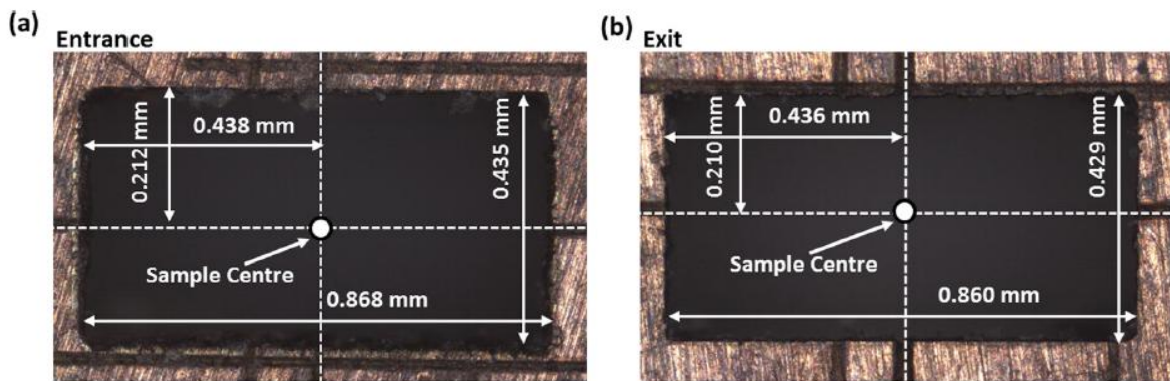


Figure 2.8. Rectangular through hole produced with two-side machining strategy: top view at its entrance (a) and at (b) the exit side [35].

2.6. Investigating a wide fluence spectrum with different focal distance lenses

Implementing lenses with different focal distance, in order to achieve a variety of beam diameter and fluence, is a solution to avoid some laser drilling limitations. As it is illustrated by Semak et. al. [39] in Figure 2.9, using lower focal distance lenses lead to the lower beam diameter. At the same time, they are sensitive to defocusing and consequently require fine adjustment in Z direction [39].

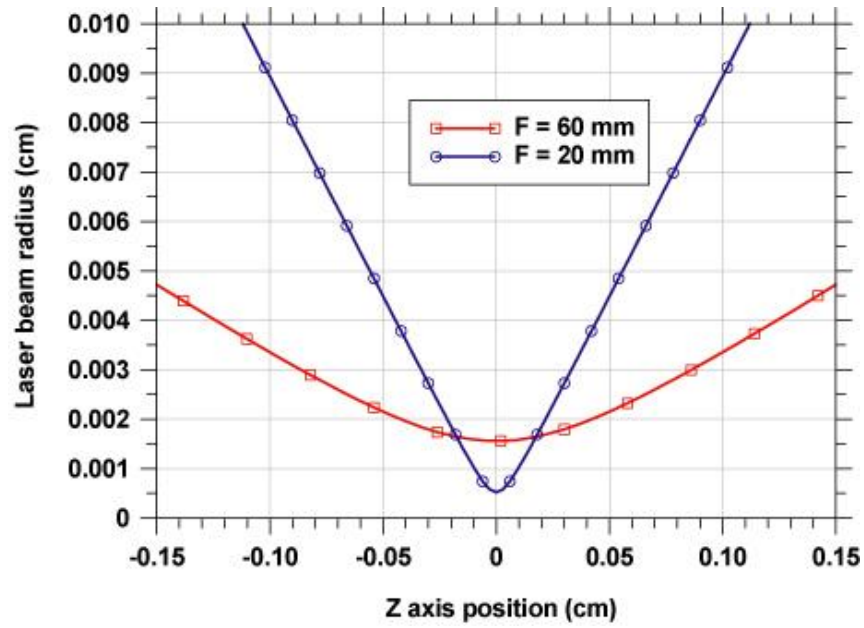


Figure 2.9. Beam radius near the focal distance for lenses with focal length of 60 and 20 mm [39].

Doring et.al [40], by implementing 5 different lenses managed to achieve higher fluences with a variety of beam diameters, as it is shown in Table 2.1.

Table 2.1. Spot size and maximum achievable fluence for each lens [40]

Lens	d_0 (μm)	F_{max} (J/cm^2)
$f = 25$ mm	10.4 ± 0.5	294 ± 26
$f = 50$ mm	15.6 ± 0.3	130 ± 6
$f = 75$ mm	20.4 ± 0.7	76 ± 5
$f = 100$ mm	27.8 ± 0.3	41 ± 1
$f = 150$ mm	37.8 ± 0.6	22 ± 1

The focus of their study was on deep drilling with ultrashort laser pulses on silicone, and as depicted in Figure 2.10, the maximum hole depth is mostly governed by the pulse energy and is independent from the irradiated spot size and the corresponding fluence.

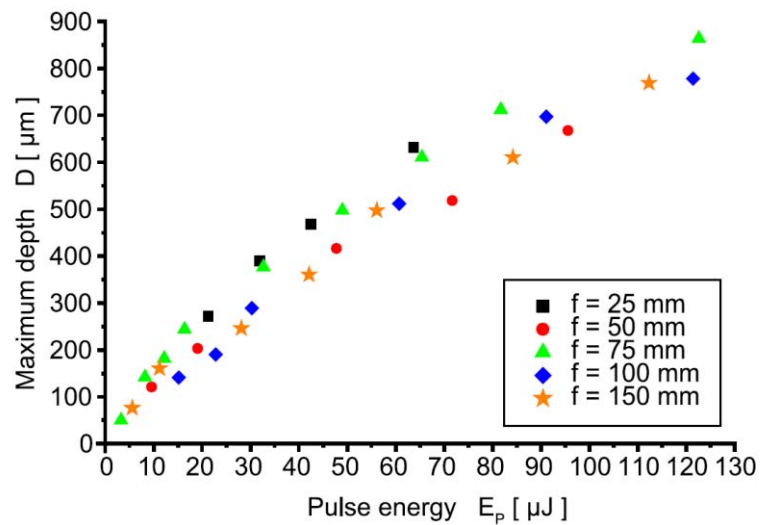


Figure 2.10. The maximum achievable hole depth for lenses with different focal distance [40]

2.7. Shaping the spatial profile of the beam

In most of the laser drilling attempts, the spatial shape of the beam is a Gaussian profile with some intrinsic drawbacks. In particular the wasted part of the energy in the wings with intensities less than ablation threshold of the material which leads to a lower throughput in the process, wider HAZ and poor edge definition [41] as it is shown in Figure 2.11.

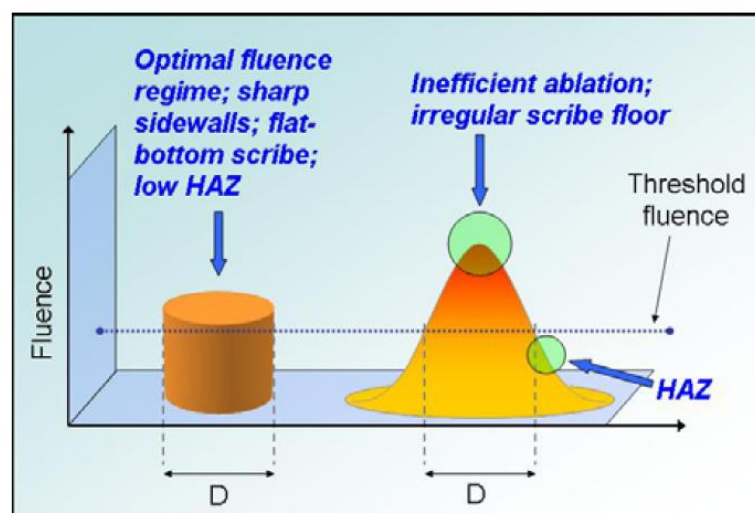


Figure 2.11. Side effects of using a Gaussian beam distribution compared to a flat-top [42]

In addition, as a result of the non-uniform energy distribution, the shape of the dimple will represent a Gaussian beam shape rather than a cylindrical one (See Figure 2.12). Predicting the shape of the hole will be even more complicated because of the refractive index dependency on the local fluence [43, 44].

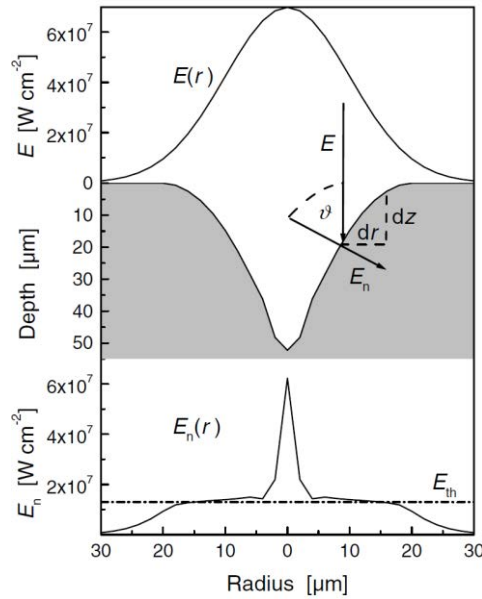


Figure 2.12. The dependency of the hole shape on the Gaussian beam distribution [44]

Hence, converting the spatial beam shape profile, for instance into a Bessel beam or top-hat can be considered as another optical solution. He et al [45] by adopting an axicon and designing a binary phase plate, produced a tailored Bessel beam, to facilitate drilling holes with 10 μm diameter in 100 μm thick Silicon with almost taper-free sidewalls. Hole characteristics for three different beam shapes of Gaussian, Conventional Bessel beam and Tailored Bessel beam is illustrated in Figure 2.13, proving the improvements when using a tailored Bessel beam. Nevertheless transparency of the material to the laser source wavelength together with the ring marks which are likely to be seen as a result of high fluence and accumulation of energy, limits Bessel beam application [46].

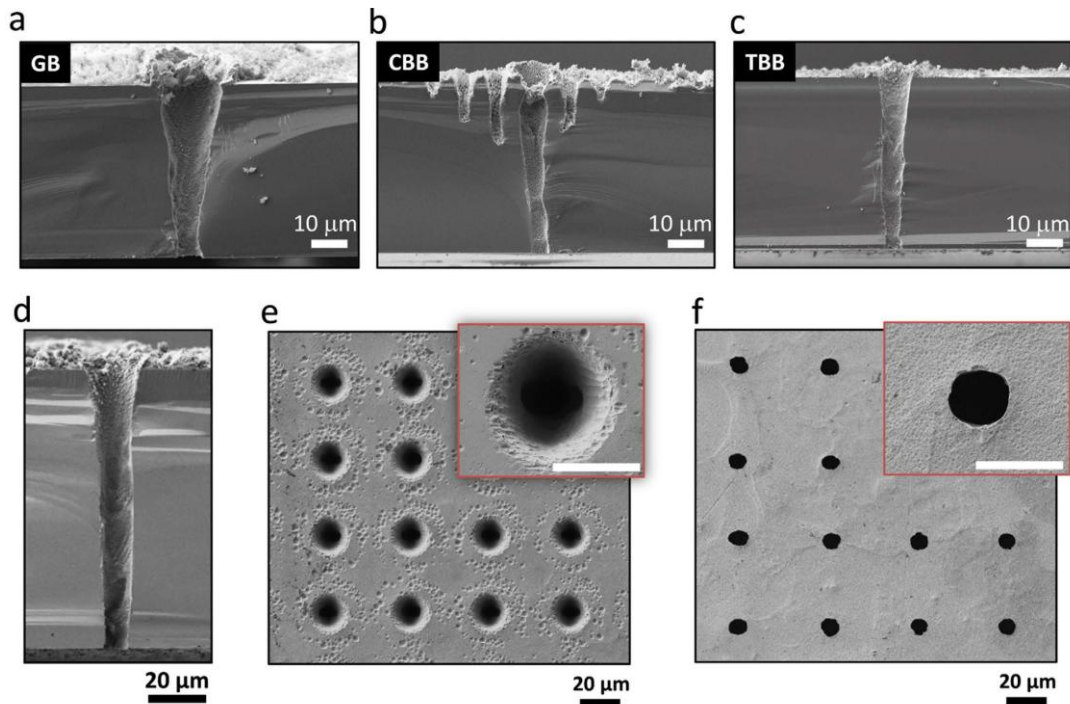


Figure 2.13. Cross sectional SEM image of drilling in 50µm thickness by (a) Gaussian (b) Conventional Bessel beam (c) Tailored Bessel beam- and in 100µm by Tailored Bessel beam (d) Cross section (e) front (f) rear view [45]

An optimum beam shaping solution should be selected taking into account application’s specific requirements and laser source properties. At the same time, beam shapers should not be considered off-the-shelf products as this could lead to several issues, i.e. divergence shifts, power fluctuations, pointing instabilities and beam spatial profile distortions [47]. Therefore, sufficient understanding of their capabilities and limitations is required before integrating them into beam delivery systems.

Beam shaping methods are generally categorized into three classes [47-49]:

- 1- *Attenuators*. These shapers basically use apertures to truncate a desirable portion of the beam. The main disadvantages of this method are the loss of some beam energy and difficulties in finding optimal position and portion of beam.
- 2- *Beam integrators*. These shapers use a lenslet array and break up the beam into beamlets. The main drawback of this beam shaping solution is the beam damage

and some deficiencies in spatial coherence because of the destructive interference phenomenon, hence it usually requires large beam dimensions.

3- *Field mapping*. This method transforms the electromagnetic field by inducing accurately one-to-one mapping. Generally, refractive, reflective or diffractive optical elements (DOE) are adopted in transforming the beams.

Shaping the beam in focal plane by using DOE have been successfully used for drilling [20]. They combined a fresnel lens and a phase plate to attain a doughnut shape for drilling stainless steel. As it is shown in Figure 2.14, beam shape and diameter are a function of the substrate position and a core remains in the middle of the hole due to the doughnut-like profile. The core falls out after drilling through thin target materials (400 μm) however for thicker materials, the core will be ablated due to multiple light reflections inside the hole.

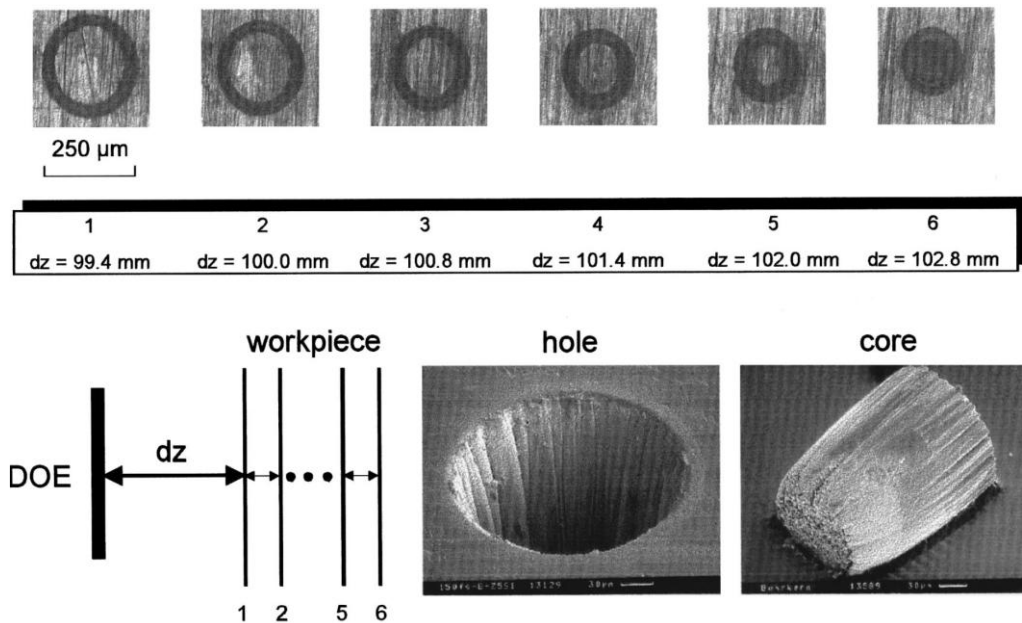


Figure 2.14. The variation of the distance between workpiece and DOE leads to different hole diameters [20]

DOEs has some problems which limits their usage in industry including complexity of the design algorithms, difficulty of manufacturing, limited diffraction efficiency and low resistance to high peak power ultra-short pulses [50].

Spatial light modulators (SLM) also as a dynamic DOE can modulate the phase of an incoming wavefront by utilizing the tuneable liquid crystal molecules [51]. They are usually limited by the shaping rate, resolution and low damage threshold [52, 53] in particular shaping the beam at focal plane which demands solving complicated algorithms [54]. In case of drilling, Sanner et al [55] implemented a versatile phase-front tailoring system to obtain doughnut and top-hat beam shape by spatial phase modulation. It can be seen in Figure 2.15 that holes with diameter of about 17 μm and depth of 15 μm are drilled by three different beam shapes. They concluded that the top-hat beams not only produce sharp edges but also unlike the Gaussian beam, the hole diameter is not fluence-dependent.

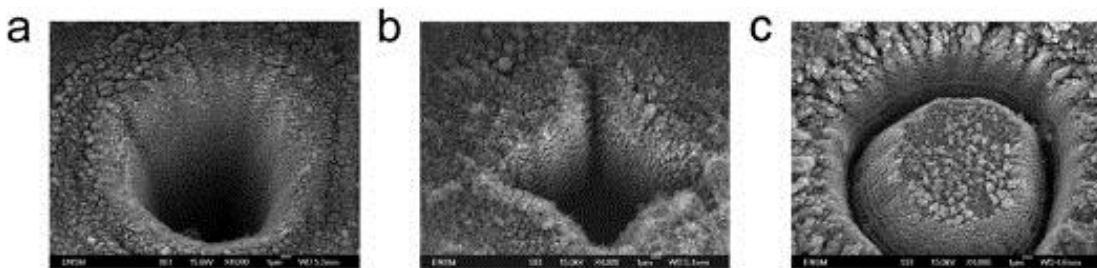


Figure 2.15. SEM image of the produced hole by (a) circular top-hat, (b) square top-hat, (c) doughnut [55]

In another attempt, Doan et al [56] produced top-hat and annular beam using a fluidic laser beam shaper and compared the resulted holes in terms of diameter, depth and HAZ. It is illustrated in Figure 2.16 that holes drilled by a top-hat beam resulted in a lower recast layer compared to a Gaussian.

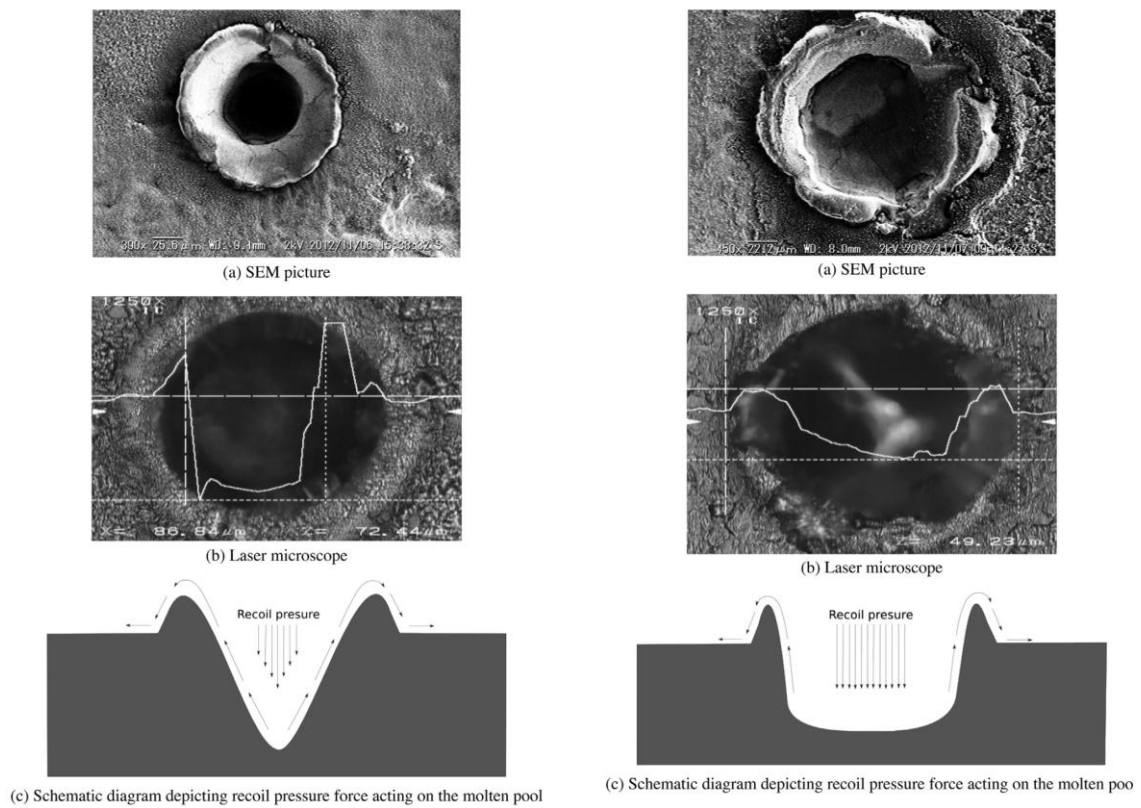


Figure 2.16. Hole drilled by a Gaussian (Left) and Top-hat (Right) after 1s

On the other hand, refractive optics compared to other methods, have a simpler structure and easier to manufacture at a low cost with high optical efficiency [50, 57, 58]. Zhang et al [58] used this method to produce a Pitchfork beam in focus and reduced the spatters around the vias. The optical elements they adopted comprise three lenses as it is illustrated in Figure 2.17: A plano-concave aspheric lens, a plano-convex aspheric lens and a commercially available aspheric focusing lens as the A, B and C elements in the figure respectively.

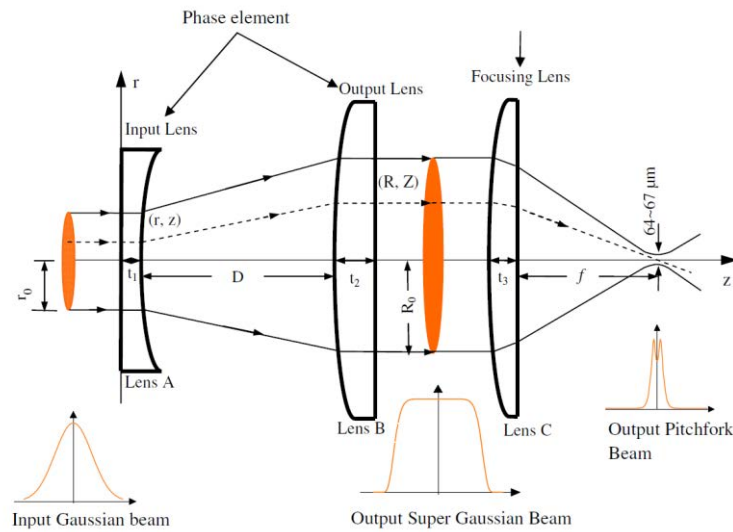


Figure 2.17. A three-lens beam shaping system to transform a Gaussian beam into a pitchfork beam [58]

2.8. Summary of open research issues

The carried out literature review reveals the limitations of laser drilling in producing high aspect ratio micron holes and different techniques for addressing these limitations. It's been shown that in comparison to the developed approaches, some techniques do not have sufficient technological maturity and need to be developed further. Specific open research issues that have to be addressed in this research are summarized as follows:

- *Key research issue 1: Two-sides laser drilling (Fully Addressed in Chapter 3)*

The main focus of the shown researches in this method was on the performance of the produced component with some qualitative evaluations. Hence there is a lack of knowledge about the capabilities in regards of achievable accuracy, repeatability and reproducibility that are essential in a manufacturing process. Thus a comprehensive quantitative study is needed to design and implement a laser processing configuration for their automation, including the necessary calibration and setting up routines. Therefore, it is important to develop an automated method that minimises and even eliminates any pre-trials in achieving a higher precision without increasing the process uncertainty. To fully automate the drilling process

from two sides, it is recommended to develop an in-situ, on-machine method for monitoring the alignment of the holes. This can be achieved by integrating in the process setup a 3D metrology sensor to carry out in-situ inspections, i.e. dimensional and other measurements to judge not only about accuracy and general quality, but also to monitor the alignment accuracy of the holes/structures produced from two sides. Therefore, the sources of errors should be identified and thus to calculate the combined uncertainty associated with different measurement procedures

- *Key research issue 2: Investigating a wide fluence spectrum with different focal distance lenses (Fully Addressed in Chapter 4)*

Limited researches have been carried out on this approach and none of them investigated systematically the effects on achievable aspect ratios and morphologies of micro holes produced by this method, in particular, quantifying the effects on achievable aspect ratios, cylindricity and taper angles of the holes in micron levels. Also, the limitations associated with the use of lenses with lower focal distances in producing high aspect ratio holes have not been investigated.

- *Key research issue 3: Shaping the spatial profile of the beam (Fully Addressed in Chapter 5)*

The majority of the researches in this field are focused on beam shaping, far from focal plane or for beam waist diameters of more than 100 μm . Hence, a systematic investigation on getting a top-hat beam in focal plane based on refractive optics for beam diameters of less than 100 μm is demanded, in particular for drilling high aspect ratio micro holes. Capabilities and limitations in laser micro drilling needs to be investigated and compared with the results achievable with a Gaussian beam. The morphology of high aspect ratio holes in terms of cylindricity, depth, taper angle and HAZ should be analysed in micron levels and the trade-off in comparison to the use of a Gaussian beam needs to be discussed.

References

- [1] J.C. Ion, *Laser Processing of Engineering Materials*, Butterworth-Heinemann, Oxford, 2005.
- [2] W.M. Steen, J. Mazumder, *Laser material processing: Fourth edition*, 2010.
- [3] S. Mishra, V. Yadava, *Laser Beam MicroMachining (LBMM) – A review*, *Optics and Lasers in Engineering*, 73 (2015) 89-122.
- [4] G.D. Gautam, A.K. Pandey, *Pulsed Nd:YAG laser beam drilling: A review*, *Optics & Laser Technology*, 100 (2018) 183-215.
- [5] C. Fornaroli, J. Holtkamp, A. Gillner, *Laser-beam helical drilling of high quality micro holes*, *Physcs Proc*, 41 (2013) 654-662.
- [6] Y. Zhang, Y. Wang, J. Zhang, Y. Liu, X. Yang, Q. Zhang, *Micromachining features of TiC ceramic by femtosecond pulsed laser*, *Ceram. Int.*, 41 (2015) 6525-6533.
- [7] M. Ghoreishi, D.K.Y. Low, L. Li, *Comparative statistical analysis of hole taper and circularity in laser percussion drilling*, *International Journal of Machine Tools and Manufacture*, 42 (2002) 985-995.
- [8] M. Ghoreishi, O.B. Nakhjavani, *Optimisation of effective factors in geometrical specifications of laser percussion drilled holes*, *Journal of Materials Processing Technology*, 196 (2008) 303-310.
- [9] G. Casalino, A.M. Losacco, A. Arnesano, F. Facchini, M. Pierangeli, C. Bonserio, *Statistical Analysis and Modelling of an Yb: KGW Femtosecond Laser Micro-drilling Process*, *Procedia CIRP*, 62 (2017) 275-280.
- [10] M.J. Jackson, W. O'Neill, *Laser micro-drilling of tool steel using Nd:YAG lasers*, *Journal of Materials Processing Technology*, 142 (2003) 517-525.
- [11] A. Schoonderbeek, C.A. Biesheuvel, R.M. Hofstra, K.J. Boller, J. Meijer, *The influence of the pulse length on the drilling of metals with an excimer laser*, *Journal of Laser Applications*, 16 (2004) 85-91.
- [12] G.K.L. Ng, L. Li, *Repeatability characteristics of laser percussion drilling of stainless-steel sheets*, *Optics and Lasers in Engineering*, 39 (2003) 25-33.
- [13] B. Adelman, R. Hellmann, *Rapid micro hole laser drilling in ceramic substrates using single mode fiber laser*, *Journal of Materials Processing Technology*, 221 (2015) 80-86.
- [14] X.C. Wang, H.Y. Zheng, P.L. Chu, J.L. Tan, K.M. Teh, T. Liu, B.C.Y. Ang, G.H. Tay, *Femtosecond laser drilling of alumina ceramic substrates*, *Applied Physics a-Materials Science & Processing*, 101 (2010) 271-278.
- [15] S.H. Kim, I.-B. Sohn, S. Jeong, *Ablation characteristics of aluminum oxide and nitride ceramics during femtosecond laser micromachining*, *Applied Surface Science*, 255 (2009) 9717-9720.
- [16] A. Bharatish, H.N. Narasimha Murthy, B. Anand, C.D. Madhusoodana, G.S. Praveena, M. Krishna, *Characterization of hole circularity and heat affected zone in pulsed CO2 laser drilling of alumina ceramics*, *Optics & Laser Technology*, 53 (2013) 22-32.
- [17] L. Romoli, R. Vallini, *Experimental study on the development of a micro-drilling cycle using ultrashort laser pulses*, *Optics and Lasers in Engineering*, 78 (2016) 121-131.
- [18] S. Nolte, C. Momma, G. Kamlage, A. Ostendorf, C. Fallnich, F. von Alvensleben, H. Welling, *Polarization effects in ultrashort-pulse laser drilling*, *Applied Physics A*, 68 (1999) 563-567.
- [19] A. Gruner, J. Schille, U. Loeschner, *Experimental study on micro hole drilling using ultrashort pulse laser radiation*, *Physics Procedia* 2016, pp. 157-166.

- [20] H.K. Tönshoff, C. Momma, A. Ostendorf, S. Nolte, G. Kamlage, Microdrilling of metals with ultrashort laser pulses, *Journal of Laser Applications*, 12 (2000) 23-27.
- [21] C. Föhl, D. Breitling, F. Dausinger, Precise drilling of steel with ultrashort pulsed solid-state lasers, *Proceedings of SPIE - The International Society for Optical Engineering* 2002, pp. 271-279.
- [22] O.J. Allegre, W. Perrie, K. Bauchert, D. Liu, S.P. Edwardson, G. Dearden, K.G. Watkins, Real-time control of polarisation in ultra-short-pulse laser micro-machining, *Applied Physics A*, 107 (2012) 445-454.
- [23] Y. Liu, C. Wang, W. Li, L. Zhang, X. Yang, G. Cheng, Q. Zhang, Effect of energy density and feeding speed on micro-hole drilling in C/SiC composites by picosecond laser, *Journal of Materials Processing Technology*, 214 (2014) 3131-3140.
- [24] C. He, F. Zibner, C. Fornaroli, J. Ryll, J. Holtkamp, A. Gillner, High-precision helical cutting using ultra-short laser pulses, *Physics Procedia* 2014, pp. 1066-1072.
- [25] A.H. Khan, W. O'Neill, L. Tunna, C.J. Sutcliffe, Numerical analysis of gas-dynamic instabilities during the laser drilling process, *Optics and Lasers in Engineering*, 44 (2006) 826-841.
- [26] A.H. Khan, S. Celotto, L. Tunna, W. O'Neill, C.J. Sutcliffe, Influence of microsupersonic gas jets on nanosecond laser percussion drilling, *Optics and Lasers in Engineering*, 45 (2007) 709-718.
- [27] J.C. Hsu, W.Y. Lin, Y.J. Chang, C.C. Ho, C.L. Kuo, Continuous-wave laser drilling assisted by intermittent gas jets, *International Journal of Advanced Manufacturing Technology*, 79 (2015) 449-459.
- [28] C.C. Ho, Y.M. Chen, J.C. Hsu, Y.J. Chang, C.L. Kuo, Characteristics of the effect of swirling gas jet assisted laser percussion drilling based on machine vision, *Journal of Laser Applications*, 27 (2015) 042001.
- [29] Y. Okamoto, K. Asako, N. Nishi, T. Sakagawa, A. Okada, Effect of surrounding gas condition on surface integrity in micro-drilling of SiC by ns pulsed laser, *Applied Physics B: Lasers and Optics*, (2015).
- [30] J. Lu, R.Q. Xu, X. Chen, Z.H. Shen, X.W. Ni, S.Y. Zhang, C.M. Gao, Mechanisms of laser drilling of metal plates underwater, *J. Appl. Phys.*, 95 (2004) 3890-3894.
- [31] C.H. Tsai, C.C. Li, Investigation of underwater laser drilling for brittle substrates, *Journal of Materials Processing Technology*, 209 (2009) 2838-2846.
- [32] L.S. Jiao, S.K. Moon, E.Y.K. Ng, H.Y. Zheng, H.S. Son, Influence of substrate heating on hole geometry and spatter area in femtosecond laser drilling of silicon, *Applied Physics Letters*, 104 (2014) 181902.
- [33] P. Penchev, V. Nasrollahi, S. Dimov, Laser micro-machining method for producing high aspect ratio features, 11th International Conference on Micro Manufacturing ICOMM, Orange County, California, USA, 2016, pp. 37.
- [34] V. Nasrollahi, P. Penchev, S. Dimov, A new laser drilling method for producing high aspect ratio micro through holes, 4M/IWMF Conference, Lyngby, Denmark, 2016, pp. 741.
- [35] P. Penchev, X. Shang, S. Dimov, M. Lancaster, Novel Manufacturing Route for Scale Up Production of Terahertz Technology Devices, *Journal of Micro and Nano-Manufacturing*, 4 (2016) 021002-021002.
- [36] G.Q. Wang, H.S. Li, N.S. Qu, D. Zhu, Investigation of the hole-formation process during double-sided through-mask electrochemical machining, *Journal of Materials Processing Technology*, 234 (2016) 95-101.
- [37] J. Bovatsek, R.S. Patel, DPSS Lasers Overcome Glass Process Challenges, *Photonic Spectra*, 46 (2012) 50-54.

- [38] K. Goya, T. Itoh, A. Seki, K. Watanabe, Efficient deep-hole drilling by a femtosecond, 400 nm second harmonic Ti:Sapphire laser for a fiber optic in-line/pico-liter spectrometer, *Sensors and Actuators B-Chemical*, 210 (2015) 685-691.
- [39] V.V. Semak, J.G. Thomas, B.R. Campbell, Drilling of steel and HgCdTe with the femtosecond pulses produced by a commercial laser system, *Journal of Physics D: Applied Physics*, 37 (2004) 2925-2931.
- [40] S. Döring, S. Richter, A. Tünnermann, S. Nolte, Evolution of hole depth and shape in ultrashort pulse deep drilling in silicon, *Applied Physics A: Materials Science and Processing*, 105 (2011) 69-74.
- [41] D.M. Karnakis, J. Fieret, P.T. Rumsby, M.C. Gower, Microhole drilling using reshaped pulsed Gaussian laser beams, *Proceedings of SPIE - The International Society for Optical Engineering*, 4443 (2001) 150-158.
- [42] J. Bovatsek, R.S. Patel, High-power, nanosecond-pulse Q-switch laser technology with flat-top beam-shaping technique for efficient industrial laser processing, 26th International Congress on Applications of Lasers and Electro-Optics, ICALEO 2007 - Congress Proceedings 2007.
- [43] S. Ahn, D.J. Hwang, H.K. Park, C.P. Grigoropoulos, Femtosecond laser drilling of crystalline and multicrystalline silicon for advanced solar cell fabrication, *Applied Physics A*, 108 (2012) 113-120.
- [44] A. Ruf, P. Berger, F. Dausinger, H. Hügel, Analytical investigations on geometrical influences on laser drilling, *Journal of Physics D: Applied Physics*, 34 (2001) 2918-2925.
- [45] F. He, J. Yu, Y. Tan, W. Chu, C. Zhou, Y. Cheng, K. Sugioka, Tailoring femtosecond 1.5- μm Bessel beams for manufacturing high-aspect-ratio through-silicon vias, *Scientific Reports*, 7 (2017).
- [46] D. M., A. C.B., Bessel and annular beams for materials processing, *Laser & Photonics Reviews*, 6 (2012) 607-621.
- [47] F.M. Dickey, *Laser Beam Shaping: Theory and Techniques*, Second ed., CRC Press, Boca Raton, FL, 2014.
- [48] F.M. Dickey, L.S. Weichman, R.N. Shagam, Laser beam shaping techniques, *High-Power Laser Ablation*, SPIE2000, pp. 11.
- [49] F.M. Dickey, S.C. Holswade, T.E. Lizotte, D.L. Shealy, *Laser beam shaping applications*, CRC Press 2005.
- [50] A. Laskin, N. Šiaulyš, G. Šlekys, V. Laskin, Beam shaping unit for micromachining, *SPIE Optical Engineering + Applications*, SPIE2013, pp. 18.
- [51] Z. Kuang, W. Perrie, J. Leach, M. Sharp, S.P. Edwardson, M. Padgett, G. Dearden, K.G. Watkins, High throughput diffractive multi-beam femtosecond laser processing using a spatial light modulator, *Applied Surface Science*, 255 (2008) 2284-2289.
- [52] J.Y. Cheng, C.L. Gu, D.P. Zhang, S.C. Chen, High-speed femtosecond laser beam shaping based on binary holography using a digital micromirror device, *Optics Letters*, 40 (2015) 4875-4878.
- [53] R.J. Beck, J.P. Parry, W.N. MacPherson, A. Waddie, N.J. Weston, J.D. Shephard, D.P. Hand, Application of cooled spatial light modulator for high power nanosecond laser micromachining, *Optics Express*, 18 (2010) 17059-17065.
- [54] Z. Kuang, J. Li, S. Edwardson, W. Perrie, D. Liu, G. Dearden, Ultrafast laser beam shaping for material processing at imaging plane by geometric masks using a spatial light modulator, *Optics and Lasers in Engineering*, 70 (2015) 1-5.

- [55] N. Sanner, N. Huot, E. Audouard, C. Larat, J.P. Huignard, Direct ultrafast laser microstructuring of materials using programmable beam shaping, *Optics and Lasers in Engineering*, 45 (2007) 737-741.
- [56] H. Duc Doan, I. Naoki, F. Kazuyoshi, Laser processing by using fluidic laser beam shaper, *Int. J. Heat Mass Transf.*, 64 (2013) 263-268.
- [57] F. Duerr, H. Thienpont, Refractive laser beam shaping by means of a functional differential equation based design approach, *Optics Express*, 22 (2014) 8001-8011.
- [58] C. Zhang, N.R. Quick, A. Kar, Pitchfork beam shaping for laser microrvia drilling, *Journal of Physics D: Applied Physics*, 41 (2008) 125105.

CHAPTER 3:

Two-side Laser Processing Method for Producing High-Aspect Ratio Micro Holes

Authors Contributions

This chapter of the alternative thesis format is published in the ASME, Journal of Micro and Nano-Manufacturing. I am the first author of this publication. The paper's detail and contributions of co-authors are outlined below. The contents of this chapter address the **key research issue 1**, characterised in section 2.8.

Nasrollahi, V.¹, Penchev, P.², Dimov, S.^{*}, Korner, L.³, Leach, R.^{**} and Kim, K.^{***}, (2017), Two-Side Laser Processing Method for Producing High Aspect Ratio Microholes. Journal of Micro and Nano-Manufacturing, 5(4), 041006

¹ **Vahid Nasrollahi**: is the main author and he conceived the ideas of two-side drilling, designed and executed experiments, performed all necessary characterization and data analysis and wrote the manuscript that was reviewed by the principal supervisor, **Prof. Stefan Dimov** (*), Prof Richard Leach (**), and Dr Kyunghan Kim (***)

² Dr Pavel Penchev contributed with the setting up of the beam delivery system.

³ Lars Korner contributed in carrying out the XCT measurement and helping in uncertainty budget analyse.

CHAPTER 3 : Two-side Laser Processing Method for Producing High-Aspect Ratio Micro Holes

ABSTRACT

Laser micro processing is a very attractive option for a growing number of industrial applications due to its intrinsic characteristics, such as high flexibility and process control and also capabilities for non-contact processing of a wide range of materials. However, there are some constraints that limit the applications of this technology, i.e. taper angles on side walls, edge quality, geometrical accuracy and achievable aspect ratios of produced structures. To address these process limitations a new method for two-side laser processing is proposed in this research. The method is described with a special focus on key enabling technologies for achieving high accuracy and repeatability in two-side laser drilling. The pilot implementation of the proposed processing configuration and technologies is discussed together with an in-situ, on-machine inspection procedure to verify the achievable positional and geometrical accuracy. It is demonstrated that alignment accuracy better than 10 μm is achievable using this pilot two-side laser processing platform. In addition, the morphology of holes with circular and square cross-sections produced with one-side laser drilling and the proposed method was compared in regards to achievable aspect ratios and holes' dimensional and geometrical accuracy and thus to make conclusions about its capabilities.

Keywords: microhole, laser microdrilling, uncertainty characterization

3.1. Introduction

There is an increasing demand for producing components incorporating micro-scale structures, especially in biomedical, optical, aerospace and automotive industries [1]. Key functional features of such components have sizes ranging from 1 to 100 μm , tolerances and surface roughness better than 5 μm and Ra 500 nm, respectively [2]. In response to this growing demand, manufacturing processes are developed to address issues related to the scalability of available technologies while achieving the required level of predictability, reproducibility, productivity and cost effectiveness in producing complex geometries in a variety of materials [3]. Both, conventional, e.g. micro milling or micro drilling, and non-conventional micromachining technologies have been used to produce such components. The non-conventional technologies used to produce micro-scale structures fall into three main categories [4]:

- Chemical and electrochemical, e.g. photochemical machining;
- Mechanical, e.g. ultrasonic and abrasive water jet machining;
- Thermal energy, e.g. electron beam, electric discharge and laser ablation.

Considering the material removal rate (MRR), the process reliability and capital investment required for cost-effective manufacture, together with components' technical requirements and batch sizes, a suitable process or processes can be selected among existing options. In some cases, especially for difficult-to-cut materials, hybrid machining solutions have been developed that combine the capabilities of two or more machining processes and thus to benefit from their complementarity in achieving acceptable manufacturing performance [2, 5, 6].

This research is focused on developing a new laser processing method that can be used for producing through structures, e.g. arrays of micro holes with high aspect ratio (depth to

diameter ratio), that are required for a range of applications in the electronics industry, i.e. interconnecting vias and printed circuit boards, and also for producing interface probe cards for 3D wafer bumps [7-10]. The target holes' diameters and pitches in such applications are less than 60 μm , whereas the holes' aspect ratios are higher than 5 with taper angle less than 10° . These are very demanding requirements considering the accuracy, repeatability and throughput required for cost-effective processing and therefore there are limited numbers of micromachining processes that are capable of producing such hole arrays. In addition, it is important to state that there is a constant demand to reduce the holes' diameters down to 10 μm . In this context, one option is the use of photolithography to produce such through holes. However, photolithography requires multi-step processing in clean room environment that make this fabrication route capital intensive and thus potentially viable only for relatively high batch sizes [11]. Another manufacturing technology that could be employed is micro EDM drilling but this process has shortcomings too, i.e. high electrode wear and low MRR [12].

In the last decade, laser micro drilling has emerged as a viable alternative for producing such holes' arrays due to its intrinsic characteristics, such as high throughput, capabilities for non-contact processing a wide range of materials and also for producing holes with diameters down to and even less than 10 μm . However, laser micro drilling has some limitations, too, such as tapered side walls, achievable geometrical accuracy and edge definition due to the heat affected zone (HAZ) and material spatters, and penetration depth constraints. Different research groups have investigated laser parameter domains, different process setups and drilling strategies to reduce and even eliminate these shortcomings. In particular, Adelman and Hellmann [7] investigated the effects of different factors affecting the process and found that the accurate setting-up of the focal plane on the workpiece was the

most influential one in producing holes with a very low taper and higher circularity in ceramic plates. Wang et al [13] tried to identify the best focus plane positioning to minimize the taper and HAZ. In particular, a drilling strategy was suggested to achieve as high as possible circularity of exit holes. Another aspect investigated by research groups was the use of assisted gases to facilitate the drilling process. For example, Khan et al [14, 15] studied the effects of different nozzle diameters and gases on achievable drilling rates. Hsu et al [16] employed an intermittent gas to minimize some side effects such as spatter and holes' taper, while Ho et al [17] compared the effects of swirling and straight gas on holes' depth. In addition, to process transparent materials such as sapphire a short pulse laser assisted wet etching was studied to attain high surface quality and efficiency for specific applications [18, 19]. Lott et al [20] investigated further to optimize the processing parameters such as repetition rate, pulse overlap and Z-axis translation speed and thus to drill 400 μm holes in sapphire wafers while minimizing taper angle, drilling speed and cracks on the surface.

The use of different drilling strategies was also investigated by researcher, e.g. by using beam rotation apparatus for helical drilling [21], and thus to minimize/eliminate some side effects of the beams' Gaussian spatial profiles, i.e. micro cracks, circularity deviations and tapers. It is stressed that the selection of an appropriate drilling strategy is even more important when high aspect ratio micro holes have to be produced as this has a major impact on the drilling condition. In particular, when percussion drilling is applied, with the increase of the pulse number the penetration rate decreases due to light scattering and blocking of the beam and deterioration of ablation and ejection conditions in general [11]. Even by applying high fluence, the hole depth achievable is limited because of multiple beam reflections from the holes' side walls and also due to re-depositioning of ejected/melted material [22]. Tokarev et al [23] reported that the absorption of the laser beam by the plasma plume and the effects of

plasma stream doubled the wall heating because of radiation and convection, and also argued that this was the main reason for the different drilling conditions in deep and shallow holes. Therefore, it was proposed to model the plasma heating of side walls and thus to judge better about its effects on the drilling process.

In this paper, a new method for two-side processing is proposed to address some of the limitations associated with the laser micro drilling process. First, the distinguishing characteristics of the proposed method are described and the relevant research is reviewed. Then, the process design is discussed with a special focus on key enabling methods and technologies for achieving high accuracy and repeatability in two-side laser drilling. Next, a pilot implementation of the proposed method is described that is then used to validate the proposed two-side laser processing method. Finally, conclusions are made about the capabilities of the proposed method together with its enabling technologies based on the obtained experimental results.

3.2. Process characteristics and literature review

The concept for two-side laser drilling is simple. The operation requires first processing from one side until the saturation point is reached, i.e. when the penetration rate decreases substantially, and then after rotating the workpiece by 180° it continues from the opposite side. The main advantages of this approach compared with one-side laser processing are [24, 25]:

- 1- The achievable aspect ratios can be doubled at least and thus to drill holes that cannot be produced due to their high aspect ratio.
- 2- The effect of taper angle that leads to considerable differences between the entry and exit holes' diameters can be eliminated.

- 3- The achievable processing efficiency is higher as drilling is performed only in its optimum processing window, i.e. the drilling process stops when the saturation point is reached.
- 4- Through holes with higher geometrical and dimensional accuracy can be produced as the number of pulses required is minimised and hence also the side effects associated with the laser drilling process.
- 5- The method is not limited to drilling only circular holes but can also be used for producing any structures, both through and blind, as high positional accuracy can be achieved in producing functional features from the two opposite sides of the workpiece [26].

Two-side holes' fabrication was reported only in two implementations. In particular, Pavel et al [26] used this method to produce sub millimetre features of waveguide of Terahertz Device. Their results confirms the dimensional improvements in particular in the exit side of the feature. In another attempt, Goya et al [27] used the two-side method to drill a hole into a 62.5 μm glass optical fibre with a femtosecond laser and thus to fabricate a micro probe for spectroscopic measurements. It was reported that the micro holes produced from the two opposite sides connected successfully and thus it was possible to produce a through hole. The diameters of the holes were found to be approximately 10 and 18 μm at the waist and at the fibre surface, respectively. The main focus of this research was the performance of a sensor produced with the proposed drilling method and its capabilities in regards of achievable accuracy, repeatability and reproducibility that are essential in the production of dense holes' arrays with high efficiency.

To perform more than one side processing it is necessary to implement multi-axis laser processing machine configurations. Such multi-axis laser machining setups (machine

tools) are available predominantly for macro-scale applications, i.e. for cutting, welding and drilling operations [28], but their use for multi-side precision machining has received less attention. In particular, some multi-axis laser micromachining setups were reported as pilot machine tool configurations to address specific application requirements. For example, a turning machine tool was reported for processing axisymmetric parts [29], while another research group proposed a laser milling process for producing freeform parts with functional features in the sub-millimetre range [30]. In other investigations 5 axis laser machining capabilities were demonstrated for fabricating complex parts, i.e. a micro globe and a micro windmill [31], while Jin et al [32] developed a mathematical model for compensating volumetric errors in multi-axis laser processing after singling out geometrical errors associated with each axis.

Laser processing systems commonly integrate scan heads that are usually combined with mechanical stages to realise complex multi-axis micromachining configurations. The scan heads allow high dynamic beam movements but with a relatively low accuracy limited to a relatively small working envelop (field of view) compared with those achievable with the CNC mechanical stages [33]. This is another important difference between laser-based machining systems and conventional CNC machine tools. Recognising these significant differences, solutions were reported to address the constraints associated with them in implementing multi-axis laser micromachining setups. In particular, Kim et al [34] reported a software solution to synchronize the movements of mechanical stages and beam deflectors of a scan head, and thus to process bigger areas than the field of view, with acceptable accuracy and speed. At the same time, Penchev et al [35] reported generic software tools to minimize the negative dynamic effects of scan heads on achievable accuracy and also to benefit fully from available high frequency laser sources [36]. In addition, generic integration tools, i.e. a

modular workpiece holding device, an automated work-piece setting up routine and an automated strategy for multi-axis processing employing rotary stages, were proposed for improving the system-level performance of laser micromachining systems [37].

3.3. Process design

3.3.1. Background and sources of errors

As it was stated above machining from two-sides is a relatively simple concept but its complexity increases when high accuracy, repeatability and reproducibility have to be achieved. In particular, the difficulties arise from the necessary high precision alignment of the holes/structures produced from two sides. This is due to geometrical errors in rotating the workpieces by 180° employing rotary stages. There are two main methods to execute such a drilling strategy: (i) quantifying various sources of errors and then compensating them; or (ii) implementing fully automated routines. In this research, the main focus is on designing and validating automated routines.

To design such routines it is essential to identify first the sources of errors in two-side drilling and then to plan a sequence of steps necessary to execute fully automated drilling operations while minimising the effects of these errors. Generally, the error sources in CNC machining operations can be grouped as follows [38]:

- i. **Thermal errors.** They are negligible in laser micro processing (LMP) since the laser sources used are with a very low average power and they are usually kept away from the processing area. In addition, most of the movements are carried out with beam deflectors (scan heads) and not with mechanical axes.
- ii. **Cutting-force induced errors.** There are no such errors in LMP as it is a non-contact method.

iii. **Geometric and kinematic errors associated with linear and rotary axes.** In particular, for each linear axis there are two straightness, one positioning, and three angular errors (pitch, yaw, roll) while for rotary axes there are two radial, one axial, two tilt and one angular positioning error. Also, there are five location errors associated with rotary axes and three squareness errors accompanying the linear axes [39].

Thus, only the last class of geometrical errors are critical in executing precise laser machining operations and therefore should be considered in designing two-side laser drilling operations. In addition, there are other compensation movements that are specifically required in executing two-side drilling routines, i.e. due to:

- *Incident beam is not normal to the workpiece:* It is shown in Figure 3.1a and b that angular displacements of the beam from the workpiece surface normal (it is assumed that the beam is parallel to the Z axis) in regards to A ($\Delta\alpha^\circ$) or B ($\Delta\beta^\circ$) axes (realised with two rotary stages) can be compensated by repositioning in the Y and X directions respectively. However, a through hole drilled from two sides will not be normal to the workpiece and therefore it is essential to minimise any angular displacements in both directions before executing drilling operations. For simplicity only the displacement between the A axis and the beam is discussed further in this section but the considerations apply to the B axis, too.
- *Incident beam is not perpendicular to A axis:* As it is shown in Figure 3.1c, although such angular displacement ($\Delta\psi^\circ$) can be compensated by repositioning in the X direction, the holes drilled from two sides will not be coaxial and therefore this error has be minimised again to an acceptable deviation range.

- *Displacement of hole positions in respect to A axis:* Depending on the displacement of holes from the A axis, the workpiece needs to be repositioned twice in the Y direction and thus to align the holes drilled from the two opposite sides as shown in Figure 3.2a.
- *A axis not being parallel to X axis:* As it is shown in Figure 3.2b, this error can be compensated by measuring the angular displacement, $\Delta\gamma$, and then calculating the required compensation movements of the X and Y stages, based on the hole position.
- *Displacements between A axis and the centre plane of the workpiece in Z direction are higher than the laser beam depth of focus (see Figure 3.3):* Such a displacement can lead to an offset of the beam focal plane after rotating the workpiece by 180° . This can be compensated with repositioning movements in the Z direction and thus to adjust the focal distance.
- *Dynamic limitations of beam deflectors* should be considered by finding the optimum laser delays [35].
- *Beam displacements in machine coordinate system (MCS)* caused by alignments and calibrations of the optical components or changing ambient conditions [40].
- *Deviations from the parallelism of mechanical and optical axes* in executing the operations.
- *Linear and rotational positioning errors:* These errors need to be considered especially for the movements in the X and Y directions and also for the A axis to minimise any undesirable radial and axial displacements as a result of the rotation by 180° .

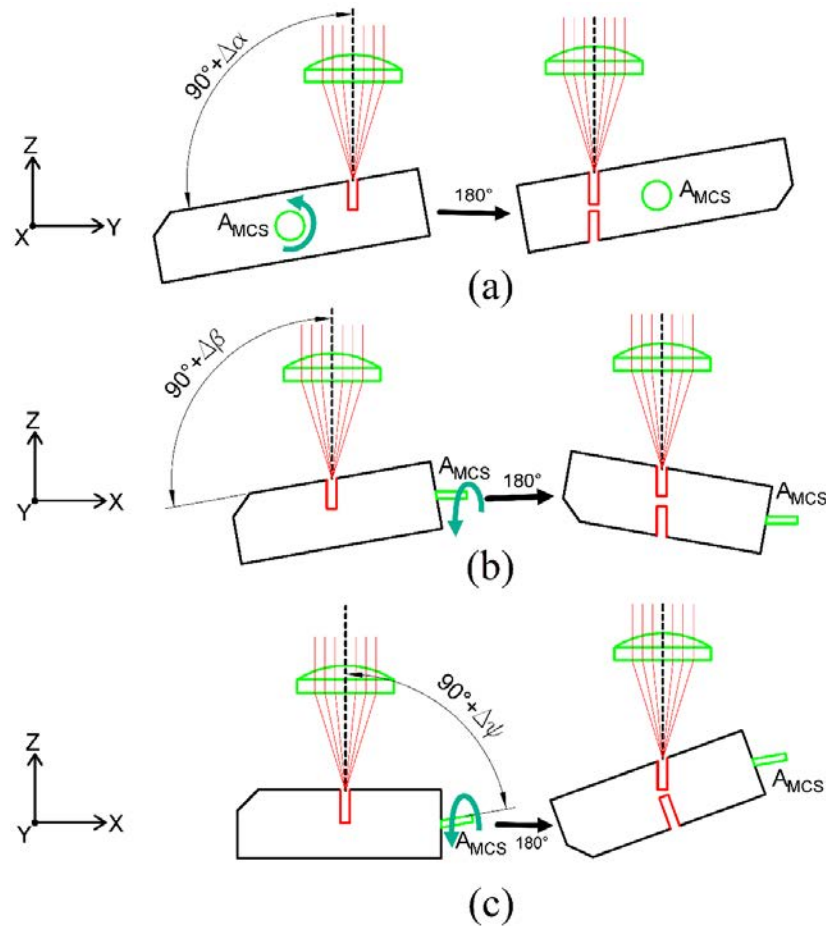


Figure 3.1. Angular displacements of incident beam and: (a) workpiece normal in regards to the A axis, $\Delta\alpha^\circ$; (b) workpiece normal in regards to the B axis, $\Delta\beta^\circ$ (c) A axis, $\Delta\psi^\circ$.

There are some other general considerations, such as sample flatness, that have to be taken into account in designing the process. Most of the potential errors listed above are systematic and can be substantially reduced by quantifying them and then calculating the required linear and rotary adjustments of the workpiece. However, residual errors associated with the required measurements, and linear and rotary movements cannot be compensated. These errors are directly dependent on the measurement equipment and the linear/rotary stages used, and can be minimised by increasing their precision, so as to reduce their combined effects.

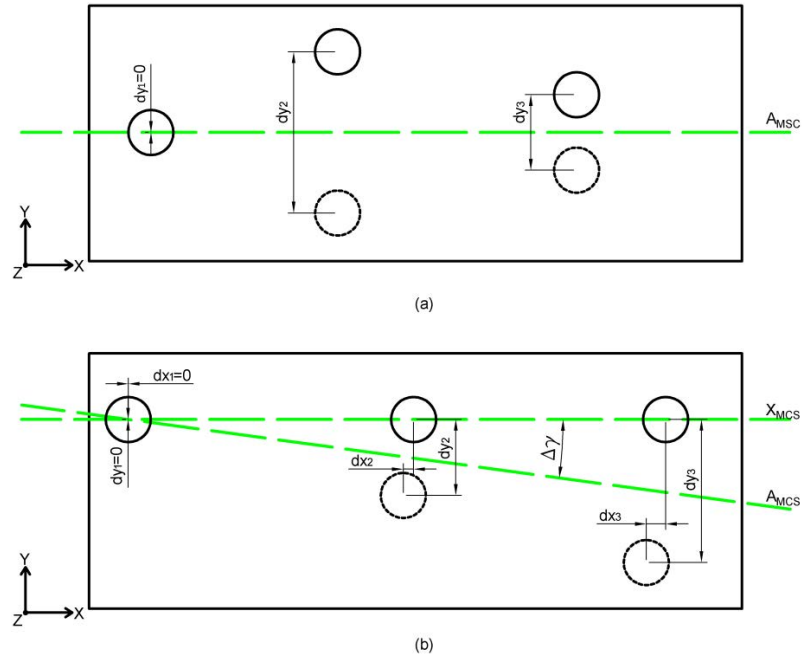


Figure 3.2. Required adjustments in X and Y directions (dx , dy) due to: (a) displacement of holes' positions in respect to the A axis; and (b) the A axis not being parallel to the X axis, $\Delta\gamma^\circ$.

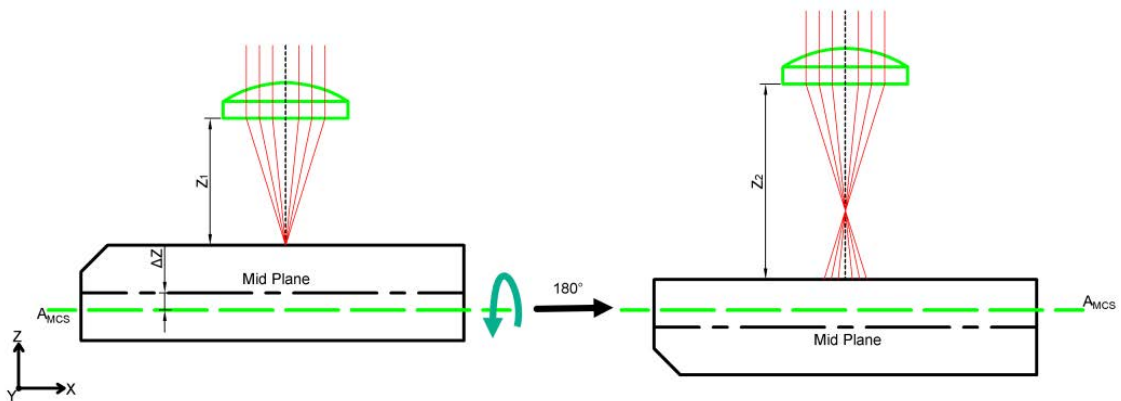


Figure 3.3. Required compensational movements in Z direction due to displacements between A axis and the centre plane of the workpiece, ΔZ

3.3.2. Design and requirements

To execute two-side laser drilling operations with required accuracy, repeatability and reproducibility it is necessary to design and implement a laser processing configuration for their automation, including the necessary calibration and setting up routines. Therefore, it is important to develop an automated method that minimises and even eliminates any pre-trials

in achieving a higher precision without increasing the process uncertainty. The implementation of fully automated two-side laser drilling operations requires not only component technologies that are always necessary to realise laser processing operations but also those required to realise multi-axis processing, specialised workpiece handling and automated process setting up routines. In particular, the first group of component technologies includes those that are selected taking into account the workpiece material, required beam spot diameter and target structure dimensions and quality, i.e. laser sources, beam conditioning devices, scan heads and focusing lenses. The second group includes additional component technologies, both hardware and software tools, that are specially configured and/or developed to address the specific requirements associated with the two-side laser drilling operations and thus to execute them with the necessary accuracy, repeatability and reproducibility. The requirements of component technologies that should be specially configured and/or developed for carrying out such drilling operations are discussed below.

3.3.2.1. *Rotary mechanical stages*

To carry out two-side laser processing, one rotational axis is required and therefore the machine configuration should integrate at least one rotary stage. The general requirements that such a stage should satisfy are:

- *The rotational axis should be perpendicular to the incident laser beam.* Assuming that the laser beam is parallel to the Z axis in the setup design, the rotary stage should realise A (rotation around X axis) or B (around Y axis) axes. Figure 3.1c depicts how an angular displacement of the incident beam from perpendicularity to the A axis can affect directly the concentricity and coaxially of holes by $\Delta\psi^\circ$. In this research, an A rotary stage was

used however two-side drilling operations could be implemented with a B stage in the same way.

- *Pre-defined resolution and repeatability in realising rotations by 180°.* The angular deviations in executing such rotations can be compensated but only down to the stage resolution. Also, if such deviations are stochastic for a given processing strategy, they can directly affect not only the holes' coaxially but also their positional accuracy. Thus, the rotary stage has to be selected taking into account the holes' positional and geometrical accuracy.
- *The rotary axis should be parallel to the X or Y axes.* Such angular displacements of $\Delta\gamma$, as shown in Figure 3.2b, can be compensated but require additional adjustment in X and Y directions, which could be avoided.
- *Minimised axial and radial errors.* Such errors can be compensated but only if they are systematic and therefore the achievable accuracy can be in the order of the rotary stage repeatability.

If the processing configuration integrates A and B rotary stages, drilling strategies can be designed to compensate any primary tilting of the workpiece in both directions (see Figure 3.1a and 1b). In addition, the integration of a C stage will allow in-situ, on-machine setting up and inspection routines to be automated.

3.3.2.2. *Linear mechanical stages*

The implementation of two-side laser processing requires a range of positional movements as discussed in Section 3.3.1. These movements introduce the following requirements in selecting the linear stages for executing automated laser drilling routines.

- *X and Y stages* have to be used in routines for detecting automatically the positions of reference marks/features, e.g. a reference through hole, before and after the rotation of the workpiece and also for correlating the beam coordinate system (BCS) to the MCS. Hence, the accuracy and resolution of these stages directly affects the achievable accuracy.
- *X and Y stages* should ensure precise initial positioning of the workpiece and then the necessary linear adjustments after the rotation by 180°. These X/Y movements are required to position the workpiece in the field of view of different sensors for process setting up and inspection. Therefore, the repeatability of the stages in executing these movements is essential for achieving the required positional accuracy of the holes.
- *The Z stage* should keep the workpiece within the laser beam depth of focus before and after the rotation by 180°. Hence, the resolution and repeatability of the Z stage should be better than the Raleigh length of the focused laser beam.
- *The straightness and angular errors of the linear stages* can be compensated automatically but their repeatability is important for achieving the required positional accuracy of the holes.

3.3.2.3. *Modular workpiece holding device*

The implementation of the two-side laser drilling method requires the development of a specialised workholding device to ensure the beam access to both sides of workpieces and a reliable, and at the same time, flexible interface between the workpiece and the stack of the mechanical stages in the laser drilling setup. Therefore, the workholding system should have a modular design and should be easily adaptable to workpieces with different sizes and shapes. In addition, the overall size and mass should be minimised to lessen the negative

dynamic effects in executing precision movements with a stack of mechanical linear and rotary stages, and cover the least possible surface area of the workpiece. In spite of the fact that laser drilling is a non-contact process, the workpiece fixturing should be sufficiently reliable, especially during or after the rotation by 180° , to eliminate any additional errors in the workpiece-workholding device sub-system.

3.3.2.4. *System level tools*

Alignment/measurement probes. To correlate the workpiece coordinate systems (WCS) to MCS, non-contact measuring probes, e.g. a chromatic confocal probe, should be employed to detect reference marks/features with the required level of accuracy and precision and also to determine the position the workpiece surface along the laser beam propagation direction (the focal plane). The working area of the probe should be easily accessible with the use of mechanical stages to determine the X, Y and Z positions of workpiece reference features/surfaces. The accuracy and resolution of the probe should be selected 5 to 10 times higher than the target positional accuracy of the laser drilled holes. Other important characteristics of the probe that determine its alignment/inspection capabilities are its working distance and the measurement range.

Fully automated process setting up routines. Process setting up routines should be developed for executing two-side laser drilling operations that employ the alignment/measurement probe to assess the errors from various sources discussed in Section 3.3.1 and then to compensate or minimise their impact on the process accuracy and repeatability. In particular, these routines should automate the following process setting up steps:

- Correlating the A axis to the BCS and thus to compensate radial displacement in the Y direction due to rotations with the A stage.
- Measuring the angular displacement between the X and A axes ($\Delta\gamma$);
- Measuring axial displacements of the A stage (ΔX_A) due to rotations around the A axis.
- Measuring angular displacement after executing a rotation by 180° with the A stage ($\Delta\theta$).
- Determining the focal planes of the laser beam on the workpiece, i.e. the initial setting up of the laser drilling process and then after the rotation by 180° , to compensate any radial displacements in the Z direction.

An automated process setting up that includes the above set of routines is described in Section 3.3.3. In addition, to set the drilling process, the laser parameters have to be optimised to achieve the required quality and throughput. This should include determining the optimum pulse number after which the penetration rate decreases substantially (the saturation point) or the mid plane of the workpiece is reached and thus to know when to continue the drilling process from the opposite side. In particular, the maximum possible thickness of the workpiece that can be drilled by this method can be estimated to be up to twice the maximum depth of blind holes or the saturation point in one side drilling.

In-situ, on-machine inspection methods. To automate the drilling process fully it is recommended to develop in-situ, on-machine methods for monitoring the drilling process. This can be achieved by integrating in the process setup a 3D metrology sensor to carry out in-situ inspections, i.e. dimensional and other measurements to judge about accuracy and general quality, but also to monitor the alignment accuracy of the holes/structures produced from two sides. Such a sensor should utilise the linear and rotary stages integrated in the laser processing setup to perform inspection and monitoring routines on both sides of the workpieces. Therefore, the sources of errors should be identified and thus to calculate the

combined uncertainty associated with different measurement procedures. The ultimate objective should be to select a 3D metrology sensor in such a way that the combined uncertainty associated with the in-situ, on-machine measurement routines does not exceed a fifth of the required positional accuracy of the drilled holes.

3.3.3. Fully automated process setting procedure

The procedure employs reference through features, i.e. two through holes produced from one side, to minimise the effect of various error sources (see Section 3.3.1) by implementing the routines outlined in Section 3.3.2.4. Figure 3.4 depicts the overall concept of finding the centres of two reference holes, located at Points 5 and 6 respectively, on the first side of the workpiece. Then, the centres of the two holes, i.e. Points 7 and 8 in Figure 3.4, are found again after rotating the workpiece by 180° and thus to calculate the resultant axial displacement of ΔX_A . The radial displacements in the Y and Z directions, resulting from the rotation, are compensated by correlating the A axis to the BCS and some adjustments in the Z direction. With this reference data, it is possible to determine the centres of all holes that have to be drilled on the workpiece after the rotation. More than two through holes can be used as references to minimise the effects of any errors in their manufacture.

This process setting up procedure requires the execution of the following steps as depicted in Figure 3.4:

1. Positioning the workpiece under a non-contact probe, scanning its surface in the X_{MCS} and Y_{MCS} directions using the mechanical stages to find the initial angular displacements of the workpiece normal relative to Z_{MCS} and then compensating them by rotating the workpiece around the A_{MCS} and B_{MCS} axes.

2. Determining the focal plane and its respective Z_{MCS} value and thus to ensure that the first side of the workpiece (z_1) is within the laser beam depth of focus.
3. Laser drilling of two through holes with well-defined edges, e.g. 500 μm in diameter, that are positioned as far as possible from each other.
4. Positioning the probe beam inside the first hole (Point 0) by using X and Y mechanical stages.
5. Scanning the hole along the X_{MCS} direction to detect Points 1 and 2 and thus to find the X_{MCS} coordinate (X_5) of the reference hole centre (Point 5).
6. Scanning of the hole along the Y_{MCS} direction to detect Point 3 and 4 and thus find the Y_{MCS} coordinate (Y_5) of the reference hole centre (Point 5).
7. Positioning of the probe beam inside the second hole and repeating Steps 5 and 6 to find the X_{MCS} and Y_{MCS} coordinates (X_6, Y_6) of its centre (Point 6).
8. Rotation of the workpiece by 180° around the A_{MCS} axis.
9. Scanning the workpiece surface in the Y_{MCS} direction to find the angular displacement ($\Delta\theta$) of the workpiece normal in regards to Z_{MCS} .
10. Repeating Step 2 for the second side of the workpiece to ensure again that the workpiece is within the laser beam depth of focus (z_2).
11. Repeating Steps 4 to 6 for the two reference holes on the second side and thus to find the X_{MCS} and Y_{MCS} coordinates of their centres, i.e. Points 7 and 8 (X_7, Y_7 and X_8, Y_8).

Based on the results, i.e. X_{MCS} and Y_{MCS} coordinates of Points 5 to 8, obtained with this process setting up procedure, the angular displacement between the A_{MCS} and X_{MCS} axes ($\Delta\gamma$), the axial error (ΔX_A), and the position of the A_{MCS} axis can be calculated by employing Eq. (1) and (2):

$$X_7 - X_5 = \Delta X_A + (Y_5 - Y_7) \cdot \tan(\Delta\gamma), \quad (1)$$

$$X_8 - X_6 = \Delta X_A + (Y_6 - Y_8) \cdot \tan(\Delta\gamma). \quad (2)$$

By solving Eq. (2), $\tan(\Delta\gamma)$ and ΔX_A are calculated, i.e.:

$$\tan(\Delta\gamma) = \frac{X_7 - X_5 - X_8 + X_6}{Y_5 - Y_7 - Y_6 + Y_8}, \quad (3)$$

$$\Delta X_A = X_7 - X_5 - \frac{(Y_5 - Y_7)(X_7 - X_5 - X_8 + X_6)}{Y_5 - Y_7 - Y_6 + Y_8}. \quad (4)$$

The general formula for calculating the symmetry points (x, y) in relation to a line, $Y = a.X + b$, would be:

$$\left(\frac{x(1-a^2)+2a(y-b)}{a^2+1}, \frac{2(ax+b)-y(1-a^2)}{a^2+1} \right). \quad (5)$$

In this research, the symmetry line $Y = a.X + b$ is the A_{MCS} axis and $a = \tan(\Delta\gamma)$.

Using Eq. (5) and the coordinates of Points 5 and 7, b_1 can be calculated as follows:

$$b_1 = \frac{Y_7(a^2+1)+Y_5(1-a^2)}{2} - a.X_5, \quad (6)$$

and then b_2 using Points 6 and 8:

$$b_2 = \frac{Y_8(a^2+1)+Y_6(1-a^2)}{2} - a.X_6. \quad (7)$$

Ideally b_1 and b_2 should be equal. However, because of the uncertainties in finding the coordinates of Points 5 to 8 there may be a difference between them. Therefore, to minimise this offset their average can be taken:

$$b = \frac{b_1+b_2}{2}. \quad (8)$$

Based on this process setting up procedure, it would be possible to execute a sequence of steps to produce an array of holes, i.e.:

- Producing the array of holes with coordinates (X, Y, z_l) on the first side by using a pre-defined number of pulses necessary to reach the saturation point or workpiece mid plane;
- Rotation by $180^\circ + \Delta\theta$ around the A_{MCS} axis to set the second side of the workpiece and thus to continue the drilling operation and also to compensate any rotational errors;

- Positioning the workpiece at z_2 along the Z_{MCS} axis to compensate any radial errors as a result of the rotation and any displacements between the centres of rotation and the workpiece (see Figure 3.3) and thus to set the focal plane of the workpiece on the second side within the laser beam depth of focus;
- By using the calculations of Eq. (3), (4) and (8), the X_{new} and Y_{new} coordinates of each hole on the workpiece's second side are determined as follows:

$$X_{new} = \frac{X(1 - \tan^2(\Delta\gamma)) + 2 \cdot \tan(\Delta\gamma) \cdot (Y - b)}{\tan^2(\Delta\gamma) + 1} + \Delta X_A, \quad (9)$$

$$Y_{new} = \frac{2(\tan(\Delta\gamma) \cdot X + b) - Y(1 - \tan^2(\Delta\gamma))}{\tan^2(\Delta\gamma) + 1}. \quad (10)$$

By applying Eq. (9) and (10), the axial rotational error (ΔX_A) and angular displacement between the X_{MCS} and A_{MCS} axes ($\Delta\gamma$) are compensated. Also, the position of the A_{MCS} axis in MCS is determined and thus the radial rotational error in the Y_{MCS} direction is also compensated.

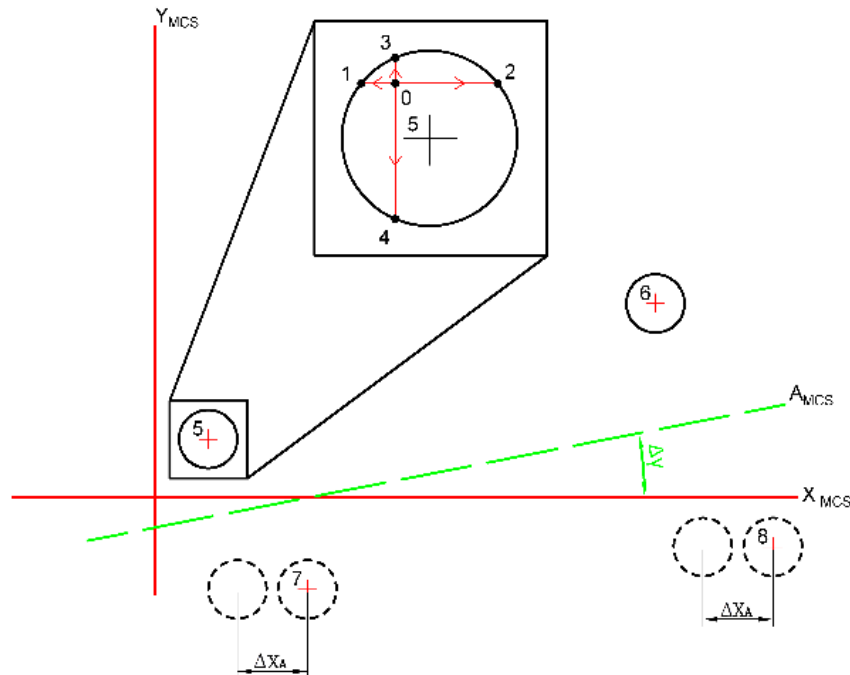


Figure 3.4. The setting up procedure for determining initial coordinates of two through holes centres (Points 5, 6) and their corresponding coordinates (points 7, 8 respectively) after a rotation by 180°

3.3.4. In-situ, on-machine inspection methodology

It is necessary to implement in-situ, on-machine monitoring and inspection methods within the laser processing setup without moving the workpiece as outlined in Section 3.3.2.4. In particular, the workpiece can be positioned in the field of view of the 3D metrology sensor by employing the C, X, Y and Z mechanical stages of the laser processing setup and thus to carry out in-situ inspection routines on both sides of the workpiece. As the 3D sensor is integrated in the laser processing setup, the alignment accuracy between pairs of holes on two opposite sides of the workpiece can be assessed by using as references through features, e.g. through holes, in the sensor coordinate system (SCS). In this way, the combined uncertainty can be minimised as both the reference features and the through micro holes are within one field of view of the sensor. The in-situ, on-machine inspection procedure to assess the alignment accuracy of the proposed drilling method includes the following steps:

- 1) Laser drilling of a reference through feature from one-side, e.g. a 500 μm circular hole but through structures with other cross-sections can be used, too;
- 2) Percussion drilling a through micro hole employing the two-side drilling operation;
- 3) Positioning the reference and micro holes within the sensor field of view using the mechanical axes as shown in Figure 3.5a;
- 4) Finding the coordinates (X_9, Y_9) and (X_{10}, Y_{10}) of the reference and micro holes' centres in the SCS, i.e. Points 9 and 10, respectively;
- 5) Rotating the sample by 180° with the rotary stage and repeating Steps 3 and 4 to find the coordinates (X_{11}, Y_{11}) and (X_{12}, Y_{12}) of the two holes on the second side in SCS, i.e. Points 11 and 12 in Figure 3.5b.
- 6) Calculating the displacement between the holes on the two sides as follows:

$$\Delta X_{s1} = X_{10} - X_9, \Delta Y_{s1} = Y_{10} - Y_9, \quad (11)$$

$$\Delta X_{s2} = X_{12} - X_{11}, \Delta Y_{s2} = Y_{12} - Y_{11}. \quad (12)$$

If the angular displacement between A_{MCS} and X_{SCS} is $\Delta\theta$, based on Eq. (5), the errors in X and Y directions are:

$$E_X = \Delta X_{s2} - \frac{\Delta X_{s1}(1 - \tan^2(\Delta\theta)) + 2 \tan(\Delta\theta) \cdot \Delta Y_{s1}}{\tan^2(\Delta\theta) + 1}, \quad (13)$$

$$E_Y = \Delta Y_{s2} - \frac{2 \tan(\Delta\theta) \cdot \Delta X_{s1} - \Delta Y_{s1}(1 - \tan^2(\Delta\theta))}{\tan^2(\Delta\theta) + 1}, \quad (14)$$

$$E = \sqrt{E_X^2 + E_Y^2}. \quad (15)$$

$\Delta\theta$ is an important factor affecting the precision of this in-situ alignment assessment method. Therefore, the effects of such angular displacement should be minimised during the integration of the 3D metrology sensor into the laser processing setup. In addition, this displacement can be measured with the optical sensor and hence can be taken into account in Eq. (13) and (14). However, the uncertainty associated with this alignment measurement needs to be included in the uncertainty evaluation of the proposed two-side drilling method. Other limitations of this in-situ inspection method is the finite sensor field of view but it is possible to extend it by stitching fields together employing software tools.

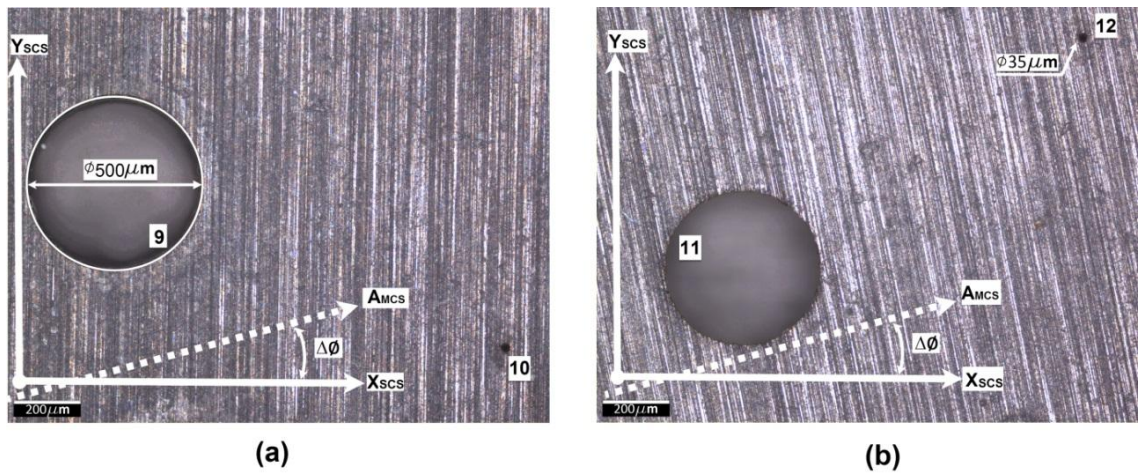


Figure 3.5. In-situ, on-machine inspection method with a 3D metrology sensor: (a) the first side field of view and (b) the second side field of view

It should be stressed that an important advantage of this in-situ inspection method is that the sources of errors discussed in Section 3.3.1 (those associated with the two-side drilling method) do not affect it, too.

3.3.5. In-situ measurement uncertainty

To apply the proposed in-situ measurement, uncertainties associated with this method should be determined. In particular, to determine to what extent it is possible to trust the alignment accuracy results when measuring holes produced using the two-side drilling method. Therefore, the expanded uncertainties associated with the proposed validation procedure have to be assessed. In this research this is carried out based on the BIPM et al. guide for expression of uncertainty in measurements (GUM) [41].

Essential part in determining the uncertainty of a measurement procedure is to identify the sources of errors that affect all its steps, especially to evaluate the uncertainties associated with them. In particular, the use of 3D metrology sensor to assess the alignment accuracy of the holes produced with the two-side drilling method involves a number of steps and the associated uncertainties with them have to be considered, i.e.:

U1. and U2. The uncertainty in measuring the micro holes' centres on two opposite sides of the workpiece.

U3. The uncertainty in measuring the reference through structure, e.g. the through hole used in this research, on the first side of the sample.

U4. The uncertainty in measuring the reference hole on the second side of the sample. It is calculated as U_3 , however since the reference hole is laser drilled from the first side, the edge definition and quality of its entrance and exit will differ. Hence, the uncertainties in determining the coordinates of their centres should be considered separately.

U5. The uncertainty associated with the use of a through hole to correlate SCSs on the two sides. Since the through holes are laser drilled, they will have a taper angle that can result in some variations of their centres on its entrance and exit sides. This can affect directly the precision of the alignment procedure and thus increases its uncertainty. Therefore, it is necessary to assess it, too.

U6. Uncertainty of detecting the angular displacement between the A_{MCS} and X_{SCS} axes which should be transformed into a lateral uncertainty to calculate the expanded uncertainty.

All of the above uncertainties are evaluated as type A, i.e. they should be calculated by using statistical methods. In addition, one type B is considered, i.e.:

U7. The resolution of the C stage. If the C stage is used to position the workpiece in the sensor field of view, the uncertainty associated with this rotation should be considered. In particular, the resolution of the rotary stage affects $\Delta\theta$.

3.4. Experimental validation

3.4.1. Material

The automated two-side drilling operation can be used for any material that can be processed by a given laser source. In this research it is validated on silicon nitride (Si_3N_4) substrates. This material has a wide application in microelectronic and microelectromechanical systems because of its properties such as insulation capabilities and its resistance in high-energy manufacturing processes [42].

The thickness of the silicon nitride substrate used in this research was 250 μm and the surface roughness of the sample was measured with a focus variation microscope (Alicona G5), i.e. S_a of its two sides was 220 nm.

3.4.2. Equipment

The automated two-side drilling operation was validated on a laser micro processing platform that integrates the following key component technologies:

- 5 W Yb-doped sub-pico laser source with wavelength of 1030 nm, pulse duration of 310 fs, frequency up to 500 kHz and beam quality factor M^2 better than 1.3;
- A telecentric lens with 100 mm focal length exchangeable with a drilling/cutting head that integrates a 50 mm focusing lens as shown in Figure 3.6b;
- High precision X and Y mechanical stages with linear motors for positioning the workpiece with a resolution of 250 nm and repeatability of $\pm 0.75 \mu\text{m}$;
- Two rotary stages to position the workpiece around the X axis (A) and the Z axis (C) with resolution and repeatability of $3.15 \mu\text{rad}$ and $\pm 19.4 \mu\text{rad}$, respectively. The A axis is a key component for implementing the proposed two-sides drilling method;

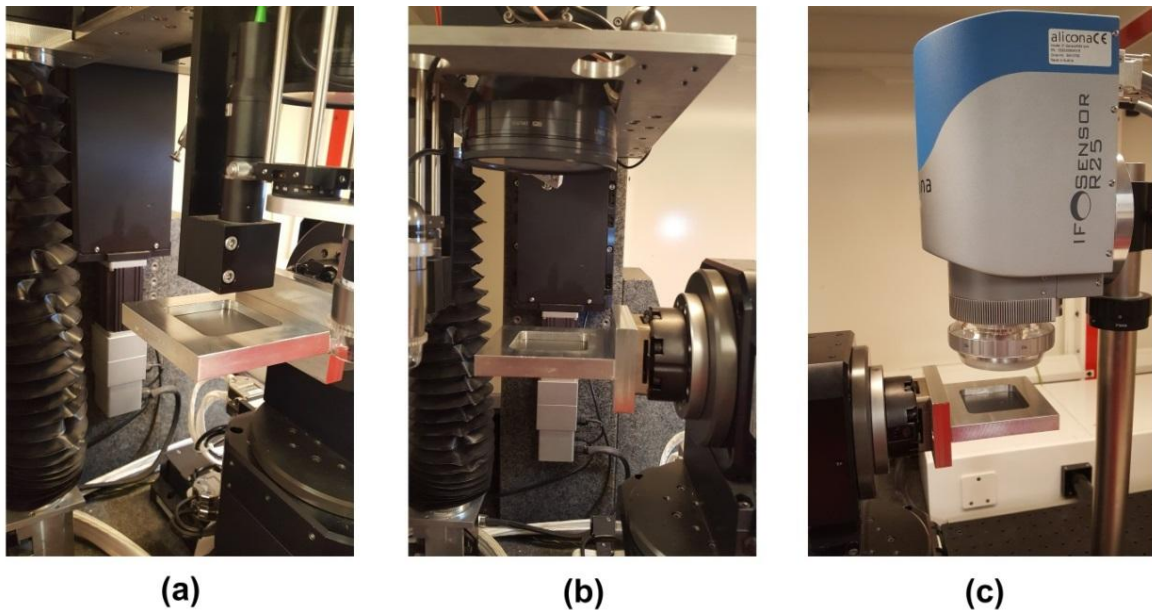


Figure 3.6. Three views of the used laser processing setup: (a) confocal sensor; (b) the focusing lens together with the stack of mechanical stages; (c) the R25 sensor

- A chromatic confocal probe [43] for executing the automated process setting up procedure described in Section 3.3.3. The probe axial resolution is 130 nm with spot radius of 3.6 μm and measuring range of 4 mm (Figure 3.6a);
- An integrated focus variation probe, i.e. Alicona IF-Sensor R25, with a 10 \times objective lens that has: field of view of 2 x 2 mm, a working distance of 15.5 mm, a vertical resolution of 100 nm and sampling distance of 1 μm (Figure 3.6c);
- A specially designed modular workholding device to provide a laser beam access to both sides of a workpiece as depicted in Figure 3.6. As it is shown in the Figure 3.7, the device includes an adapter and spacers and thus the laser processing setup can accommodate workpieces with different sizes and thicknesses.

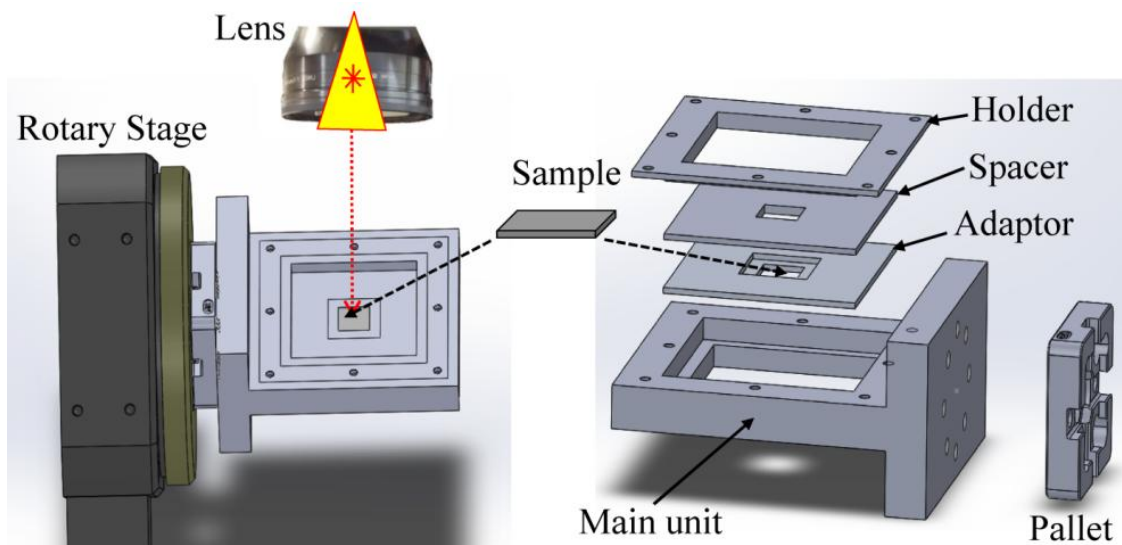


Figure 3.7. The specially designed modular work holding device

3.4.3. Percussion drilling

As stated in Section 3.3.2.4 to setup the process it is necessary to determine the optimum pulse number after which the penetration rate decreases substantially. To do so, arrays of blind holes with a varying number of pulses was produced and their depth measured. The other laser parameter settings that affected the penetration depth were the pulse frequency

and energy. They were selected based on the results reported by other researchers [44-47] and also the author's experience with the laser source used in this research. In particular, the following laser settings were selected, pulse frequency of 100 kHz and average power 0.68 W. The focal plane was kept at the substrate surface to drill arrays of blind holes.

The depth of the produced blind holes was measured employing X-ray computed tomography (XCT), a Zeiss XRADIA Versa XRM-500 system. The acceleration voltage was set to 50 kV, with a current of 79 μ A. The exposure time of each projection was 1750 ms. The projection image of 1013 by 1013 pixels is described with a 16 bit grey level. A geometric magnification of 3.35 was achieved, and combined with the optical magnification of 4 yielded to a projected pixel size of 2 μ m, using a pixel binning of 2. The volume was reconstructed over a grid of cubic voxels with a side length of the 2 μ m. The data set generated with the XCT system was analysed in VG studio 3.0, Volume Graphics GmbH Heidelberg Germany. The surface model was created using VG's advanced surface determination, starting from an ISO 50 surface determination.

Two sets of blind holes were drilled. The first set was produced employing the 100 mm telecentric lens with 35 μ m beam spot diameter and the holes' depth as a function of pulse numbers was analysed as shown in Figure 3.8. It can be seen that the "saturation" point was reached after 1000 pulses while the achieved depth was 115 μ m. Considering the silicon nitride substrate thickness of 250 μ m used in this research, this depth was not sufficient to penetrate it even by applying the two-side drilling method. The second set of blind holes was produced using the 50 mm focusing lens with 25 μ m beam diameter and thus a higher fluence was used. A higher depth at the saturation point was achieved, i.e. 150 μ m, after delivering 1600 pulses. These process settings were used to validate the proposed two-side drilling method.

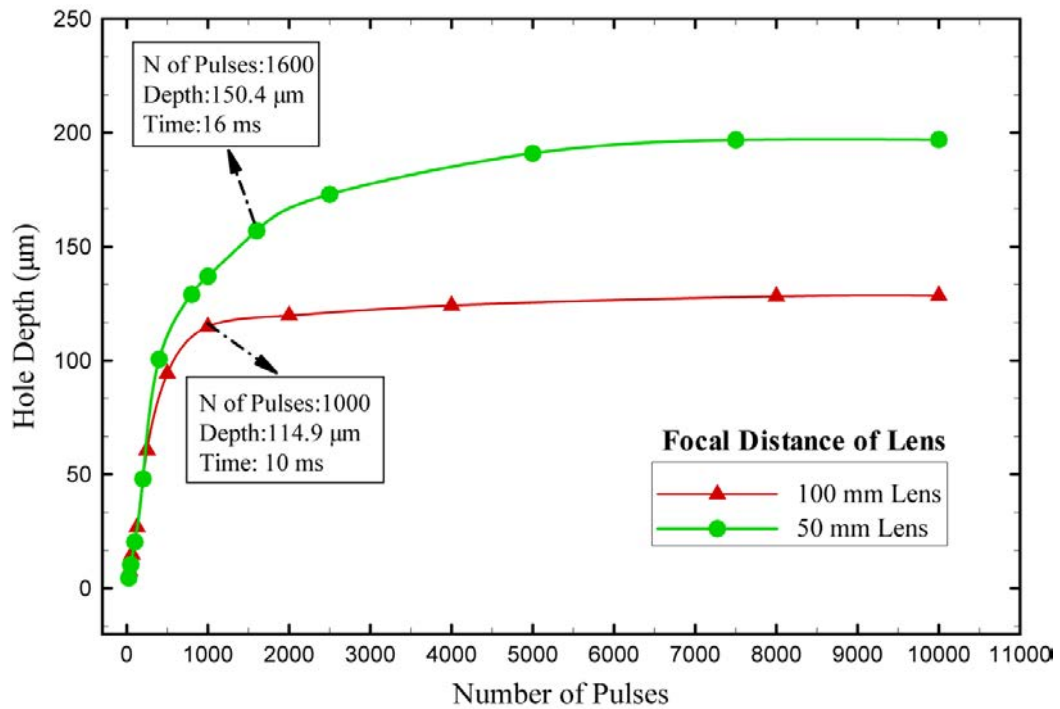


Figure 3.8. Determining the optimum numbers of pulses with two different lenses

3.4.4. Design of experiments

3.4.4.1. *In-situ, on-machine measurement uncertainty*

As was stated in Section 3.3.5, before implementing the proposed in-situ inspection methodology, the uncertainty associated with such measurements needs to be determined. The sources of type A uncertainties were identified and the following experiments were carried out to quantify them:

U1. and *U2.* To determine the uncertainty of measuring micro holes' coordinates in SCS, a single micro hole was produced by laser percussion drilling. The hole was scanned ten times with the R25 sensor and then the standard deviation of its coordinates was calculated.

U3. The uncertainty of measuring the entrance of a reference hole on one side of the sample was determined in the same way as *U1* but a 500 µm diameter through hole produced by laser drilling was used.

U4. The exit side of the reference hole was measured ten times to determine the uncertainty in the same way as *U3*.

U5. To access the uncertainty of correlating the SCSs on the two sides of the sample, 20 through holes were laser drilled as shown in Figure 3.9 and the distances between them were compared on both sides. To minimise the additional uncertainty due to this measurement, it was carried out on the Alicona G5 system with 50× objective lens with higher lateral and vertical resolutions, i.e. 640 nm and 20 nm, respectively.

U6. The angular deviation of the A_{MCS} and X_{SCS} were measured ten times, and their standard uncertainty was computed based on the sensitivity coefficient and probability divisor.

The type A uncertainties, *U1-U6*, have been assumed to be of normal distribution with the divisor of 1; and a degree of freedom (DoF) of $n - 1$, where n is the number of samples. The sensitivity coefficient of the uncertainties has been taken as one, except for *U6* for which the uncertainty of detecting the angular displacement between the A_{MCS} and X_{SCS} axes is a geometric function of the angle and the field of view of the sensor. Given that the angle is small, the sensitivity coefficient for the maximum displacement can be assumed based on the maximum field of view of the sensor.

U7. Given the digital readout of the resolution of the C_{MCS} axis, the probability distribution of the resolution has been assumed to be rectangular, with a divisor of $\sqrt{3}$, and DoF of infinity.

After finding the standard uncertainty of all the steps associated with the proposed in-situ alignment measurement method, its combined uncertainty was calculated using the root-square-sum of the standard uncertainties as follows:

$$U_c = \sqrt{(U1)^2 + (U2)^2 + (U3)^2 + (U4)^2 + (U5)^2 + (U6)^2 + (U7)^2} \quad (16)$$

The effective DoF has been calculated as 41, using the Welch-Satterthwaite formula. This effective DoF yields to a k-factor of 1.93 at a 97% confidence level. Hence the expanded uncertainty, U , can be stated as:

$$U = k \cdot U_c \quad (17)$$

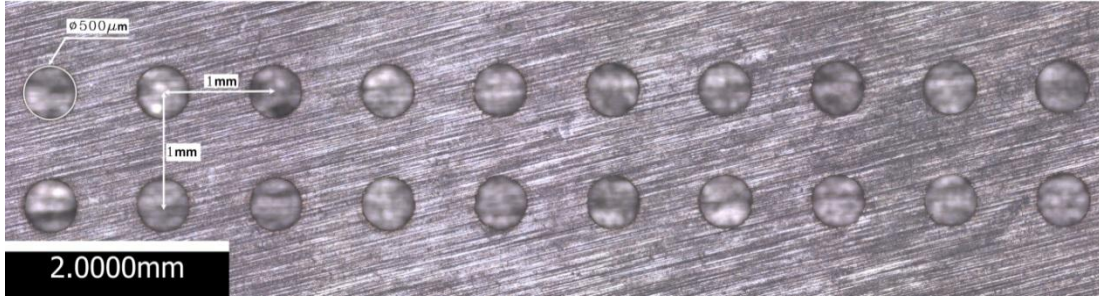


Figure 3.9. The array of holes used to evaluate uncertainty in correlating SCSs on the sample two sides

3.4.4.2. *Hole alignment accuracy*

Considering the measurement uncertainty associated with the proposed in-situ inspection method, it would be possible to verify the alignment accuracy of holes produced employing the two-side drilling method. In particular, 10 pairs of holes were produced on two opposite sides of a sample and their alignment accuracy was measured with the in-situ, on-machine inspection method. The holes' positions were selected in different areas within the working envelope of the laser processing setup and thus to consider the worst-case scenario in assessing the achievable alignment accuracy.

3.4.4.3. *Hole morphology*

Micro holes with different cross-sections were produced by employing both the one-side and the proposed two-side drilling methods. A test sample was designed, as shown in Figure 3.10, to compare their capabilities. It includes 4 arrays of holes:

Array A: The holes in each row were produced employing percussion drilling from one side with the laser settings selected in Section 3.4.3. The only difference between the rows was the number of pulses used as stated in Figure 3.10.

Array B: The same as Array A but percussion drilling from two sides was employed. Again, the pulse numbers were varied to see how the holes evolved before and after reaching the substrate depth with 1600 pulses.

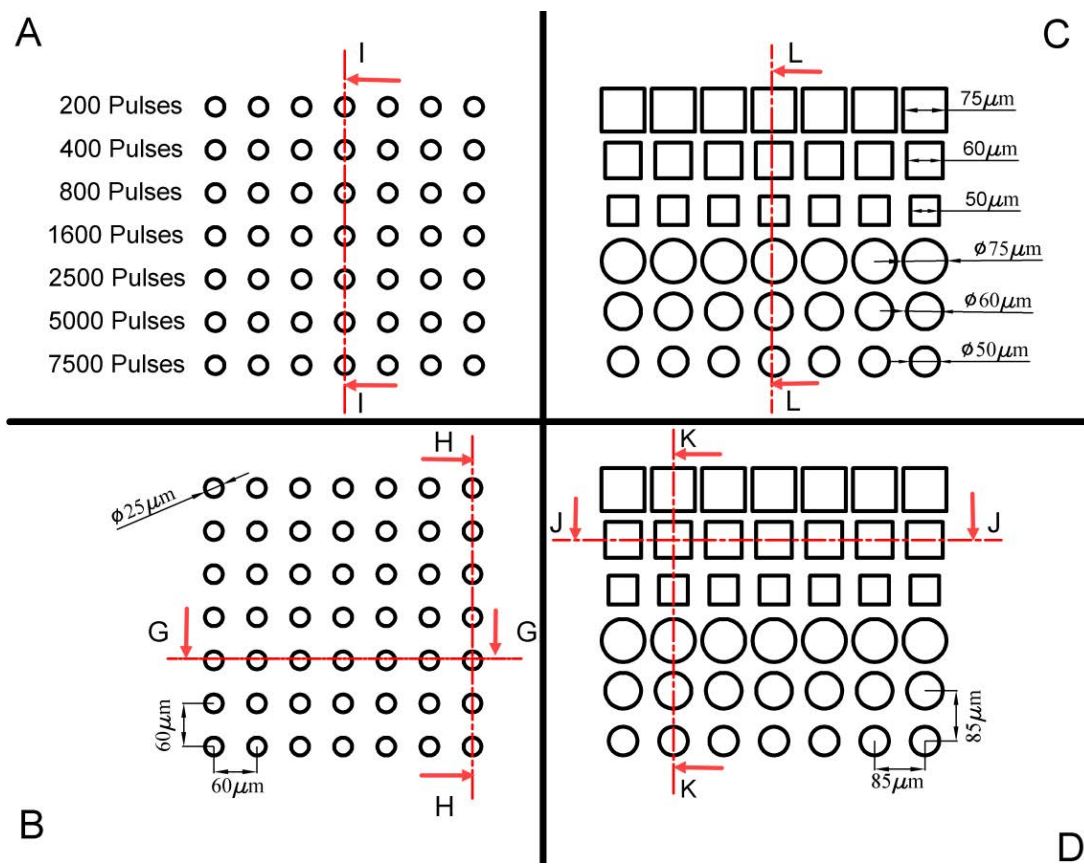


Figure 3.10. The test sample designed to compare one- and two-side drilling methods

Array C: Holes with nominal square and circular cross-sections were produced employing a helical drilling strategy that involved layer based hatching with the laser beam by changing the hatching direction 45° at each layer. The hatching distance was set on $4\ \mu\text{m}$ and the hole edges were outlined at each layer. By using this strategy the holes on one side were

drilled using again the laser settings selected in Section 3.4.3. The holes in each row are identical and the sizes and cross-sections were varied as shown in Figure 3.10.

Array D: The same as Array C but produced employing the two-side processing method.

All four holes' arrays were measured with the XCT system and the hole sizes and shapes in different cross sections were compared.

3.5. Results and discussion

3.5.1. In-situ, on-machine measurement uncertainty

The different sources of uncertainty were assessed experimentally as described in Section 3.3.4.2 and thus to calculate the expanded uncertainty associated with the proposed in-situ inspection method. The results are provided in Table 3.1. It can be seen that the greatest uncertainty contribution was U6 which depends on both the lateral and vertical resolutions of the R25 sensor. To minimise U6 the R25 resolution can be increased by using higher magnification objectives but this will reduce the sensor field of view. As a consequence, it may be required to “stitch” fields with the associated uncertainty with this and also the time necessary to execute in-situ, on-machine inspection routines will increase. U1 to U5 are directly dependent on the geometrical accuracy of the laser drilled holes and their edge definition. For example, it is clear from the values of U3 and U4 that the edge definition of the reference hole entrance is worse than its exit due to the laser drilling side effects. Hence, the contributions of U1 to U5 can be reduced by optimising further the laser drilling settings. The expanded uncertainty calculated using Eq. (16) and (17) is 0.9 μm with a confidence level of 97%. This is in line with the requirements stated in Section 3.3.2.4, i.e. the uncertainty associated with the proposed in-situ measurement routines to be within a fifth of required positional accuracy of the drilled holes (in the range from 5 to 10 μm).

Table 3.1. The uncertainty budgets allocated to different error sources in performing in-situ, on-machine alignment measurements

	Uncertainty source	Standard uncertainty (μm)
U1	Measuring the microhole center in SCS	0.129
U2	Measuring the microhole center in SCS, second side	0.129
U3	Measuring the reference hole entrance in SCS	0.211
U4	Measuring the reference hole exit in SCS	0.096
U5	Correlating SCSs on the two sides	0.225
U6	Detecting the angular displacement between the A_{MCS} and X_{SCS} axes	0.285
U7	Resolution of the C_{MCS} axis	0.005
UC	Combined standard uncertainty	0.467
U	Expanded uncertainty (97% confidence level)	0.904

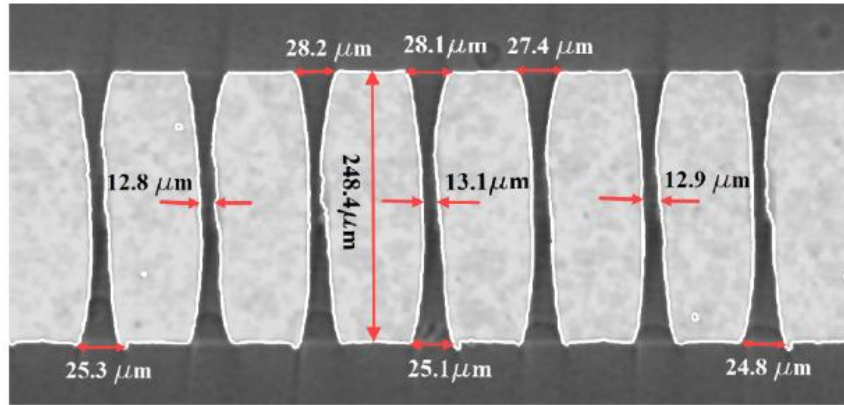
3.5.2. Hole alignment accuracy

The statistical results obtained by using R25 sensor to assess the alignment accuracy of 10 pair of holes with the proposed in-situ, on-machine measurement method are: Min: 1.22 μm , Max: 8.33 μm , Average: 4.46 μm and Standard Deviation: 2.52 μm . These variations in the achieved alignment accuracy are mainly due to errors associated with the edge detection by using the chromatic confocal sensor and can be minimised by optimising the laser parameter setting for producing the through reference holes and by choosing a chromatic confocal sensor with a higher resolution. However, there are trade-offs as a higher resolution sensors entail shorter working distances and hence impact on the flexibility of the alignment procedure and increase the possibilities for collisions. Another reason for these variations is the resolution and repeatability of mechanical stages that can be improved by selecting stages with higher resolution and/or precision.

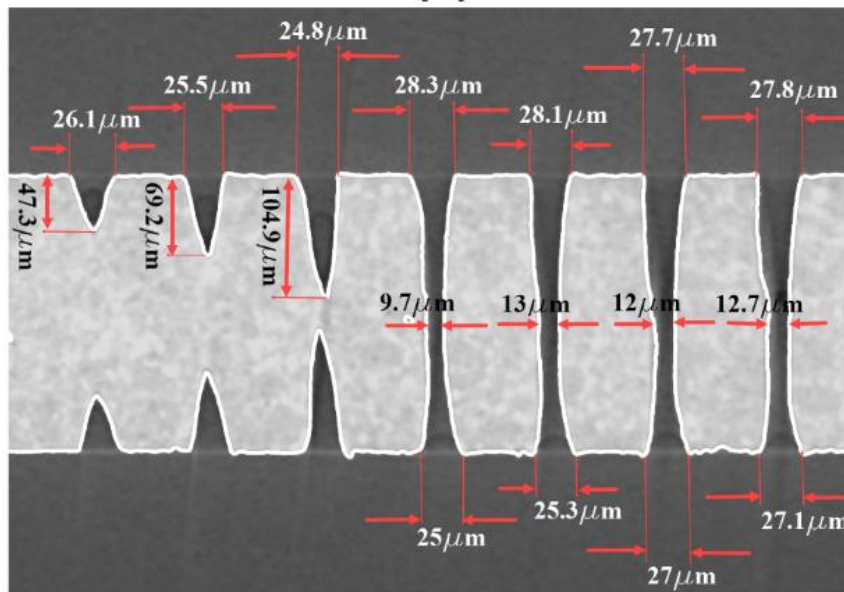
Taking into account the measurement uncertainty, it can be stated that the misalignment between the entrances and exits of through holes produced with the proposed two-side laser drilling method is better than $(8.3 \pm 0.9) \mu\text{m}$.

3.5.3. Hole morphology

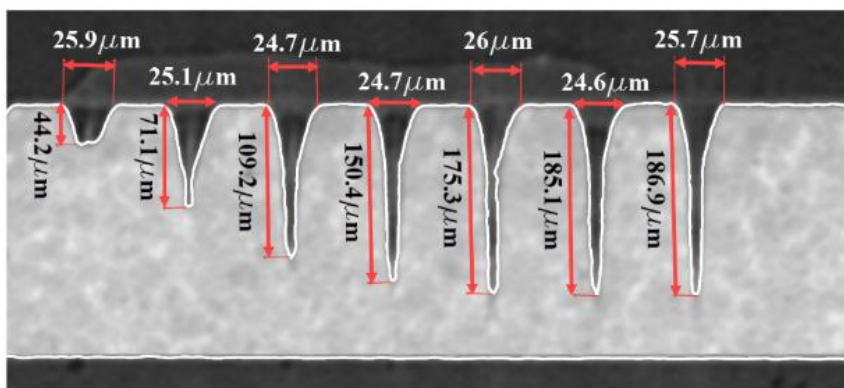
The hole morphology was analysed with the XCT system. The cross sections of hole arrays (see Figure 3.10) produced by percussion drilling are shown in Figure 3.11. The evolution of the holes and the way the pairs of holes meet when the two-side drilling method is applied are shown in Figure 3.11b. It can be seen that the entrance and exit holes' diameters are approximately identical. Comparing the results in Figure 3.11c it is apparent that the through holes that were not possible to produce with the one-side method were drilled successfully with the proposed two-side method. In addition, as can be seen in Figure 3.11a good repeatability can be achieved in producing holes with 2500 pulses employing the two-side method. The evolutions of holes' diameters with the increase of pulse numbers are shown in Figure 3.12 and Figure 3.13 for one- and two-side drilling methods, respectively. There are only marginal differences in the morphology of the holes drilled with 5000 and 7500 pulses from one-side, which shows again that the saturation point is already reached at these pulse numbers. Considering the holes' evolution in the two-side drilling method, 200, 400 and 800 pulses were not sufficient to penetrate the sample while at 1600 pulses the hole shape has started to emerge and then to arrive at the final shape of the holes at 2500 pulses. A further increase of pulse number, i.e. 5000 and 7500 pulses, leads to only marginal changes, i.e. a slight increase of exit diameter while the necking diameter decreases. Thus, the results are quite conclusive in regards to the optimum number of pulses necessary to produce through holes in the 250 μm silicon nitride substrate with the two-side drilling method.



(a)



(b)



(c)

Figure 3.11. Holes' cross-sections generated using the XCT system: (a) section G-G of holes' array B produced by two-side drilling with 2500 pulses; (b) section H-H of holes' array B produced by two-side drilling with pulse numbers of 200, 400, 800, 1600, 2500, 5000 and 7500; (c) section I-I of holes' array A produced by one-side drilling with pulse numbers of 200, 400, 800, 1600, 2500, 5000 and 7500.

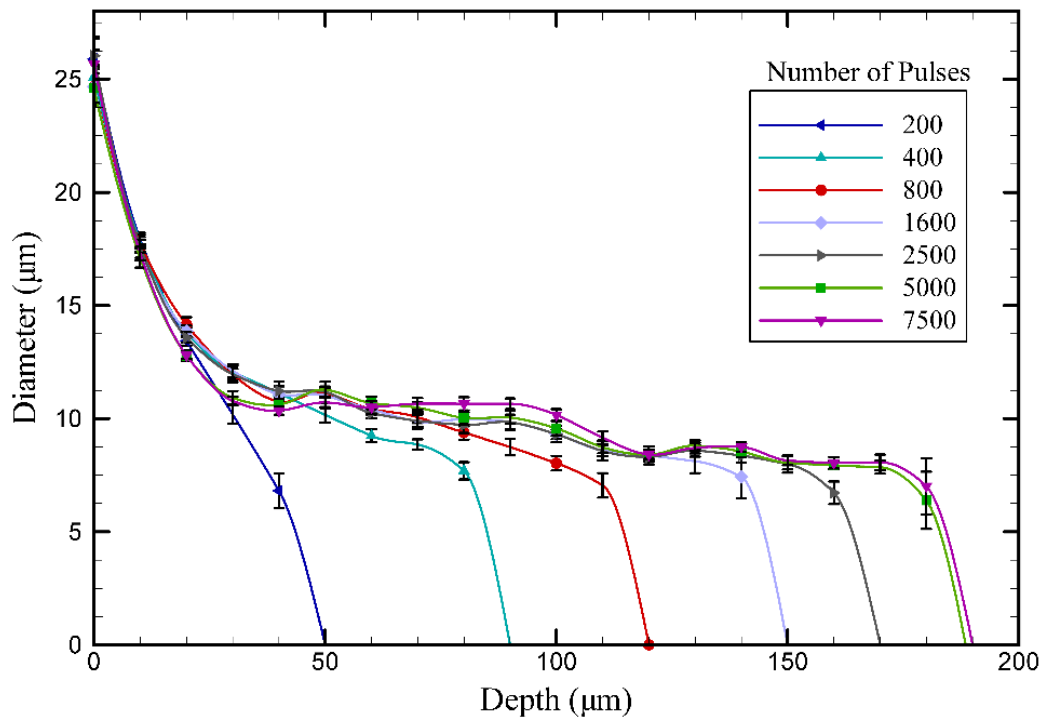


Figure 3.12. Morphology analysis of holes produced employing one-side percussion drilling with different pulse numbers

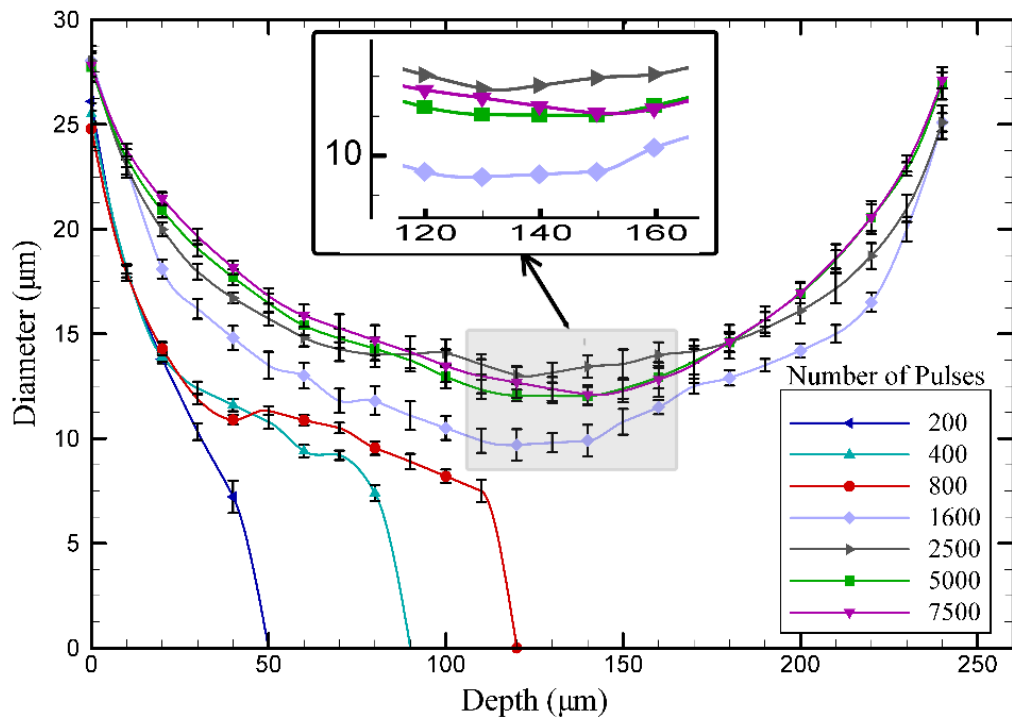
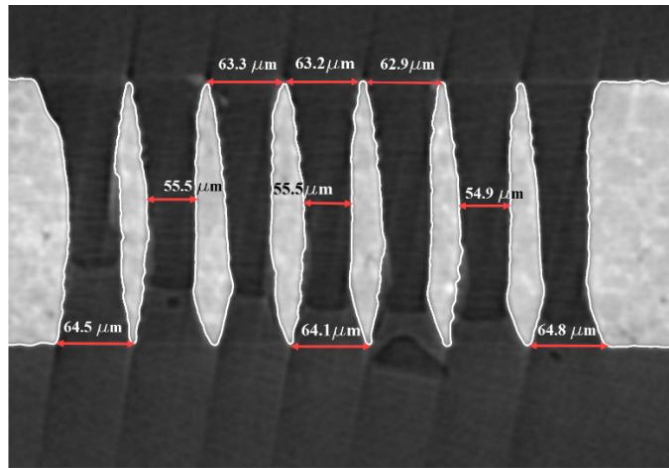


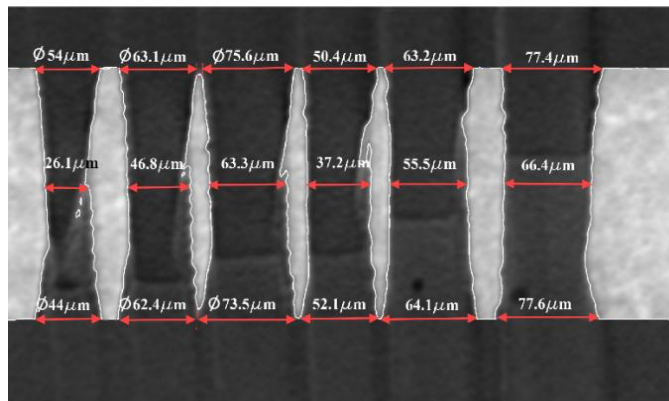
Figure 3.13. Morphology analysis of holes produced employing two-side percussion drilling with different pulse numbers

The holes' cross sections of arrays C and D (see Figure 3.10) resulting from the use of a different drilling strategy from one- and two sides are depicted in Figure 3.14. Again good repeatability is achieved with the two-side drill method in producing 60 μm rectangular holes (Figure 3.14a). The tapering effect in drilling the holes from one-side is very pronounced in Figure 3.14c while it is almost negligible in the two-side approach (Figure 3.14b). The evolutions of holes' sizes with the increase of pulse numbers in both drilling approaches provided in Figure 3.15 and Figure 3.16 also shows clearly the resulting differences in regards to the tapering effects.

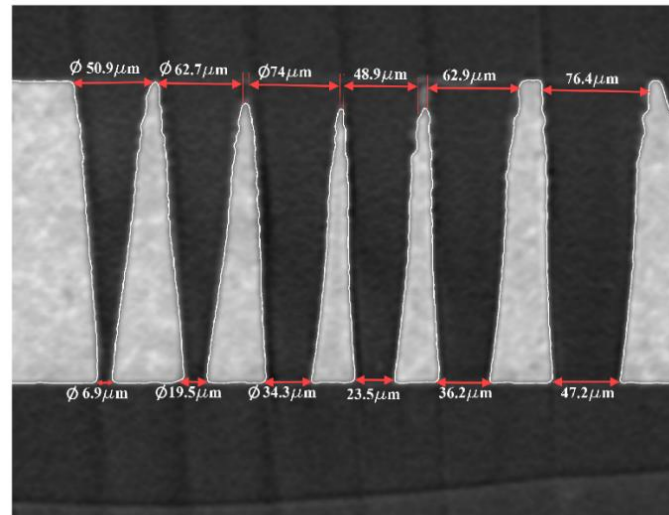
In addition, the deviations from holes' geometrical accuracy in both drilling methods, i.e. roundness and tapering angle in producing 75 μm holes, are depicted in Figure 3.17. Although the outer hole diameter is bigger when the two-side drilling is used, the average circularity of the holes is still better. For example, the roundness deviation of the three cross sections shown in Figure 3.17 decreased when the two-side approach was used while the holes' profile was much closer to the circular shape in all three cross-sections. The circularity of the holes' exits is almost the same for two-side and one-side drilling (8.5 μm and 8.9 μm respectively), however holes' diameters and profiles are quite different and only in the two-side drilling method are close to the hole target size and form, i.e. cylindricity.



(a)



(b)



(c)

Figure 3.14. Holes' cross-sections generated using the XCT system: (a) section J-J of 60 μm square holes (Array D) produced by two-side drilling; (b) section K-K of square and circular holes with different dimensions (Array D) produced by two-side drilling; (c) section L-L of square and circular holes with different dimensions (Array C) produced by one-side drilling

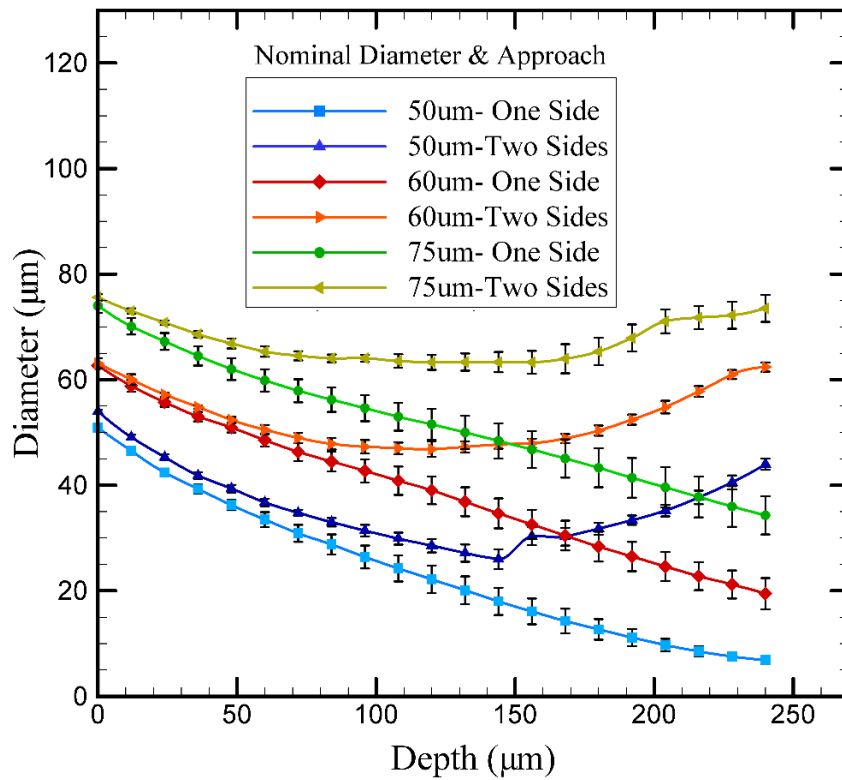


Figure 3.15. Morphology analysis of circular holes (arrays C and D) produced employing one- and two-side drilling

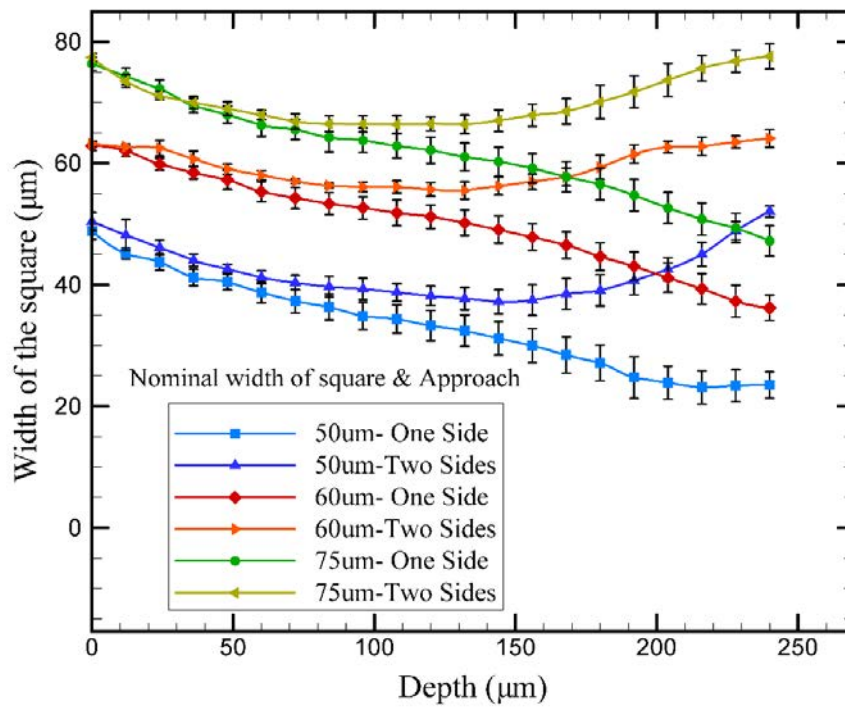


Figure 3.16. Morphology analysis of square holes (Arrays C and D) produced employing one- and two-side drilling

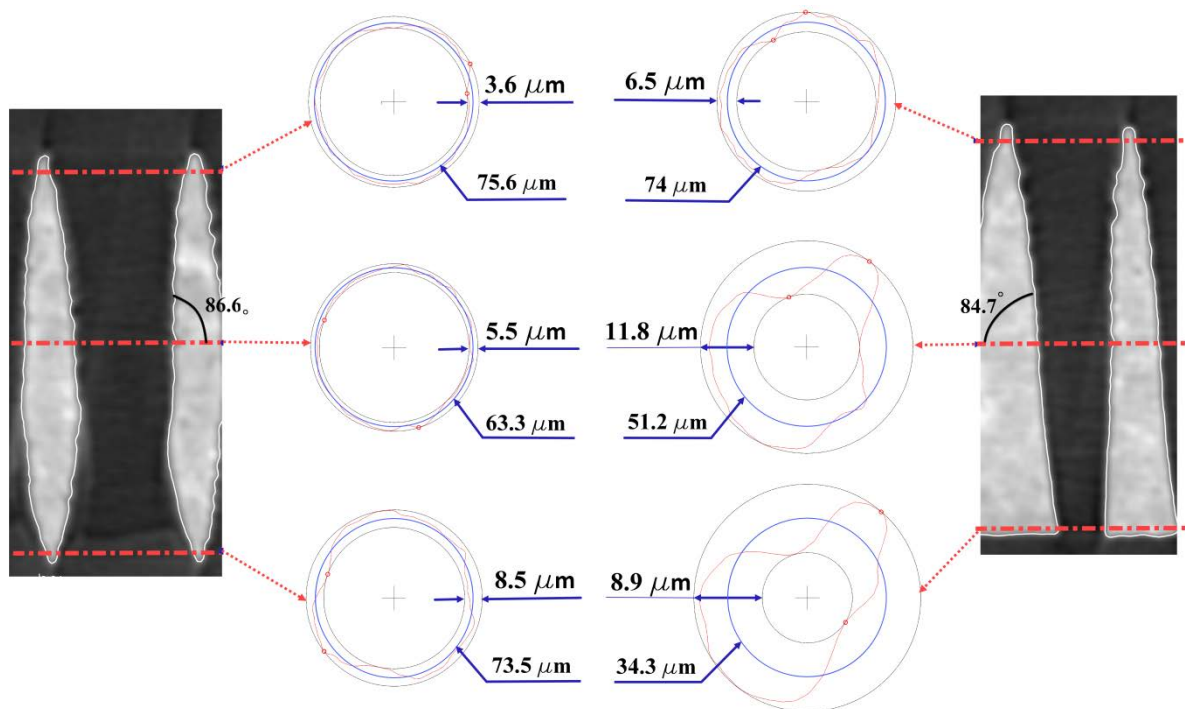


Figure 3.17. Roundness and tapering angles of 75 μm circular holes (arrays C and D) produced by one- and two-side drilling

3.6. Conclusion

In this paper, a new two-side drilling method is proposed. A pilot two-side laser processing setup was designed and for its implementation the following enabling tools and technologies were developed and validated:

- A specially designed laser processing setup that integrates two rotary and three linear mechanical stages together with a modular workpiece holding device to ensure the required motion control, accuracy and repeatability in executing two-side laser processing routines;
- System level tools for fully automated process setting up that allow errors from various sources to be compensated and thus to minimise their impact on achievable accuracy and repeatability in two-side laser processing;

- A fully automated laser processing method for drilling holes with high alignment accuracy and repeatability from two opposite sides;
- A method for fully automated correlation of working coordinate systems in two-side laser processing;
- In-situ, on-machine inspection method for verifying the alignment accuracy achievable with the proposed two-side laser processing method.

The new two-side drilling method was validated experimentally and the following conclusions can be made based on the obtained results.

- The achievable alignment accuracy of through holes with different cross-sections produced with the proposed two-side drilling method is better than 10 μm . It is important to note that this accuracy can be improved by optimising the laser parameter settings and also by employing a higher accuracy and resolution stages and sensors for process setting up.
- Micro holes with very good repeatability and dimensional and geometrical accuracy were produced by two-side drilling that cannot be achieved employing one-side drilling.
- The achievable aspect ratios can be more than doubled in comparison with the one-side drilling method while improving the holes' dimensional and geometrical accuracy.

In addition, it is worth mentioning the application area of the proposed method can be broaden to two-side drilling of workpiece with not parallel surfaces, e.g. for drilling intersecting holes and micro channels inside components for fluid flow and heat exchange applications.

Acknowledgments

The research reported in this paper was supported by Korea Institute for Advancement of Technology (KIAT), i.e. the project on “Laser Machining of Ceramic Interface Cards for 3D wafer bumps”, European Commission H2020 FoF programme, i.e. the project on “Modular laser based additive manufacturing platform for large scale industrial applications” (MAESTRO), and the Engineering and Physical Sciences Research Council (EPSRC Grants EP/M008983/1 and EP/L01534X/1). The authors would like to thank Alicona Imaging GmbH for their support and advice in implementing the in-situ measurement method reported in this paper and also to acknowledge the contribution of Martin Corfield in carrying out the XCT measurements.

References

- [1] T. Özel, Editorial: Special section on micromanufacturing processes and applications, *Materials and Manufacturing Processes*, 24 (2009) 1235-1235.
- [2] S.Z. Chavoshi, X. Luo, Hybrid micro-machining processes: A review, *Precision Engineering*, 41 (2015) 1-23.
- [3] X. Luo, K. Cheng, D. Webb, F. Wardle, Design of ultraprecision machine tools with applications to manufacture of miniature and micro components, *Journal of Materials Processing Technology*, 167 (2005) 515-528.
- [4] S.P. Leo Kumar, J. Jerald, S. Kumanan, R. Prabakaran, A review on current research aspects in tool-based micromachining processes, *Materials and Manufacturing Processes*, 29 (2014) 1291-1337.
- [5] A.M.A. Al-Ahmari, M.S. Rasheed, M.K. Mohammed, T. Saleh, A Hybrid Machining Process Combining Micro-EDM and Laser Beam Machining of Nickel-Titanium-Based Shape Memory Alloy, *Materials and Manufacturing Processes*, 31 (2016) 447-455.
- [6] C.R. Dandekar, Y.C. Shin, J. Barnes, Machinability improvement of titanium alloy (Ti-6Al-4V) via LAM and hybrid machining, *International Journal of Machine Tools and Manufacture*, 50 (2010) 174-182.
- [7] B. Adelman, R. Hellmann, Rapid micro hole laser drilling in ceramic substrates using single mode fiber laser, *Journal of Materials Processing Technology*, 221 (2015) 80-86.
- [8] W.C. Choi, J.Y. Ryu, Fabrication of a guide block for measuring a device with fine pitch area-arrayed solder bumps, *Microsyst Technol*, 18 (2012) 333-339.
- [9] N. Watanabe, M. Suzuki, K. Kawano, M. Eto, M. Aoyagi, Fabrication of a membrane probe card using transparent film for three-dimensional integrated circuit testing, *Jpn. J. Appl. Phys.*, 53 (2014) 06JM06.
- [10] W.C. Choi, J.Y. Ryu, A MEMS guide plate for a high temperature testing of a wafer level packaged die wafer, *Microsyst Technol*, 17 (2011) 143-148.
- [11] H. Huang, L.-M. Yang, J. Liu, Micro-hole drilling and cutting using femtosecond fiber laser, *Optical Engineering*, 53 (2014) 051513.
- [12] H.S. Lim, Y.S. Wong, M. Rahman, M.K. Edwin Lee, A study on the machining of high-aspect ratio micro-structures using micro-EDM, *Journal of Materials Processing Technology*, 140 (2003) 318-325.
- [13] X.C. Wang, H.Y. Zheng, P.L. Chu, J.L. Tan, K.M. Teh, T. Liu, B.C.Y. Ang, G.H. Tay, Femtosecond laser drilling of alumina ceramic substrates, *Applied Physics a-Materials Science & Processing*, 101 (2010) 271-278.
- [14] A.H. Khan, S. Celotto, L. Tunna, W. O'Neill, C.J. Sutcliffe, Influence of microsupersonic gas jets on nanosecond laser percussion drilling, *Optics and Lasers in Engineering*, 45 (2007) 709-718.
- [15] A.H. Khan, W. O'Neill, L. Tunna, C.J. Sutcliffe, Numerical analysis of gas-dynamic instabilities during the laser drilling process, *Optics and Lasers in Engineering*, 44 (2006) 826-841.
- [16] J.C. Hsu, W.Y. Lin, Y.J. Chang, C.C. Ho, C.L. Kuo, Continuous-wave laser drilling assisted by intermittent gas jets, *International Journal of Advanced Manufacturing Technology*, 79 (2015) 449-459.
- [17] C.C. Ho, Y.M. Chen, J.C. Hsu, Y.J. Chang, C.L. Kuo, Characteristics of the effect of swirling gas jet assisted laser percussion drilling based on machine vision, *Journal of Laser Applications*, 27 (2015) 042001.

- [18] Q.K. Li, Q.D. Chen, L.G. Niu, Y.H. Yu, L. Wang, Y.L. Sun, H.B. Sun, Sapphire-Based Dammann Gratings for UV Beam Splitting, *IEEE Photonics Journal*, 8 (2016).
- [19] S. Juodkazis, K. Nishimura, S. Tanaka, H. Misawa, E.G. Gamaly, B. Luther-Davies, L. Hallo, P. Nicolai, V.T. Tikhonchuk, Laser-Induced Microexplosion Confined in the Bulk of a Sapphire Crystal: Evidence of Multimegabar Pressures, *Physical Review Letters*, 96 (2006) 166101.
- [20] G. Lott, N. Falletto, P.J. Devilder, R. Kling, Optimizing the processing of sapphire with ultrashort laser pulses, *Journal of Laser Applications*, 28 (2016) 022206.
- [21] H. Zhang, J. Di, M. Zhou, Y. Yan, R. Wang, An investigation on the hole quality during picosecond laser helical drilling of stainless steel 304, *Applied Physics a-Materials Science & Processing*, 119 (2015) 745-752.
- [22] Y. Zhang, Y. Wang, J. Zhang, Y. Liu, X. Yang, Q. Zhang, Micromachining features of TiC ceramic by femtosecond pulsed laser, *Ceram. Int.*, 41 (2015) 6525-6533.
- [23] V.N. Tokarev, E.A. Cheshev, V.V. Bezotosnyi, V.Y. Khomich, S.I. Mikolutskiy, N.V. Vasil'yeva, Optimization of plasma effect in laser drilling of high aspect ratio microvias, *Laser Physics*, 25 (2015) 056003.
- [24] P. Penchev, V. Nasrollahi, S. Dimov, Laser micro-machining method for producing high aspect ratio features, 11th International Conference on Micro Manufacturing ICOMM, Orange County, California, USA, 2016, pp. 37.
- [25] V. Nasrollahi, P. Penchev, S. Dimov, A new laser drilling method for producing high aspect ratio micro through holes, 4M/IWMF Conference, Lyngby, Denmark, 2016, pp. 741.
- [26] P. Penchev, X. Shang, S. Dimov, M. Lancaster, Novel Manufacturing Route for Scale Up Production of Terahertz Technology Devices, *Journal of Micro and Nano-Manufacturing*, 4 (2016) 021002-021002.
- [27] K. Goya, T. Itoh, A. Seki, K. Watanabe, Efficient deep-hole drilling by a femtosecond, 400 nm second harmonic Ti:Sapphire laser for a fiber optic in-line/pico-liter spectrometer, *Sensors and Actuators B-Chemical*, 210 (2015) 685-691.
- [28] T.L. VanderWert, Laser processing aircraft and turbine engine parts, *SAE Techni. Paper.*, (1993).
- [29] Sivarao, S. Thiru, K. Jusoff, M. Yusoff, J. SahayaAnand, T. Qumrul Ahsan, Baharudin, A. Shaaban, M. Razali Muhamad, A. Abdullah, N. Izan, A. Hambali, RajaIzam, Taufik, M. Hadzley, M. Amran, W. Hasrulnizzam, M. Shahir, M. Amri, M. Warikh, M. Rizal, D. Sivakumar, C.F. Tan, A. Abdullah, Establishing a hybrid laser lathing technology, *World Appl. Sci. J.*, 21 (2013) 53-59.
- [30] J.L. Ocaña, C. Molpeceres, J.J. Garcia-Ballesteros, S. Lauzurica, D. Iordachescu, Micromachining of 2D-3D structures with high intensity laser pulses, *J. Optoelectron. Adv. Mat.*, 13 (2011) 976-980.
- [31] Y. Kawamura, A. Kai, K. Yoshii, Various kinds of pulsed ultraviolet laser micromachinings using a five axis microstage, *J. Laser Micro Nanoeng.*, 5 (2010) 163-168.
- [32] S.Y. Jin, K.T. Lee, K. Kim, Volumetric error compensation of multi-axis laser machining center for direct patterning of flat panel display, *J Manuf Sci Eng Trans ASME*, 128 (2006) 239-248.
- [33] D. Bhaduri, P. Penchev, S. Dimov, S.L. Soo, An investigation of accuracy, repeatability and reproducibility of laser micromachining systems, *Meas J Int Meas Confed*, 88 (2016) 248-261.
- [34] K. Kim, K. Yoon, J. Suh, J. Lee, Laser scanner stage on-the-fly method for ultrafast and wide area fabrication, 6th International WLT Conference on Lasers in Manufacturing, LiM, Munich, 2011, pp. 455-461.

- [35] P. Penchev, S. Dimov, D. Bhaduri, S.L. Soo, B. Crickboom, Generic software tool for counteracting the dynamics effects of optical beam delivery systems, *Proceedings of the Institution of Mechanical Engineers, Part B: Journal of Engineering Manufacture*, (2015) 1-17.
- [36] P. Penchev, S. Dimov, D. Bhaduri, Experimental investigation of 3D scanheads for laser micro-processing, *Optics & Laser Technology*, 81 (2016) 55-59.
- [37] P. Penchev, S. Dimov, D. Bhaduri, S.L. Soo, Generic integration tools for reconfigurable laser micromachining systems, *Journal of Manufacturing Systems*, 38 (2016) 27-45.
- [38] R. Ramesh, M.A. Mannan, A.N. Poo, Error compensation in machine tools — a review: Part I: geometric, cutting-force induced and fixture-dependent errors, *International Journal of Machine Tools and Manufacture*, 40 (2000) 1235-1256.
- [39] H. Schwenke, W. Knapp, H. Haitjema, A. Weckenmann, R. Schmitt, F. Delbressine, Geometric error measurement and compensation of machines—An update, *CIRP Annals - Manufacturing Technology*, 57 (2008) 660-675.
- [40] R. Schmitt, G. Mallmann, K. Winands, M. Pothen, Inline Process Metrology System for the Control of Laser Surface Structuring Processes, *Physics Procedia*, 39 (2012) 814-822.
- [41] BIPM, IFCC, ISO, IUPAP, IUPAC, IEC, ILAC, OIML, Evaluation of measurement data—Guide to the Expression of Uncertainty in Measurement, Joint Committee for Guides in Metrology. JCGM 100.2008.
- [42] D. Dergez, M. Schneider, A. Bittner, U. Schmid, Mechanical and electrical properties of DC magnetron sputter deposited amorphous silicon nitride thin films, *Thin Solid Films*, 589 (2015) 227-232.
- [43] R. Artigas, Imaging Confocal Microscopy, in: R. Leach (Ed.) *Optical Measurement of Surface Topography*, Springer Berlin Heidelberg, Berlin, Heidelberg, 2011, pp. 237-286.
- [44] C.-N. Chen, J.-J. Huang, Characteristics of thin-film transistors based on silicon nitride passivation by excimer laser direct patterning, *Thin Solid Films*, 529 (2013) 449-453.
- [45] G. Poulain, D. Blanc, A. Focsa, M.D. Vita, B. Semmache, M. Gauthier, Y. Pellegrin, M. Lemiti, Laser Ablation Mechanism Of Silicon Nitride Layers In A Nanosecond UV Regime, *Energy Procedia*, 27 (2012) 516-521.
- [46] C.Y. Ho, J.K. Lu, A closed form solution for laser drilling of silicon nitride and alumina ceramics, *Journal of Materials Processing Technology*, 140 (2003) 260-263.
- [47] P.A. Atanasov, E.D. Eugenieva, N.N. Nedialkov, Laser drilling of silicon nitride and alumina ceramics: A numerical and experimental study, *J. Appl. Phys.*, 89 (2001) 2013-2016.

CHAPTER 4:

Drilling of micron-scale high aspect ratio holes with ultra-short pulsed lasers: critical effects of focusing lenses and fluence on the resulting holes' morphology

Authors Contributions

This chapter of the alternative thesis format is published in the Optics and Lasers in Engineering Journal. I am the first author of this publication. The paper's detail and contributions of co-authors are outlined below. The contents of this chapter address the **key research issue 2**, characterised in section 2.8.

Nasrollahi, V.¹, **Penchev, P.²**, **Jwad, T.³**, **Dimov, S.^{*}**, **Kim, K.^{**}**, and **Im, C.³** (2018), Drilling of micron-scale high aspect ratio holes with ultra-short pulsed lasers: Critical effects of focusing lenses and fluence on the resulting holes' morphology. Optics and Lasers in Engineering, 110, 315-322

¹ **Vahid Nasrollahi**: is the main author and he conceived the ideas of assessing a wide fluence spectrum by employing lenses with different focal distances, designed and executed experiments, performed all necessary characterization and data analysis and wrote the manuscript that was reviewed by the principal supervisor, **Prof. Stefan Dimov (*)** and Dr Kyunghan Kim (**).

² Dr Pavel Penchev contributed with the setting up of the beam delivery system.

³ Dr Tahseen Jwad and Changmin Im contributed in interpretation of obtaining results.

CHAPTER 4 : Drilling of micron-scale high aspect ratio holes with ultra-short pulsed lasers: critical effects of focusing lenses and fluence on the resulting holes' morphology

Abstract

Micro drilling employing ultra-short pulsed lasers is a promising manufacturing technology for producing high aspect ratio holes, particularly on ceramic substrates due to the growing range of application in electronic industry. Controlling the morphology and quality of the holes is an important factor in fulfilling the requirements of such applications. In this research, the effects of a wide fluence spectrum associated with the use of femto-second lasers on achievable aspect ratios were investigated by employing lenses with different focal distances. The holes' morphology and quality were analysed utilising high resolution X-ray tomography (XCT). It was demonstrated that the achievable aspect ratio can be increased from 3 to 25 just by varying the lenses focal distances. In addition, the quality of produced holes in terms of taper angle and cylindricity was investigated and the results showed that the quality would be improved by increasing the fluence and/or decreasing the focal distance. At the same time, the limitations of drilling holes with low focal distance lenses were discussed, i.e. sensitivity to defocusing and increased risks of recast formations inside the holes and bending effects, that should be considered in designing processes for high aspect ratio percussion drilling.

Keywords: Laser microdrilling; hole morphology; high aspect ratio holes; focusing lenses.

4.1. Introduction

The trend toward product miniaturisation and thus for manufacturing micro scale functional features and components demand new tools, methods and also a better understanding of materials' behaviour at such scales [1]. High aspect ratio (depth to diameter ratio) micro holes are common features in products, e.g. the channels for delivering media in micro-electromechanical systems (MEMS), nozzles for diesel fuel injection, cooling channels for turbine blades, drug delivery orifices, etc. [2-4]. Different methods have been used for producing such holes, in particular photo-etching, electro-chemical machining, electro-discharge machining and laser drilling, and their capabilities and limitations have been investigated by researchers [3, 5]. One of these technologies, particularly ultra-short pulsed laser drilling, has attracted a significant interest due to its non-contact nature and efficiency in producing micro-scale holes in almost any material [1]. Another advantage of this method is the possibility to control inner surface topology and thus to tune its properties by generating laser induced periodic surfaces structures (LIPSS). In particular, it is possible to control hydrophobicity of the holes that can be of interest to automotive industry, e.g. to decrease the risk of coking deposition and nozzle clogging [6, 7].

Another important and growing application area for high aspect ratio micro holes is in electronic industry, i.e. interconnecting vias of printed circuit boards and guide blocks of interface probe cards for testing 3D integrated circuits and electronic devices [8-11]. In particular, it is necessary in such applications to produce arrays of holes usually in ceramic substrates with aspect ratios more than 5 while their diameters and pitches are less than 60 μm and taper angle does not exceed 10° . Also, such arrays of holes should fulfil stringent requirements in regards to their accuracy, repeatability and processing speed that introduce further constraints and thus limit the available options for their cost effective manufacture.

Moreover, considering the growing demand for drilling micro holes with diameters down to 10 μm , laser micro drilling is becoming even a more attractive option that potentially can fulfil these requirements.

At the same time, the laser micro drilling process has some limitations, i.e. the achievable aspect ratios, holes tapering, circularity deviations, a heat affected zone (HAZ), spatters, recast formations and micro cracks. They are more pronounced in stationary beam drilling methods such as percussion drilling, compared with lower throughput, moving beam methods like trepanning and helical drilling [12]. To address these issues, for both drilling categories, new methods and tools have been developed, in particular changing the focusing position [8, 13], the use of assisted gases [14-17], beam rotation [18, 19], drilling under water [20], two-side drilling [21, 22], new drilling cycles [12] and also different modelling and optimizing approaches to identify the optimum processing window [23-27]. Furthermore, the effects of process settings were investigated, too, especially peak power and pulse width effects on holes' repeatability in regards to the entry diameters [28] the evolution of shallow craters' diameter and depth in regards to number of pulses (NoP) and fluence [29] and the effect of different laser parameters such as average power on circularity, HAZ and taper angle [30]

Other parameters that affect the laser drilling process, especially pulse energy, fluence and intensity, have been investigated, too. For instance, how the laser intensity at three different wavelength affects the drilling rate [31]. Also, pulse duration effects in the nano-second range and laser intensity on drilling speed was investigated and a conclusion was made that the melt expulsion was the most efficient material removal mechanism in this regime [32]. These three process parameters have an impact on holes' quality, too, especially on their circularity, edge definition and taper angles [33, 34]. However, it should be noted that

these conclusions are predominantly based on analysis of thin plates' surfaces after the drilling operations or just on morphology of shallow dimples. In addition, it should be noted that the maximum achievable depth, holes' aspect ratio and the ways to increase it in ultra-short pulsed drilling have not been studied and this applies to all materials including ceramics.

This research, by employing lenses with different focal distance, reports an investigation into the effects of a wide fluence spectrum in ultra-short percussion drilling on achievable holes' aspect ratio and quality. The morphology of the holes in terms of cylindricity and taper angle was investigated in details by employing a high resolution XCT system. The limitations of using lower focal distance lenses were also analysed, especially their depth of focus, recast formations inside the holes and bending effects that should be considered in designing percussion drilling processes for such lenses.

4.2. Materials and Methods

4.2.1. Experimental and measurement setups

Silicon nitride (Si_3N_4) wafers with a material specification to meet the requirements of a wide range of application in microelectronic and microelectromechanical systems, i.e. resistance in high-energy manufacturing processes and insulation capabilities, were used in the research [35]. The thickness of the substrates was $250\mu\text{m}$ and their surface roughness (S_a) was 220 nm, measured with a focus variation microscope (Alicona G5).

A 5 W Yb-doped sub-pico laser source with pulse duration of 310 fs, beam quality factor (M^2) better than 1.3, 1030 nm wavelength and pulse frequencies up to 500 kHz from Amplitude Systems was used in this research. The beam delivery system includes a quarter-wave plate to obtain a circular polarisation and exchangeable focusing lenses, in particular to use 100, 50 and 20 mm focal distance lenses. To maintain the focal distance with high

accuracy and repeatability, the lens was mounted on a mechanical Z stage with positional resolution of 500 nm while the workpiece was mounted on a stack of high precision X and Y mechanical stages with resolution of 250 nm.

A percussion drilling strategy was employed in this research and the focal position was maintained the same during the processing. The pulse frequency used in the experiments was 100 kHz. It should be noted that this pulse frequency was selected by conducting some initial trials while the maximum achievable pulse energy with the used laser source was utilised. In particular, through these trials the trade-offs between holes' quality, i.e. the recast formation, and processing speed that affect directly the achievable penetration depth were considered and thus to identify the optimum pulse frequency for the used laser source and substrate material.

A range of inspection methods to characterise laser drilled high aspect ratio holes, i.e. optical instruments and producing replicas of the holes by infiltrating liquid PMMA into the holes under vacuum conditions, were considered but was concluded that they did not provide sufficient insight into the process and therefore were not used in this research. Also, destructive methods such as cutting and then grinding the cross sections of the samples were examined, too. It was judged that they would introduce uncertainty in the inspection process that would be in order of difference of compared measurands and therefore would not meet the requirements of this experimental study. Taking into account the limitations of these non-destructive and destructive inspection methods, high resolution X-ray tomography was selected to assess the depth and morphology of the laser drilled micro-holes. In particular, a Zeiss XRADIA Versa XRM-500 system was employed in this research. The measurements settings selected to minimise the measurement uncertainty, especially the acceleration voltage, current and exposure time for each projection were set to 50 kV, 79 μ A and 7 s,

respectively. In this way projection images of 1013 by 1013 pixels were used to reconstruct the volumes of the drilled substrates over a grid of 1 μm cubic voxels. Then, this data set was analysed employing VG studio 3.0 from Volume Graphics and the surface model was defined by applying the VG's advanced surface determination, starting with the ISO 50 surface determination.

4.2.2. Design of experiments

To compare the laser drilling results obtained with three different lenses in terms of drilling rate and optimum NoP after which the penetration rate decreases substantially (referred to as a saturation point), arrays of blind holes with varying NoP were produced with three lenses. The NoP range was selected to cover the early stages of the hole formation before the saturation point is reached and also beyond. i.e. 100, 500, 1000, 1600, 2000, 2500, 5000, 10000 and 15000. The maximum pulse energy achievable with the used laser source i.e. 9 μJ was used in this experiment and each combination of drilling settings was repeated 7 times to assess repeatability and reliability of the results obtained in this research.

Next, the effects of a wide fluence spectrum were assessed by employing three different lenses with focal distances of 100, 50 and 20 mm and beam diameters of 45, 23 and 9 μm (measured using a beam profile analyser of Dataray Beam R2), respectively. The fluence ranges achieved for each lens by utilising the full range of pulse energies available with the used laser source are shown in Table 4.1. The highest fluence levels for the three lenses were different as a result of their different beam spot diameters while utilising the maximum deliverable pulse energy for the used laser source, i.e. 9 μJ . Hence, the same fluence for the three lenses can be obtained by decreasing the pulse energy and thus to investigate a wider spectrum of fluence effects on the percussion drilling process. The lowest

level of fluence for each lens was selected taking into account the silicon nitride ablation threshold, 0.24 J/cm^2 , calculated experimentally using Liu's method [36]. Thus, employing the three lenses all the experiments were carried out with 1,000 and 10,000 pulses to examine the fluence effects, both before and after the saturation point. Again, the experiments for each set of parameters were repeated 7 times.

Table 4.1. Design of experiments for assessing the fluence effects, employing three focusing lenses

Exp. trials	Number of pulses	Pulse energy	Corresponding fluence		
			100 mm lens	50 mm lens	20 mm lens
1 to 6	1000, 10,000	9 μJ	0.57 J/cm^2	2.17 J/cm^2	14.15 J/cm^2
7 to 12	1000, 10,000	7.7 μJ	0.48 J/cm^2	1.85 J/cm^2	12.10 J/cm^2
13 to 18	1000, 10,000	6.1 μJ	0.38 J/cm^2	1.47 J/cm^2	9.59 J/cm^2
19 to 24	1000, 10,000	4.1 μJ	0.26 J/cm^2	0.99 J/cm^2	6.44 J/cm^2
25 to 28	1000, 10,000	2.2 μJ	0.14 J/cm^2	0.53 J/cm^2	3.46 J/cm^2
29 & 30	1000, 10,000	0.9 μJ	0.06 J/cm^2	0.22 J/cm^2	1.41 J/cm^2

4.2.3. Depth of focus analysis

The issues associated with off-focus processing are common in laser machining but they could be ignored if their effects are negligible. However, lenses with small focal distances are sensitive to defocusing and consequently require fine adjustment in Z direction [37]. Therefore, higher resolution stages and sensors for setting up the focal plane are necessary for such lenses and this can have an impact on process flexibility and also increases the setup cost. The term, depth of focus (DOF), can be used to assess the sensitivity of a given laser machining setup to off-focus processing. As a laser beam with a Gaussian energy profile is employed in this research, the theoretical DOF can be calculated using Eq (1).

$$DOF = \frac{8\lambda}{\pi} \left(\frac{f}{D}\right)^2 \cdot M^2 \quad (1)$$

where: λ is the wavelength of the laser beam, f - the lens focal distance and D is the input beam diameter at the lens.

Thus, the theoretical DOF of the 100, 50 and 20 mm lenses calculated using Eq (1) are 2375 μm , 621 μm and 95 μm , respectively. There is a substantial DOF reduction when lenses with small focal distances are used and therefore their sensitivity to off-focus processing was analysed in this research. Therefore, additional experiments were carried out with a defocused beam, especially ± 50 μm , ± 100 μm and ± 200 μm , for all three lenses. The pulse energy in these experiments was fixed at 9 μJ while NoP were kept at 500 and 5,000 to examine the effects both, before and after the saturation point. Again, as in all experiments in this research each process setting was repeated 7 times to assess the reliability of the obtained results.

4.3. Results and Discussion

4.3.1. Saturation point

The capabilities of the three lenses in regards to achievable aspect ratios in percussion laser drilling of micro holes were examined in these first series of experiments. The arrays of blind holes produced with each lens by varying NoP were analysed by extracting the cross sectional views from the XCT results as depicted partly in Figure 4.1 for the holes drilled using 500, 1000, 5000 and 10000 pulses with 3 repetitions in each case. It can be clearly seen that the penetration stops at the early stages when the 100 mm lens was employed. The functional dependence between NoP and achievable penetration depth for the three lenses is given in Figure 4.2. It highlights clearly the benefits of employing lenses with smaller focal distances and thus to achieve higher fluence. The saturation point for the 100 mm lens was below the 110 μm mark while it was increased to 152 and 200 μm for 50 and 20 mm lenses, respectively. In all cases, any further increases of NoP after the saturation point did lead only to small improvements in regards to the achieved penetration depth.

The decrease of the drilling rates has been attributed to different factors such as plasma shielding and the angular dependence of laser absorption. In this research, the increase of the holes' surface area during the drilling process that led to a decrease of the effective fluence were considered a dominant factor in limiting the penetration depth [38]. This phenomenon is consistent across all three lenses, however since the fluence was much closer to the ablation threshold when the 100 mm lens was employed the saturation occurred in early stages of the drilling process.

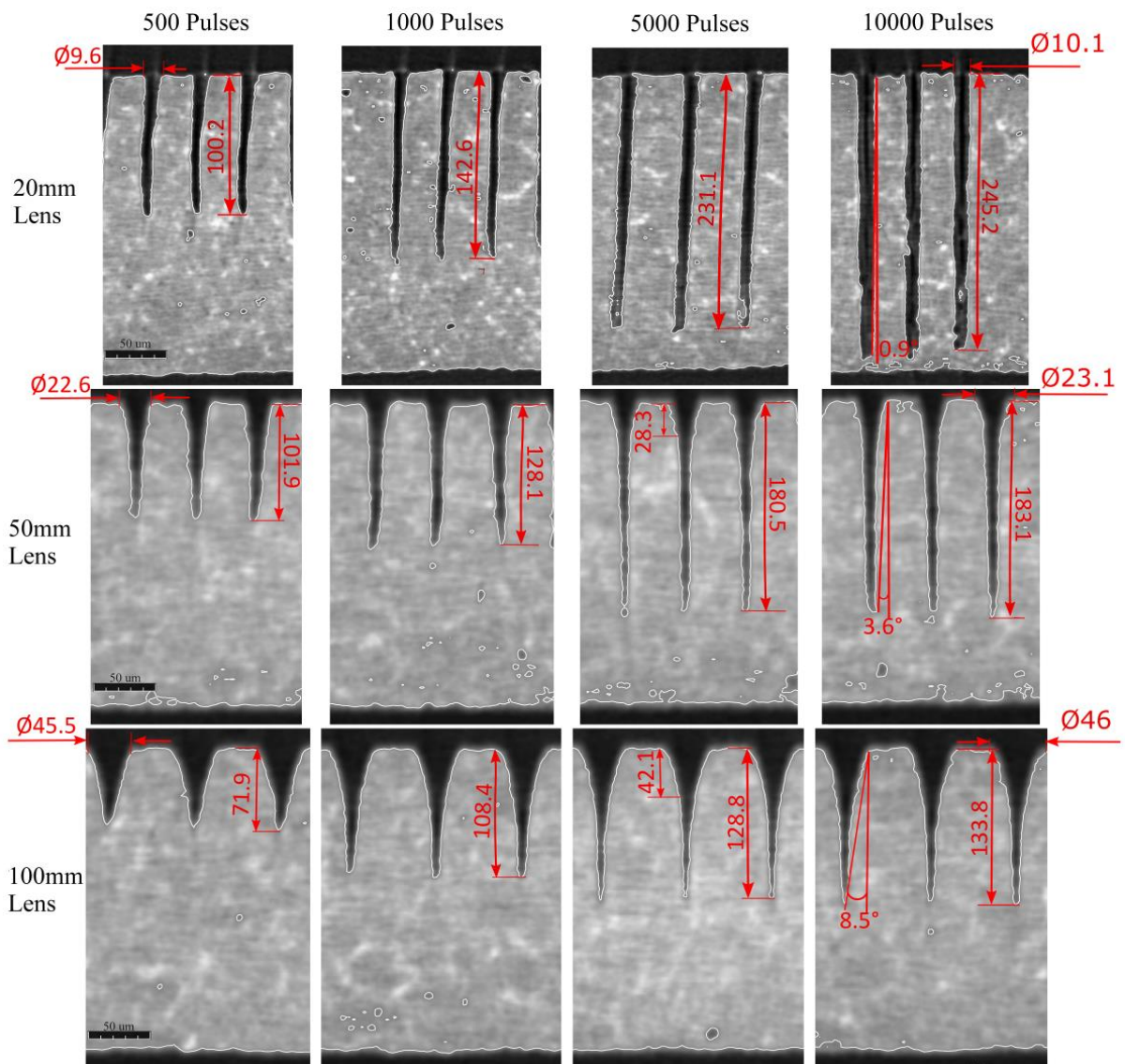


Figure 4.1. The XCT cross sections of the holes produced with the three lenses by delivering 500, 1000, 5000 and 10000 pulses. Note: all measurements are in micrometer and were taken employing VG studio 3.0.

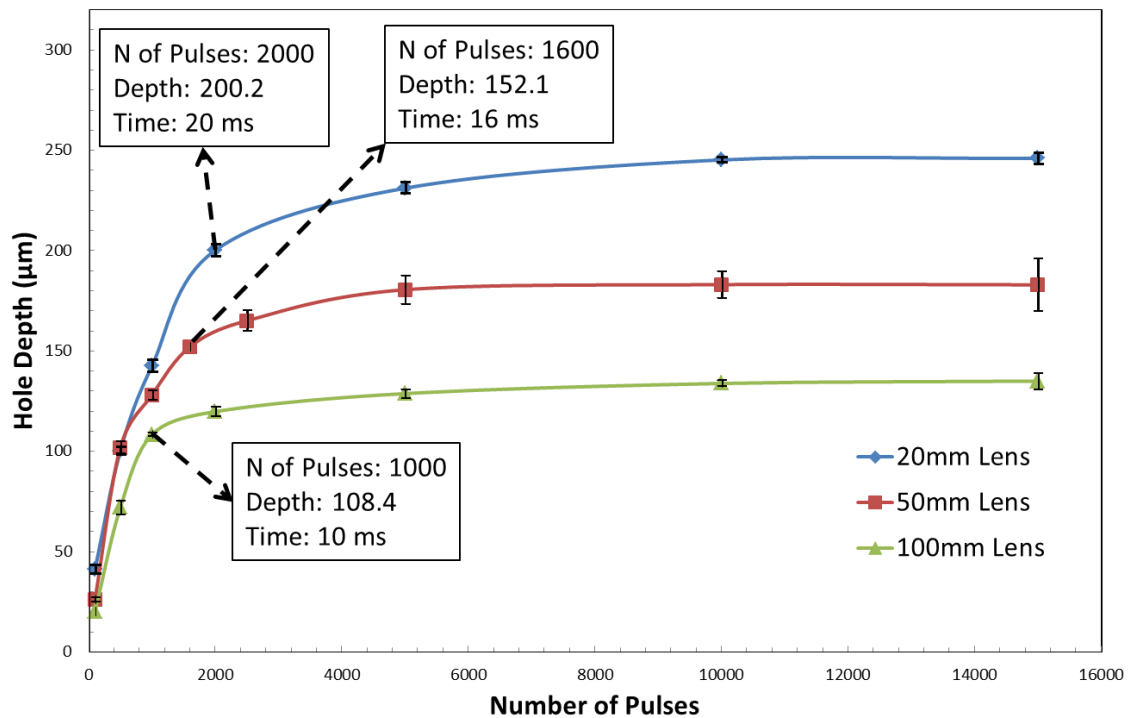


Figure 4.2. Percussion drilling saturation points for the three lenses

4.3.2. Fluence effects

The effects of fluence on achievable depth when employing the three different lenses was investigated by completing the experiments described in Table 4.1. The results obtained for the two different NoP used in the experiments are provided in Figure 4.3. It shows clearly how the increase of fluence affects the achievable penetration depth for each lens. This trend is more pronounced for the lenses with a bigger focal distance. At the same time, the lenses with a smaller focal distance can cover wider fluence ranges and thus to maintain the effective fluence at higher levels for longer that translates in a higher penetration depth. This is very well pronounced when 10,000 pulses were used, especially the penetration depth increases from 134 µm for the 100 mm lens to 183 µm and 245 µm for the 50 and 20 mm lenses, respectively.

If the achievable penetration depth with the same fluence levels of 1.4 J/cm^2 with 10,000 pulses are compared for 20 and 50 mm lenses, i.e. 25 and $120 \mu\text{m}$, respectively, there is a sharp increase. The same was observed when the depths achieved with 0.55 J/cm^2 employing the 50 and 100 mm lenses were compared, especially an increase from 29 to $134 \mu\text{m}$, respectively. This should be attributed to the high pulse energies used to achieve the same fluence levels as shown in Table 4.1 and this is in line with the results reported by Doring et.al. [39]. Another factor that contributes to the increase of the penetration depth is the bigger entry diameter of the holes drilled by the lenses with bigger focal distances (see Figure 4.1) as this facilitates the evacuation of the ablated material. Therefore, if these results are used to analyse the functional dependence between the fluence and achievable aspect ratios, as shown Figure 4.4, the same increasing trend can be observed. In particular, the increase of achievable aspect ratios was from 3 for the 100 mm lens to 8 and 25 for the 50 and 20 mm lenses, respectively, when 10,000 pulses were deployed.

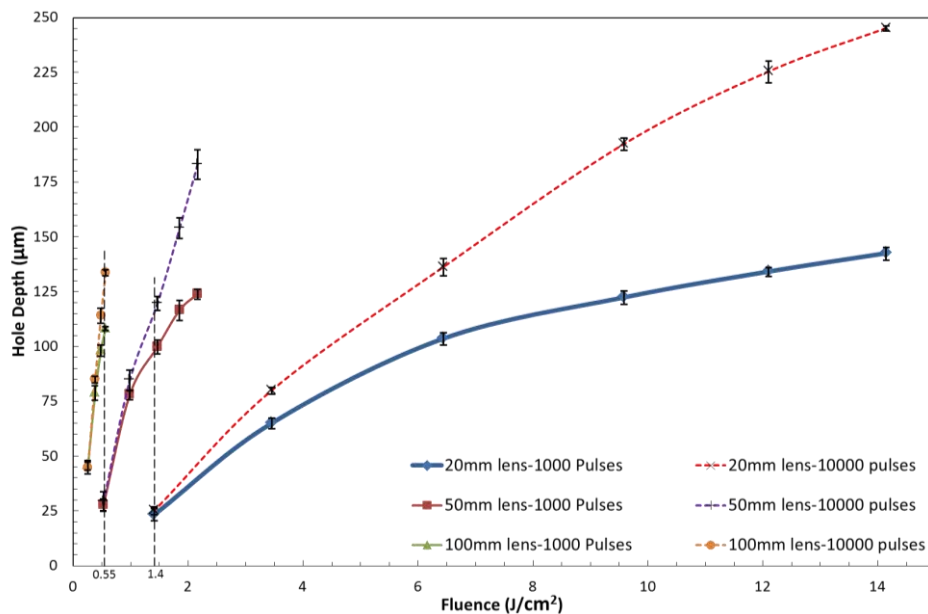


Figure 4.3. The penetration depths achieved with the different fluence levels for the three lenses when 1,000 and 10,000 pulses were used.

The other point which can be extracted from this graph, is the marginal difference in hole depth when increasing number of pulses in low fluences for each lens. It's because of the closeness of the ablation threshold to the pulse fluence which makes the subsequent pulses ineffective.

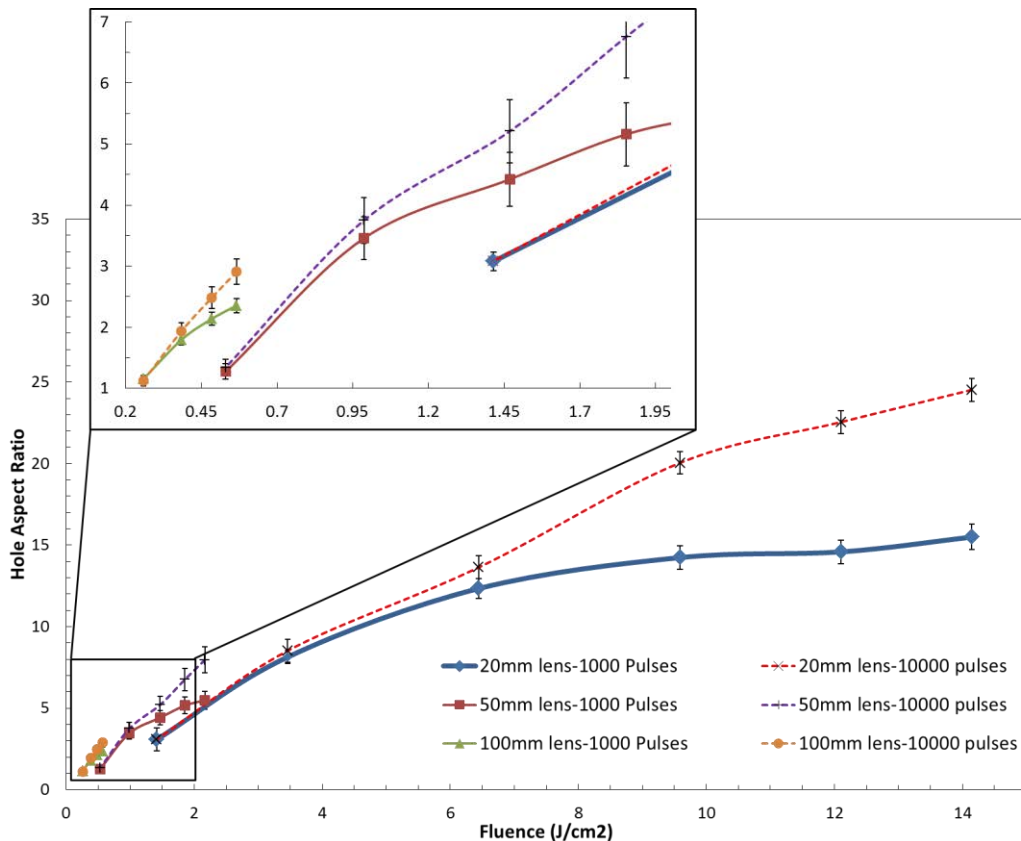


Figure 4.4. The achievable aspect ratios with the different fluence levels for the three lenses when 1,000 and 10,000 pulses were used.

4.3.3. Depth of focus analysis

The use of lenses with smaller focal distances is an attractive option for drilling higher aspect ratio micro holes but requires a careful analysis of their sensitivity to potential off-focus processing. The results obtained for the conducted DOF analysis with 500 and 5,000 pulses described in Section 4.2.3 are provided in Figure 4.5 and depicts the same trend before and after the saturation point.

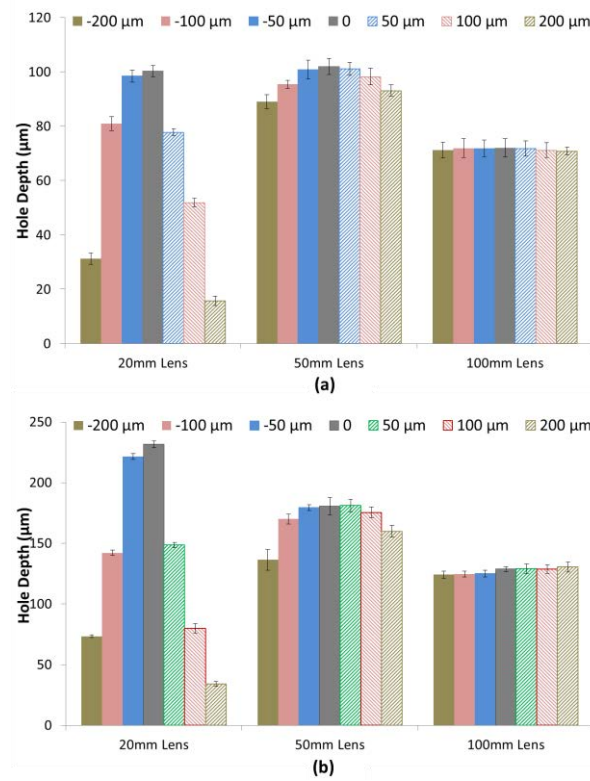


Figure 4.5. The achieved penetration depth with three lenses when a defocusing is applied, (a) 500 pulses and (b) 5,000 pulses.

While only negligible differences between the penetration depths were observed with the 100 mm lens when the beam was defocused up to $\pm 200 \mu\text{m}$ the differences are much more pronounced for the 50 mm lens, especially the penetration depth achieved with 5,000 pulses dropped approximately 24% (from 180 to 136 μm). The results obtained with the 20 mm lens are distinctly different and show a higher sensitivity to off-focus drilling. In particular, the penetration depth achieved with 5,000 pulses after only a small defocusing of +50 μm dropped from 232 to 149 μm , approximately 36%, that was less than the depth achieved with the 50mm lens. A further defocusing of +100 μm and +200 μm resulted in a drop of the hole depth to 80 μm (65% drop) and 34 μm (85% drop), respectively, that was less than the achieved depth with the 100 mm lens. The main reason for this sharp drop is the large divergence angle of the beam that leads to a significant fluence drop. In particular, the beam radius in focus (ω_0) can be calculated as follows:

$$\omega_0 = \frac{2\lambda \cdot f \cdot M^2}{\pi \cdot D} \quad (2)$$

By applying some defocusing of z, the beam radius would change to:

$$\omega(z) = \omega_0 \sqrt{1 + \left(\frac{M^2 \cdot \lambda \cdot z}{\pi \cdot \omega_0^2} \right)^2} \quad (3)$$

And, also the fluence due this z defocusing changes as follows:

$$F(z) = \frac{E}{\pi \omega(z)^2} = \frac{4\pi \cdot E \cdot f^2 \cdot D^2}{16\lambda^2 \cdot f^4 \cdot (M^2)^2 + \pi^2 \cdot D^4 \cdot z^2} \quad (4)$$

where: E is the pulse energy.

Substituting Eqs (2) and (3) in Eq (4), the first derivative of F(z) is:

$$\frac{dF(z)}{dz} = \frac{-8\pi^3 \cdot E \cdot D^6 \cdot z \cdot f^2}{(16\lambda^2 \cdot f^4 \cdot (M^2)^2 + \pi^2 \cdot D^4 \cdot z^2)^2} \quad (5)$$

Eq (5) shows how the rate of the fluence changes as a result of the beam defocusing dependence on the lenses' focal distance. Thus, the rate of fluence drop $\left(\frac{dF}{dz}\right)$ in this study with a defocusing of 10 μm would be -115, -0.511 and -0.008 J/cm^2 per mm for the 20, 50 and 100 mm lenses, respectively, that explains the substantial effect of defocusing when lenses with smaller focal distances are used. This is shown in figure 4.6.

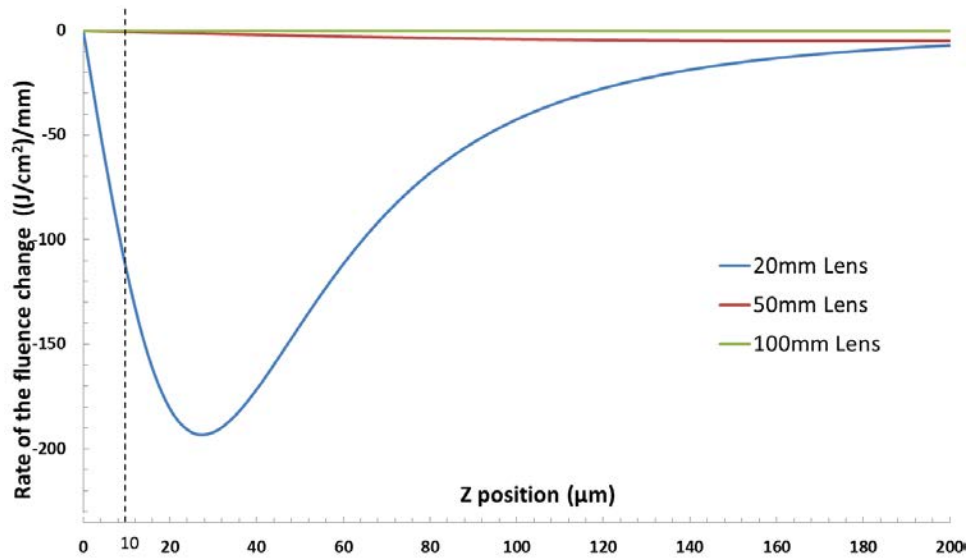


Figure 4.6. Rate of the fluence change for 3 different lenses

The beam divergence and spatial beam profiles of all three lenses calculated using Eq (3) that result from four different defocusing values are provided in Figure 4.7. The Gaussian beam spatial profile of the 20 mm lens for $z = 0$ has a sharp peak that is much higher than those of other two lenses and also the ablation threshold of silicon nitride, i.e. 0.24 J/cm^2 . By applying $200 \text{ }\mu\text{m}$ defocussing, the maximum fluence is for the 50 mm lens. Further increase of defocusing to $1,000 \text{ }\mu\text{m}$ results in a complete reverse fluence order, especially the 100 mm lens taking the top spot. However, it should be noted that in such high off-focus processing most of the beam spatial profiles of the 50 and 100 mm lenses are less than the silicon nitride ablation threshold while for the 20 mm lens it is completely under the threshold line.

The other phenomenon regarding the 20 mm lens that is clearly pronounced in Figure 4.5 is the large discrepancy between the achieved penetration depths when positive and negative defocusing is applied, i.e. $222 \text{ }\mu\text{m}$ compared with $149 \text{ }\mu\text{m}$ when $-50 \text{ }\mu\text{m}$ and $+50 \text{ }\mu\text{m}$ defocusing was used in case of 5,000 pulses. The difference is maintained for -100 and $+100 \text{ }\mu\text{m}$ off-focus drilling, too, i.e. 142 and $80 \text{ }\mu\text{m}$, respectively. This could be explained with the effects of the increasing distance between the focus and the holes' bottom, when a positive defocusing was applied. Thus, it could be expected that a negative defocusing could lead to better results than laser drilling in focus; however, for percussion drilling with the 20 mm lens this was not the case as shown in Figure 4.5. The reason for this is that the beam defocusing leads to a substantial fluence reduction accompanied with a significant change of the beam spatial profile that increases substantially the “filtered out” pulse energy in the drilling process as depicted in Figure 4.8. Thus, the use of negative defocusing is not effective in percussion laser drilling with small focal distance lenses.

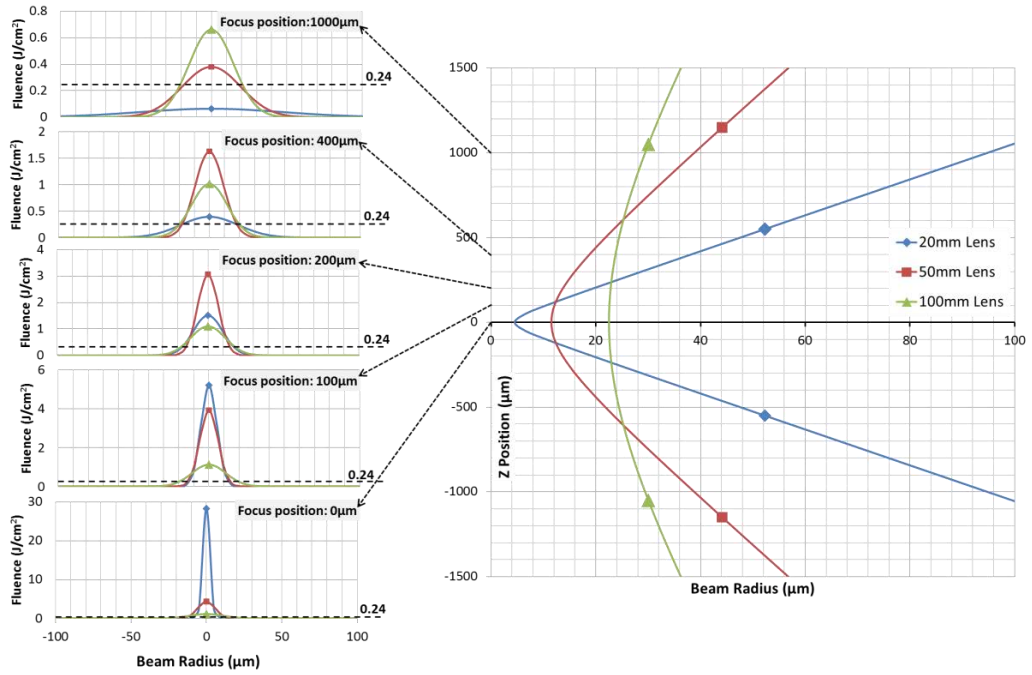


Figure 4.7. Beam spatial profiles of the three lenses at the substrate surface when different levels of defocusing are applied.

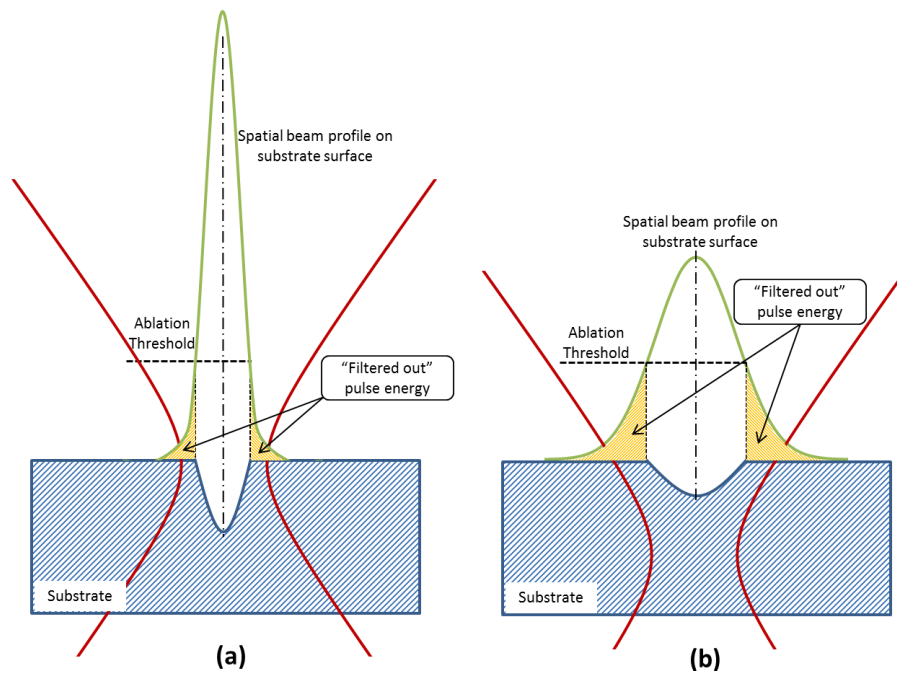


Figure 4.8. The filtered out portions of beam intensity: (a) a focused beam and (b) a negative defocused beam.

4.3.4. Hole morphology

So far the focus was on the achievable penetration depth but the effects on holes' morphologies (see Figure 4.1) should be discussed, too. It is clear that the NoP increase does not affect holes' entry diameters. Also, it is apparent that lenses with a higher focal distance produce holes with bigger openings due to their bigger focal spot diameter. The other option available to drill holes with bigger diameters is the use of trepanning or helical drilling but this would have a high impact on achievable processing speed compared to percussion drilling. In addition, it should be noted that the implementation of helical drilling employing scan heads requires the use of telecentric lenses to keep the beam normal to the substrate surface and also to prevent any defocusing when moving the beam. However, telecentric lenses are available only with relatively bigger focal distances, e.g. 70 or 100 mm, due to manufacturing constrains [40]. Also, it is possible to produce holes with bigger diameters by defocusing, however as it is shown in Section 4.3.3 it is not easy to set up the drilling process due to high sensitivity to off-focus processing. So, there is less flexibility in regards to the resulting holes' diameters when percussion drilling strategies are used and therefore the focusing lens should be selected very carefully taking into account the targeted hole diameter, aspect ratio, and processing speed.

The other common morphological issue is the cone shape entry with a necking that leads to deep narrow holes as shown in Figure 4.1, especially 42 and 28 μm for the holes produced with the 100 and 50 mm lenses using 5,000 pulses, respectively. At the same time, high aspect ratio uniform cylindrical holes were produced with the 20 mm lens. The average taper angles of the holes after 10,000 pulses were 9° , 4° and 1° for the 100, 50 and 20 mm lenses, respectively.

It should be stressed that recasts inside high aspect ratio hole are more likely to occur when lenses with a small focal distance are used because of the poor evacuation of the ablated material, in particular approximately 5% of the holes produced with the 20 mm lens had such issues as shown in Figure 4.9a. The other problem of high aspect ratio holes is the bending effect, however only 3% of the holes produced with the 20 mm lens exhibited such an effect as depicted in Figure 4.9b. One of the reasons for this phenomenon is the beam deflection by the ablated materials or the formed vapour cloud [41] that are more likely to occur in high aspect ratio holes.

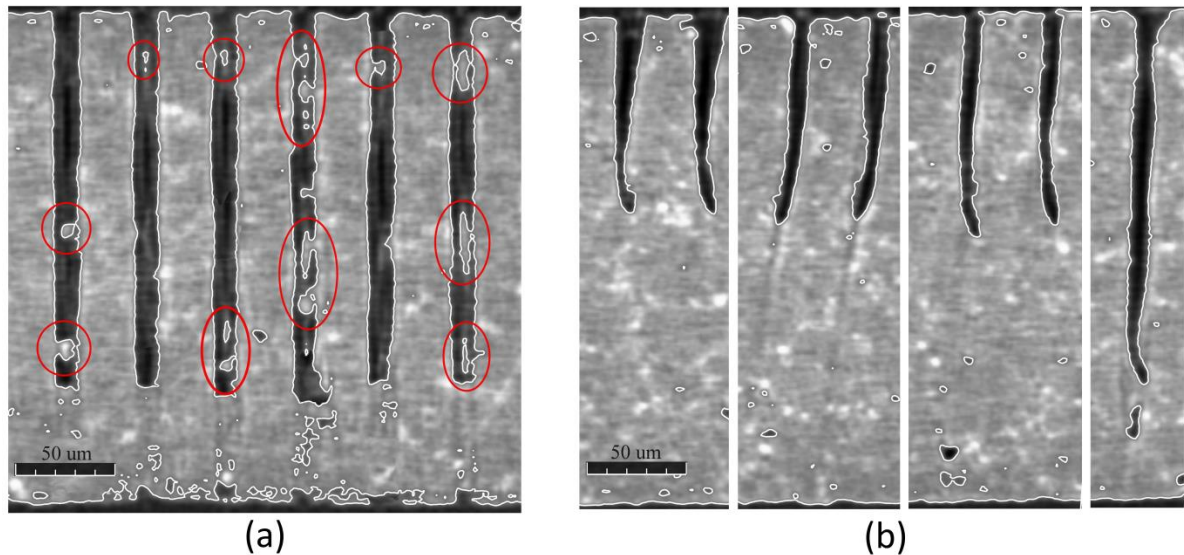


Figure 4.9. Issues with high aspect ratio holes, (a) recasts and (b) bending.

4.4. Conclusions

The effects of a wide fluence spectrum in ultra-short percussion drilling with different focal distance lenses are reported in this research. Especially, the effects on achievable aspect ratios and morphologies of the micro holes produced in Silicon nitride substrates were investigated. Based on the obtained results the following conclusions were made:

- Generally, the achievable holes' aspect ratio can be increased by employing lower focal distance lenses. In particular, aspect ratios up to 25 was achieved with the

maximum pulse energy available, 9 μj , by using the 20 mm lens compared with only 8 and 3 for 50 and 100 mm lenses, respectively.

- Holes with much better cylindricity and lower taper angle can be percussion drilled with smaller focal distance lenses. In particular, the taper angle decreased from almost 9° to less than 1° when the lens focal distance was reduced from 100 to 20 mm. In addition, lenses with smaller focal distance led to a substantial reduction of the resulting cone shape entries with necking.
- Both, the use of high fluence and high pulse energy lead to a high penetration depth.
- There are some limitations associated with the use of smaller focal distance lenses, i.e. smaller beam focal spot diameters and a higher sensitivity to defocusing. In addition, when such lenses are used to produce high aspect ratio holes the risks for recast formations inside the holes and the bending effects increase.

Acknowledgment

The research reported in this paper was supported by Korea Institute for Advancement of Technology (KIAT), i.e. the project on “Laser Machining of Ceramic Interface Cards for 3D wafer bumps”, and two H2020 Factory of the Future projects, “Modular laser based additive manufacturing platform for large scale industrial applications” (MAESTRO) and “High-Impact Injection Moulding Platform for mass-production of 3D and/or large micro-structured surfaces with Antimicrobial, Self-cleaning, Anti-scratch, Anti-squeak and Aesthetic functionalities” (HIMALAIA). The authors would like to acknowledge the contribution of Martin Corfield and Lars Korner from the University of Nottingham in carrying out the XCT measurements.

References

- [1] Y. Qin, A. Brockett, Y. Ma, A. Razali, J. Zhao, C. Harrison, W. Pan, X. Dai, D. Loziak, Micro-manufacturing: research, technology outcomes and development issues, *The International Journal of Advanced Manufacturing Technology*, 47 (2010) 821-837.
- [2] E. Ferraris, V. Castiglioni, F. Ceyskens, M. Annoni, B. Lauwers, D. Reynaerts, EDM drilling of ultra-high aspect ratio micro holes with insulated tools, *CIRP Annals - Manufacturing Technology*, 62 (2013) 191-194.
- [3] Z.Y. Yu, Y. Zhang, J. Li, J. Luan, F. Zhao, D. Guo, High aspect ratio micro-hole drilling aided with ultrasonic vibration and planetary movement of electrode by micro-EDM, *CIRP Annals - Manufacturing Technology*, 58 (2009) 213-216.
- [4] C. Diver, J. Atkinson, H.J. Helml, L. Li, Micro-EDM drilling of tapered holes for industrial applications, *Journal of Materials Processing Technology*, 149 (2004) 296-303.
- [5] T. Masuzawa, State of the Art of Micromachining, *CIRP Annals - Manufacturing Technology*, 49 (2000) 473-488.
- [6] L. Romoli, C.A.A. Rashed, G. Lovicu, G. Dini, F. Tantussi, F. Fuso, M. Fiaschi, Ultrashort pulsed laser drilling and surface structuring of microholes in stainless steels, *CIRP Annals*, 63 (2014) 229-232.
- [7] L. Romoli, C.A.A. Rashed, M. Fiaschi, Experimental characterization of the inner surface in micro-drilling of spray holes: A comparison between ultrashort pulsed laser and EDM, *Optics & Laser Technology*, 56 (2014) 35-42.
- [8] B. Adelman, R. Hellmann, Rapid micro hole laser drilling in ceramic substrates using single mode fiber laser, *Journal of Materials Processing Technology*, 221 (2015) 80-86.
- [9] W.C. Choi, J.Y. Ryu, Fabrication of a guide block for measuring a device with fine pitch area-arrayed solder bumps, *Microsyst Technol*, 18 (2012) 333-339.
- [10] N. Watanabe, M. Suzuki, K. Kawano, M. Eto, M. Aoyagi, Fabrication of a membrane probe card using transparent film for three-dimensional integrated circuit testing, *Jpn. J. Appl. Phys.*, 53 (2014) 06JM06.
- [11] W.C. Choi, J.Y. Ryu, A MEMS guide plate for a high temperature testing of a wafer level packaged die wafer, *Microsyst Technol*, 17 (2011) 143-148.
- [12] L. Romoli, R. Vallini, Experimental study on the development of a micro-drilling cycle using ultrashort laser pulses, *Optics and Lasers in Engineering*, 78 (2016) 121-131.
- [13] X.C. Wang, H.Y. Zheng, P.L. Chu, J.L. Tan, K.M. Teh, T. Liu, B.C.Y. Ang, G.H. Tay, Femtosecond laser drilling of alumina ceramic substrates, *Applied Physics a-Materials Science & Processing*, 101 (2010) 271-278.
- [14] A.H. Khan, S. Celotto, L. Tunna, W. O'Neill, C.J. Sutcliffe, Influence of microsupersonic gas jets on nanosecond laser percussion drilling, *Optics and Lasers in Engineering*, 45 (2007) 709-718.
- [15] A.H. Khan, W. O'Neill, L. Tunna, C.J. Sutcliffe, Numerical analysis of gas-dynamic instabilities during the laser drilling process, *Optics and Lasers in Engineering*, 44 (2006) 826-841.
- [16] J.C. Hsu, W.Y. Lin, Y.J. Chang, C.C. Ho, C.L. Kuo, Continuous-wave laser drilling assisted by intermittent gas jets, *International Journal of Advanced Manufacturing Technology*, 79 (2015) 449-459.
- [17] C.C. Ho, Y.M. Chen, J.C. Hsu, Y.J. Chang, C.L. Kuo, Characteristics of the effect of swirling gas jet assisted laser percussion drilling based on machine vision, *Journal of Laser Applications*, 27 (2015) 042001.

- [18] H. Zhang, J. Di, M. Zhou, Y. Yan, R. Wang, An investigation on the hole quality during picosecond laser helical drilling of stainless steel 304, *Applied Physics a-Materials Science & Processing*, 119 (2015) 745-752.
- [19] C. He, F. Zibner, C. Fornaroli, J. Ryll, J. Holtkamp, A. Gillner, High-precision helical cutting using ultra-short laser pulses, *Physics Procedia* 2014, pp. 1066-1072.
- [20] N. Iwatani, H.D. Doan, K. Fushinobu, Optimization of near-infrared laser drilling of silicon carbide under water, *Int. J. Heat Mass Transf.*, 71 (2014) 515-520.
- [21] V. Nasrollahi, P. Penchev, S. Dimov, L. Korner, R. Leach, K. Kim, Two-Side Laser Processing Method for Producing High Aspect Ratio Microholes, *Journal of Micro and Nano-Manufacturing*, 5 (2017) 041006-041014.
- [22] K. Goya, T. Itoh, A. Seki, K. Watanabe, Efficient deep-hole drilling by a femtosecond, 400 nm second harmonic Ti:Sapphire laser for a fiber optic in-line/pico-liter spectrometer, *Sensors and Actuators B-Chemical*, 210 (2015) 685-691.
- [23] H. Huang, L.-M. Yang, J. Liu, Micro-hole drilling and cutting using femtosecond fiber laser, *Optical Engineering*, 53 (2014) 051513.
- [24] Y. Zhang, Y. Wang, J. Zhang, Y. Liu, X. Yang, W. Li, Effects of Laser Repetition Rate and Fluence on Micromachining of TiC Ceramic, *Materials and Manufacturing Processes*, (2015).
- [25] Y. Zhang, Y. Wang, J. Zhang, Y. Liu, X. Yang, Q. Zhang, Micromachining features of TiC ceramic by femtosecond pulsed laser, *Ceram. Int.*, 41 (2015) 6525-6533.
- [26] M. Ghoreishi, O.B. Nakhjavani, Optimisation of effective factors in geometrical specifications of laser percussion drilled holes, *Journal of Materials Processing Technology*, 196 (2008) 303-310.
- [27] M. Ghoreishi, D.K.Y. Low, L. Li, Comparative statistical analysis of hole taper and circularity in laser percussion drilling, *International Journal of Machine Tools and Manufacture*, 42 (2002) 985-995.
- [28] G.K.L. Ng, L. Li, Repeatability characteristics of laser percussion drilling of stainless-steel sheets, *Optics and Lasers in Engineering*, 39 (2003) 25-33.
- [29] S.H. Kim, I.-B. Sohn, S. Jeong, Ablation characteristics of aluminum oxide and nitride ceramics during femtosecond laser micromachining, *Applied Surface Science*, 255 (2009) 9717-9720.
- [30] A. Bharatish, H.N. Narasimha Murthy, B. Anand, C.D. Madhusoodana, G.S. Praveena, M. Krishna, Characterization of hole circularity and heat affected zone in pulsed CO₂ laser drilling of alumina ceramics, *Optics & Laser Technology*, 53 (2013) 22-32.
- [31] M.J. Jackson, W. O'Neill, Laser micro-drilling of tool steel using Nd:YAG lasers, *Journal of Materials Processing Technology*, 142 (2003) 517-525.
- [32] A. Schoonderbeek, C.A. Biesheuvel, R.M. Hofstra, K.J. Boller, J. Meijer, The influence of the pulse length on the drilling of metals with an excimer laser, *Journal of Laser Applications*, 16 (2004) 85-91.
- [33] G. Thawari, J.K.S. Sundar, G. Sundararajan, S.V. Joshi, Influence of process parameters during pulsed Nd:YAG laser cutting of nickel-base superalloys, *Journal of Materials Processing Technology*, 170 (2005) 229-239.
- [34] Y. Liu, C. Wang, W. Li, L. Zhang, X. Yang, G. Cheng, Q. Zhang, Effect of energy density and feeding speed on micro-hole drilling in C/SiC composites by picosecond laser, *Journal of Materials Processing Technology*, 214 (2014) 3131-3140.
- [35] D. Dergez, M. Schneider, A. Bittner, U. Schmid, Mechanical and electrical properties of DC magnetron sputter deposited amorphous silicon nitride thin films, *Thin Solid Films*, 589 (2015) 227-232.

- [36] J.M. Liu, Simple technique for measurements of pulsed Gaussian-beam spot sizes, *Optics Letters*, 7 (1982) 196-198.
- [37] V.V. Semak, J.G. Thomas, B.R. Campbell, Drilling of steel and HgCdTe with the femtosecond pulses produced by a commercial laser system, *Journal of Physics D: Applied Physics*, 37 (2004) 2925-2931.
- [38] A. Ruf, P. Berger, F. Dausinger, H. Hügel, Analytical investigations on geometrical influences on laser drilling, *Journal of Physics D: Applied Physics*, 34 (2001) 2918-2925.
- [39] S. Döring, S. Richter, A. Tünnermann, S. Nolte, Evolution of hole depth and shape in ultrashort pulse deep drilling in silicon, *Applied Physics A: Materials Science and Processing*, 105 (2011) 69-74.
- [40] Qioptiq, LINOS F-Theta Ronar fused silica lenses: Custom adaptations to the latest market trends, *LASER World of Photonics* 2013.
- [41] B. Xia, L. Jiang, X. Li, X. Yan, Y. Lu, Mechanism and elimination of bending effect in femtosecond laser deep-hole drilling, *Optics Express*, 23 (2015) 27853-27864.

CHAPTER 5:

Laser drilling with a top-hat beam of micro-scale high aspect ratio holes in silicon nitride

Authors Contributions

This chapter of the alternative thesis format is just submitted. I am the first author of this publication. The paper's detail and contributions of co-authors are outlined below. The contents of this chapter address the **key research issue 3**, characterised in section 2.8.

Nasrollahi, V.¹, Penchev, P.², Batal, A.³, Dimov, S.^{*}, Kim, K.^{}**, (2019), Laser drilling with a top-hat beam of micro-scale high aspect ratio holes in silicon nitride. **(Submitted in journal of materials processing technology)**

¹ **Vahid Nasrollahi**: is the main author and he conceived the ideas of implementing refractive optics for beam shaping, designed and executed experiments, performed all necessary characterization and data analysis and wrote the manuscript that was reviewed by the principal supervisor, **Prof. Stefan Dimov** (*) and Dr Kyunghan Kim (**).

² Dr Pavel Penchev contributed with the setting up of the beam delivery system.

³ Afif Batal contributed in interpretation of obtaining results.

CHAPTER 5 : Laser drilling with a top-hat beam of micro-scale high aspect ratio holes in silicon nitride

Abstract

High aspect ratio micro holes are very important functional features in many products, in particular in electronics industry. Especially, the critical requirements that such holes in electronic devices should satisfy, concern their morphology and quality that can impact directly the products' functional performance. At the same time, ultra-short lasers have shown that they have the capabilities to match such tight requirements due to their unique processing characteristics. The typical beam spatial profile of the laser sources used for drilling is Gaussian and this entails some constraints and limitations. In this study, a beam shaping system for laser micro drilling has been designed and implemented to achieve a top-hat spatial profile. The morphology of the high aspect ratio holes in terms of cylindricity, circularity, tapering angle, heat affected zone (HAZ) and penetration depth was investigated by a high resolution X-Ray Computed Tomography (XCT). The capabilities and limitations of such beam shaping solutions for producing micro-scale high aspect ratio holes has been discussed, i.e. their sensitivity to defocusing, and compared to Gaussian beam spatial distribution. It's been shown that the penetration depth and aspect ratios achievable with a Gaussian beam are higher but the use of a top-hat beam improves the holes geometrical accuracy, especially the deviations of the holes from cylindricity are less and also the holes are with a lower tapering angle. The top-hat spatial distribution minimises not only HAZ but also fluence at the beam spot area can be tailored accurately in respect to the ablation threshold.

Keywords: Laser micro-drilling; High aspect ratio holes, Flat-top distribution, beam shaping

5.1. Introduction

The continuous advances of electronic devices and microelectromechanical systems, especially their miniaturisation and the integration of more functions in a smaller package, demand new manufacturing methods that could address the increasing requirements regarding their dimensional accuracy, repeatability and cost-effectiveness [1]. Micro holes are common and often critical features in such devices and also are used as micro vias in PCBs. Vertical probe cards are a notable example that incorporate arrays of micro holes into silicon nitride substrates to support and position micro pins with high accuracy [2-5]. In particular, to satisfy the constantly increasing functional requirements for these pins, the holes have to be produced with higher density, i.e. smaller diameters and pitch distances, and geometrical accuracy, i.e. circularity, cylindricity and perpendicularity. So, this translates into stringent technical requirements for the holes' manufacture, e.g. aspect ratios 5:1, diameters and pitches less than 60 μm , taper angles less than 10° , minimum deviation from cylindricity and positional accuracy better than 4 μm , while increasing the drilling speed in order to produce the holes cost-effectively. In this context, laser micro drilling offer significant advantages compared with alternative machining processes, i.e. high throughput, any material could be processed, a contactless process and small beam diameters in micro level range. However, there are some limitations, too, e.g. achievable aspect ratios, heat affected zone (HAZ), tapered walls and material spatters.

There are different approaches to address such limitations and the most common is to find the optimum processing window, in particular the optimum fluence and pulse durations [6-13]. Other processing solutions have been used successfully, too, such as beam rotation [14, 15], using a background gas [16-19], two side drilling [20, 21] and dynamic focus positioning [2, 22]. Also, changes in the beam delivery system have been utilized, e.g.

employing lenses with different focal distances [23, 24], varying the polarization of the beam either by mechanical rotation of half wave plate [25, 26] or using fast-response liquid-crystal polarization rotator [27].

Predominantly in these investigations to addressing the laser drilling limitations, the spatial beam shape was Gaussian and this entailed a number of intrinsic drawbacks. In particular, only part of the beam energy profile is above the ablation threshold of any given material and as a result the process efficiency is reduced, HAZ is widened and edge definition is worsen [28]. In addition, the non-uniform energy distribution affects cylindricity of the resulting holes and also there are refractive index variations as a function of the local fluence that affect the hole morphology [29, 30]. Thus, converting the spatial beam profile into Bessel or top-hat beam can be considered as another optical solution. For example, He et al [31] adopted an axicon and designed a binary phase plate to produce a tailored Bessel beam that facilitated drilling holes with 10 μm diameter in 100 μm thick Silicon with almost taper-free sidewalls. However, the material transparency to the laser source wavelength and likely ring marks due to high fluence and energy accumulation, limit Bessel beam applications [32]. Other beam shapes were also investigated, e.g. implementing diffracted optical elements (DOE) to attain a doughnut beam shape [26] or top-hat beam to produce clean and sharp edges for scribing purposes [33]. Percussion drilling of holes larger than the beam spot size by employing different annular beam shapes [34, 35] is another advantage of beam shaping. The reduction of material spatter around vias by using a Pitchfork beam in the focus produced by comprising three lenses was also investigated [36].

Spatial light modulators (SLM) are another option for beam shaping [37, 38]. For drilling, Sanner et al [39] implemented a phase-front tailoring system employing SLM to obtain doughnut and top-hat beams. Especially, holes with a diameter of approximately 17

μm and depth of $15\ \mu\text{m}$ were drilled by using a top-hat beam and they were not only with sharp edges but also unlike those drilled with a Gaussian beam, their diameters were not fluence-dependent. Doan et al [40] also investigated top-hat and annular drilling using a fluidic laser beam shaper and compared the resulting holes in regards to their diameters, depths and HAZ.

In most of these investigations the effects of the spatial beam shape on holes' morphology were not thoroughly studied and were limited to shallow holes with low aspect ratios. In addition, the beam shaping techniques used in some cases were sensitive to any defocusing or optical misalignment that limited their flexibility for scale up production or were not applicable for beam diameters less than $100\ \mu\text{m}$.

In this research, a beam delivery system with refractive beam shaping was designed to produce a top-hat beam and the resulting holes were compared with those produced with a Gaussian beam. The morphology of the holes in terms of circularity and taper angle together with the penetration depth were investigated by a high-resolution X-ray Computed Tomography (XCT). The capabilities of top-hat drilling together with its limitations were contrasted to the results obtainable with a Gaussian beam and conclusions were made regarding their sensitivity to defocusing and trade-offs in holes' morphologies.

5.2. Refractive field mapping beam shapers

An optimum beam shaping solution should be selected taking into account application's specific requirements and laser source properties. At the same time, beam shapers should not be considered off-the-shelf products as this could lead to several issues, i.e. divergence shifts, power fluctuations, pointing instabilities and beam spatial profile

distortions [41]. Therefore, sufficient understanding of their capabilities and limitations is required before integrating them into beam delivery systems.

The suitability of beam shaping methods for a given application could be assessed based on the following criteria [42]:

- 1- The transformation should result in the desired beam shape with acceptable accuracy for the application;
- 2- The energy losses should be as low as possible;
- 3- Minimal sensitivity to minor changes in the process or input beam size;
- 4- Minimal beam brightness reduction.

Taking into account these criteria, it is necessary to consider the process limitations and laser source characteristics before selecting a beam shaper.

In this research, the focus is on micro drilling of holes smaller than 50 μm and therefore the focusing lens should be positioned after the beam shaper into the beam delivery system. A top-hat beam is simply obtainable in planes other than the focal plane by integrating a beam shaper before the lens, as it is shown in Figure 5.1b. Nevertheless, the laser intensity in this case is not sufficient and it is usually below the ablation threshold.

Based on diffraction theory, the resulting beam shape at the focal plane of a lens is proportional to Fourier transform of the input beam [43]. For instance, the Fourier transform of Gaussian function is still Gaussian function and thus if such beam is used its spatial distribution at the focal plane is the same as the input beam (see Figure 5.1a). Considering Fourier transformation from Eq (1), a Sinc function with an Airy pattern is required before the lens in order to produce a top-hat beam shape in the focal plane, as it is depicted in Figure 5.1c [43].

$$\mathcal{F}(A \cdot \text{sinc}(ar)) = \frac{A}{|a|} \cdot \text{rect}\left(\frac{\xi}{a}\right) \quad (1)$$

Taking into account that the ultrashort laser sources commonly used for laser micro drilling have Gaussian spatial profiles and also considering the specific application in this research, i.e. laser drilling arrays of micro holes, the following specific requirements should be satisfied in selecting an appropriate beam shaper:

- 1- Transformation of a Gaussian beam into of a beam with Airy spatial profile before the lens and thus to obtain a top-hat one at the focal plane;
- 2- Adaptability to the beam diameter of a given laser source;
- 3- Achieving the required beam diameter in focus;
- 4- Compatibility with optical X-Y scanners;
- 5- Beam shape and size consistency within relatively small focus deviations;
- 6- Damage thresholds compatible with fluence and wavelength achievable with a given laser source.

To select the most appropriate beam shaping method for addressing these requirements, it is necessary to map them against the available methods and consider their limitations. In particular, the beam shaping methods fall into three main classes [41, 44, 45]:

- 1- *Attenuators*. These shapers basically use apertures to truncate a desirable portion of the beam. The main shortcomings of this method are the loss of some beam energy and difficulties in finding an optimal position in relation to the aperture and also to decide what portion of the beam should be used. In the context of the micro drilling application in this research these are significant shortcomings and therefore this approach is undesirable.
- 2- *Beam integrators*. These shapers use a lenslet array and break up the beam into beamlets. The main drawback of this beam shaping solution is the beam damage and

some deficiency in spatial coherence due to destructive interference phenomena. So, usually a large beam size is required and therefore this approach is impractical in the context of the micro drilling application.

3- *Field mapping*. This method transforms the electromagnetic field by inducing an one-to-one mapping. Generally, refractive, reflective or diffractive optical elements (DOE) are adopted in transforming the beams.

DOEs have been used to produce a top-hat beam in the focal plane and applied successfully in laser micro machining [33] and drilling [26]. However, it has some shortcomings, too, e.g. the complexity of the used design algorithms, manufacturing difficulties, the limited diffraction efficiency and the low resistance to the high peak power of ultra-short pulses, that make this method not so attractive for industrial applications [46]. At the same time, SLM as a dynamic DOE can modulate the phase of incoming wavefronts by employing tuneable liquid crystal molecules [47] but again it has some limitation. E.g., the shaping rate, resolution and low damage threshold are common constrains [48, 49] in particular for shaping the beam at focal plane due to the complexity of the SLM design algorithms [37].

As an alternative, refractive optics can be deployed for beam shaping as it has a simpler structure, offers a higher optical efficiency and also is much easier to manufacture [36, 46, 50]. So, after considering the available field mapping methods with their limitations and constraints against the specific requirements in drilling arrays of micro holes, it was judged that Focal- π Shapers could address them and therefore was investigated in this research.

Focal- π Shapers employ refractive optical elements, i.e. aspheric optical surfaces, and operate as a Galilean type telescope. Thus, any internal focusing associated with high power

or ultra-short lasers can be avoided [51]. The magnification of about $1\times$ facilitates its integration into beam delivery systems without the need to perform any specific modifications in the beam path. In addition, Focal- π Shapers produce a collimated beam as an output and therefore offer sufficient flexibility in selecting where to position them along the beam delivery path and hence this facilitates their integration [52]. Therefore, the installation and alignment requirements of these beam shapers are relatively simple but still a good understanding of their main operational principals is required and also to follow as closely as possible their setting up procedures.

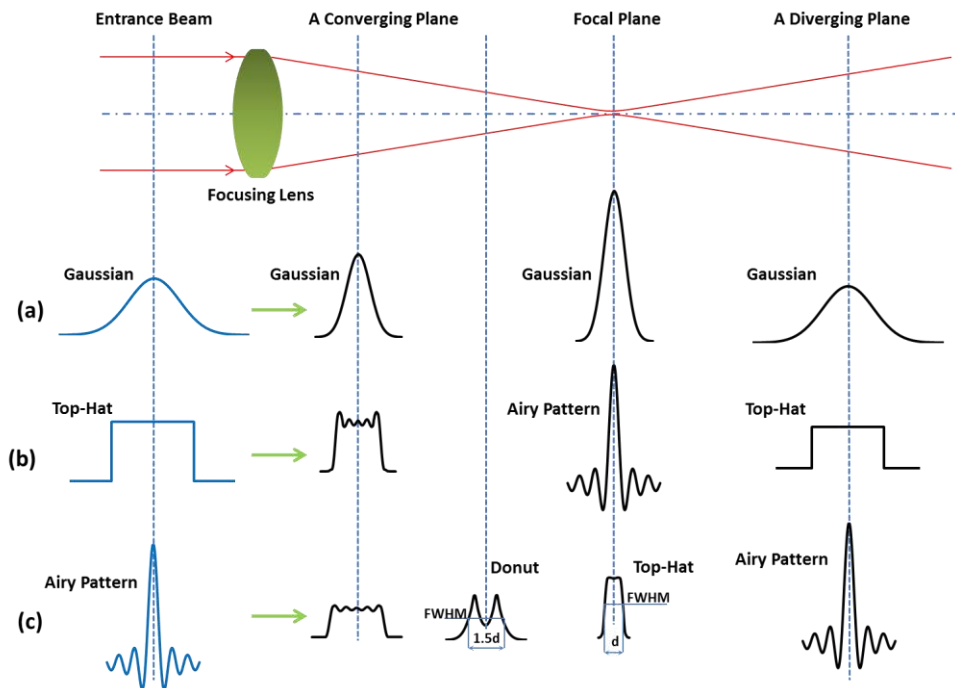


Figure 5.1.The beam propagation after the focusing lens: (a) Gaussian (b) Top-hat and (c) Sinc entrance beams.

The beam delivery systems should integrate other optical components to achieve the required beam diameter and depth of focus (DOF) in realizing the laser micro drilling operations. Since Focal- π Shaper is a $1\times$ magnifier, the FWHM beam diameter of the top-hat beam at focus (d) and DOF can be calculated using the following equations:

$$d = \frac{4\lambda \cdot f \cdot M^2}{\pi \cdot D} \quad (2)$$

$$DOF = \frac{8\lambda}{\pi} \left(\frac{f}{D}\right)^2 \cdot M^2 \quad (3)$$

where: λ is the wavelength of the laser beam; f - the lens focal distance; M^2 - the beam quality factor; and D - the input beam diameter at the beam shaper.

It is shown in Figure 5.1c, how by defocusing, the beam shape can be changed from flat-top to donut [52].

5.3. Experimental

5.3.1. Experimental setup and measurement procedure

The micro drilling setup designed to investigate the Focal- π Shaper capabilities is shown in Figure 5.2. The technical specifications of the key components integrated in the beam delivery system are provided below:

- **Laser source.** The laser source is an ultra-short pulsed Yb-doped fibre laser with pulse duration of 310 fs from Amplitude Systems. Its maximum average power is 5 W and 500 kHz is its maximum pulse repetition rate. The output is a linearly polarised Gaussian beam with quality factor (M^2) better than 1.3 and wavelength of 1030 nm.
- **Polariser.** Elliptical hole shapes and tapered walls are inevitable phenomena in drilling high aspect ratio holes and a way of minimising these effects is to convert the polarisation to circular [53, 54]. Therefore, a quarter-wave plate is integrated after the laser source in the beam path.
- **Beam Shaper.** Taking into account the wavelength and max beam intensity of the laser source together with the requirements that the beam shaper should satisfy (see Section 5.2), *Focal- π Shaper 9_1064_HP* was selected in this research. The $1/e^2$ input beam diameter was set in the range from 4 to 5 mm based on the manufacturer

recommendation [52] and thus was similar to the output beam diameter of the laser source. Therefore, it was considered that the beam expander which can be potentially a source of misalignments and beam quality deterioration is not necessary to be implemented in the beam delivery system. The beam shaper installation and alignment was performed following the step by step manufacturer instruction [55].

- **X Y scanner.** Since the objective of this research is to implement and validate a beam delivery system for producing arrays of holes with high efficiency, beam deflectors was used instead of mechanical stages. The chosen beam shaper allows beam deflectors to be integrated without affecting the beam spatial distribution in the focal plane.
- **Telecentric lens.** A telecentric lens was integrated to insure the orthogonality of the beam across the field of view. The focal length of the lens was 100 mm and thus the beam spot diameter at the focal plane was 47 μm based on Eq (2). Thus, the calculated DOF was 2.6 mm based on Eq (3) that was acceptable in the context of this research on laser micro drilling. This lens was mounted on a mechanical Z stage with resolution of 500 nm and thus to be able to position the focal plane with sufficient accuracy and repeatability on workpieces.

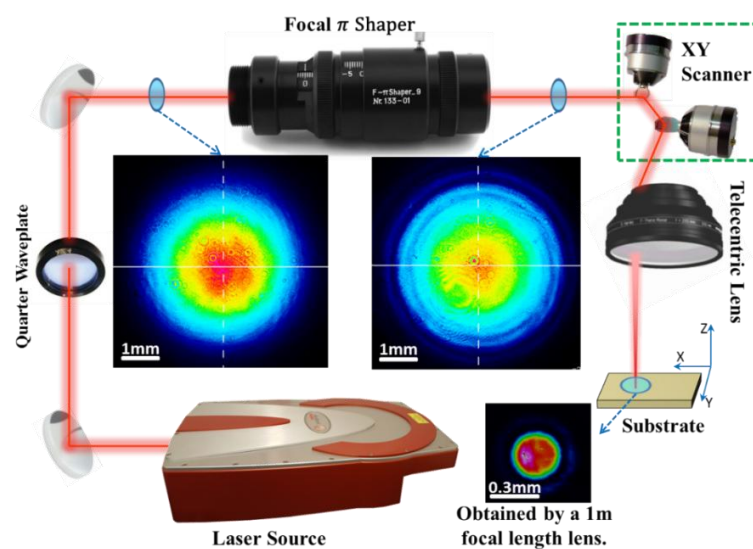


Figure 5.2. Laser drilling setup with beam profiles at different positions along the beam path

The beam shape was analysed employing a DataRay Inc WinCamD CMOS scanning beam profiler with a measurement area of 11.3 x 11.3 mm and pixel size of 5.5 μm . Beam measurements were taken at three critical points along the beam propagation axis, in particular before and after the beam shaper and also at the focal plane after the focusing lens. As it is shown in Figure 5.2, the beam spatial profiles were as expected Gaussian, Airy and top-hat at the three measurement points, respectively. The CMOS beam profiler had some resolution limitations and therefore the top-hat distribution was captured by using a 1 m focal distance lens.

Silicon Nitride (Si_3N_4) substrates were used to investigate the capabilities of Focal- π Shaper for drilling high aspect ratio micro holes because of their wide range of applications in microelectronic and microelectromechanical systems [56]. The thickness of the used Si_3N_4 wafers was 250 μm while their surface roughness was Sa 220 nm, measured with a focus variation microscope (Alicona G5). The drilling strategy applied in the research was percussion drilling without changing the focus position in process and pulse frequency of 100 kHz was selected as a trade-off between holes' quality, i.e. the edge definition, and the processing speed. The maximum available pulse energy with the used laser source was deployed, i.e. 9 μJ .

It is extremely difficult and even impossible to analyse properly the morphology of such high aspect ratio micro holes, i.e. diameters and circularity at different depths, employing solely conventional optical measurement methods, especially by making replicas or cutting and grinding of suitable cross-sections. In most of these cases, uncertainty of the measurement procedures would be in order of the measurands. Therefore, high resolution X-ray tomography was utilised in this research to evaluate the resulted morphology, in particular by analysing a sequence of cross-sections at different depths along the holes' axes. A Zeiss

XRADIA Versa XRM-500 system was used with the following scanning settings: acceleration voltage and current were 50 kV and 79 μ A, respectively; and the exposure time of each projection was 7 s. As a result, projection images of 1013 by 1013 pixel was captured with pixel binning of 2 reconstructing the volume over a grid of cubic voxels with a side length of 2 μ m. This data set was analysed with the Volume Graphics studio 3.0 software and the surface model was defined by VG's advanced surface determination, starting with the ISO 50 surface determination.

5.3.2. Design of experiments

A set of experiments was designed to investigate the capabilities of a top-hat beam in drilling high aspect ratio micro holes and compare them with the drilling results achievable with a Gaussian beam. Especially, holes with different number of pulses (NoP) were produced with both spatial beam distributions. The resulting holes' shape and morphology were analysed after pre-set NoPs, i.e. 100, 200, 400, 600, 1000, 2000, 5000 and 7500, and the drilling experiments with each process setting was repeated 7 times.

As it is depicted in Figure 5.1, the beam diameter and shape can be continuously changed by defocusing. Therefore, laser setups that are highly sensitive to defocusing could not only limit the process flexibility, but also could increase the setup costs due to tighter requirements towards positioning stages and sensors. Therefore, the sensitivity of the investigated laser drilling setup to defocusing in the range from +200 μ m to -1000 μ m in 200 μ m step was analysed, too.

5.4. Results and Discussion

5.4.1. Effects of beam shape on holes' morphology

The effects of the top-hat beam shape on holes' morphology was analysed and compared to the results obtained with a Gaussian beam. Cross sections of XCT results were extracted and the resulting holes' morphology after different NoP is depicted in Figure 5.3. Depth profiles of each two holes produced with the same processing parameters are shown and thus to judge about the repeatability of the drilling process. The morphological evolution of the holes' shape, especially penetrated depth, HAZ, circularity and cylindricity for both top-hat and Gaussian spatial beam profiles are presented.

5.4.1.1. Penetration depth

The XCT results in Figure 5.3 confirm that a higher penetration depth is achievable with a Gaussian beam. The effect of NoP on penetration depth is provided in Figure 5.4 and it is evident that at a given NoP the penetration rate drops significantly, indicating that the ablation efficiency has been reduced noticeably. In particular, the efficiency drop was observed at 1000 and 600 NoP for Gaussian and top-hat beam shapes, respectively, while the maximum hole depth was reached at 7500 NoP, i.e. 139 and 74 μm , for the two respective profiles. There are competing factors leading to these differences and thus determining the achievable penetration depth. Specially, plasma shielding and the angular dependence of the laser absorption affect the laser drilling process but the increasing surface area during the drilling process is considered as a dominating factor in decreasing the effective fluence and also in inhibiting the penetration into the material [30].

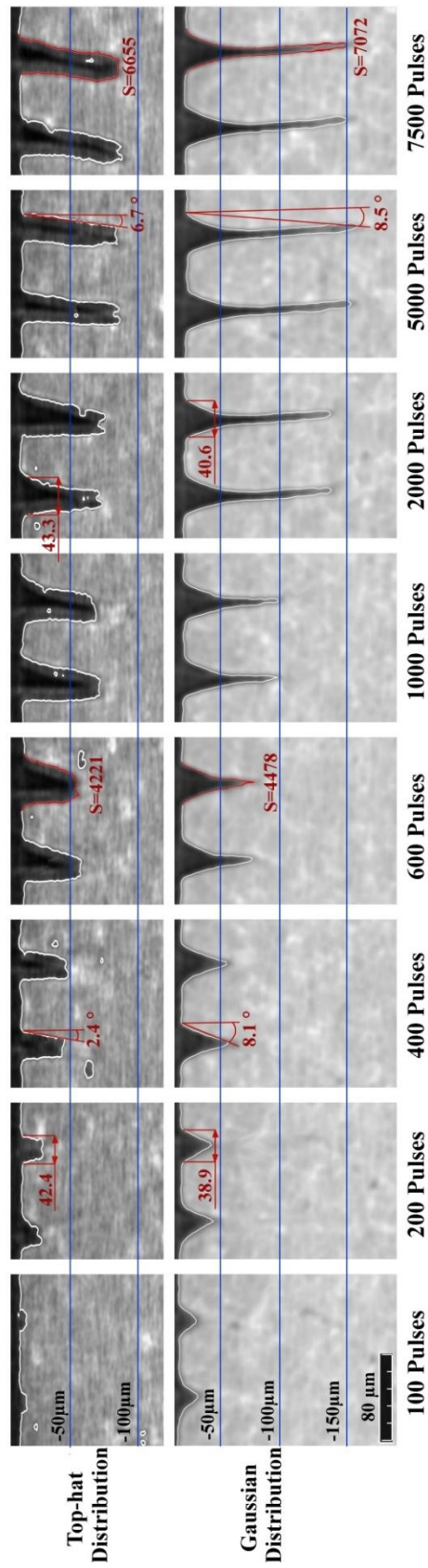


Figure 5.3. XCT results of Gaussian and Top-hat distribution for different NoP. Note: S is the surface area inside the hole and is in μm^2 . All other measurements are in micrometers.

Therefore, the effect of increasing irradiated surface area inside the holes was analysed and presented in Figure 5.5 as a function of NoP. It is apparent that there is only a marginal difference between the surface areas resulting after laser drilling with both profiles. For instance, the area of the holes irradiated with the Gaussian beam was approximately $7000 \mu\text{m}^2$ at 7500 NoP and this was only $400 \mu\text{m}^2$ higher than the respective areas resulting after top-hat processing. This relatively negligible difference could be attributed to the Gaussian energy distribution that provides a locally higher fluence at the centre of the beam for further ablation. The effective fluence represented as the pulse energy per area is nearly at the same level for both beam profiles, as shown in Figure 5.5, and this supports the hypothesis that the increasing surface area is the dominant factor in determining the saturation penetration depth. Unlike the top-hat profile, the holes' deviation from cylindricity was bigger when the Gaussian beam was used and also the penetration depth was higher while the holes' surface areas were maintained with only a small offset for the two beam shapes.

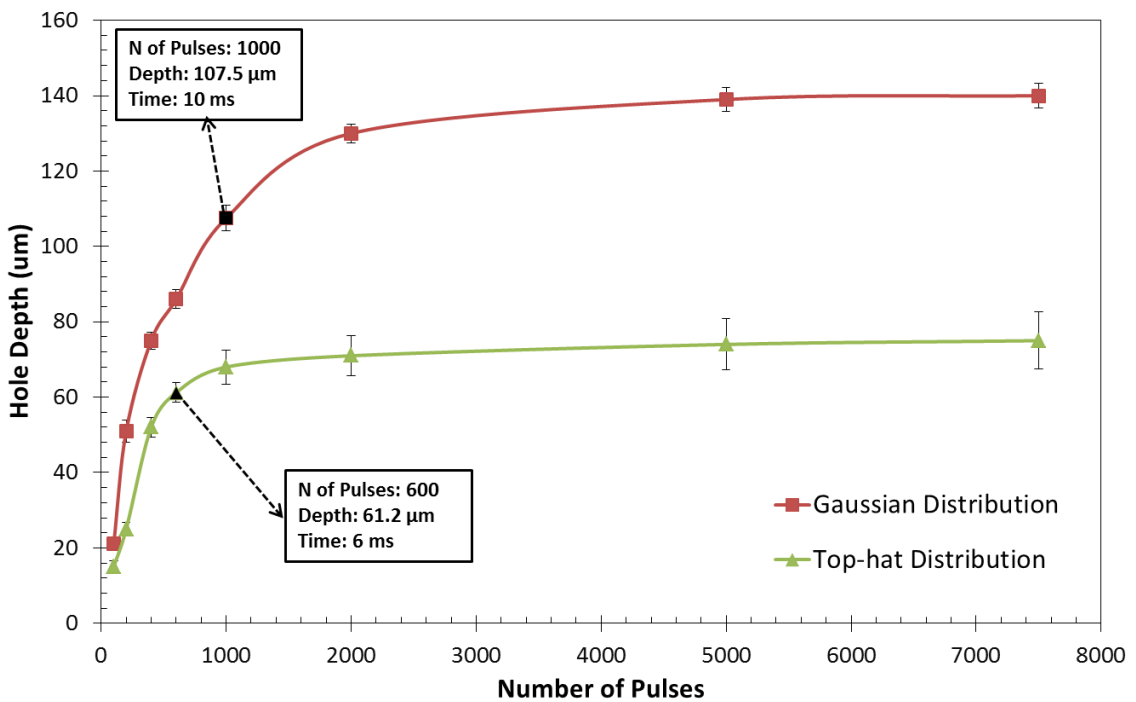


Figure 5.4. The penetration depths achievable with Gaussian and top-hat beams with an increasing number of pulses

Another difference was the higher spread of holes' depth when the top-hat beam was used as indicated by the standard deviation in Figure 5.4. The variation of holes' depth was more obvious for the top-hat beam, i.e. the standard deviation for the 7 repeats at 7500 NoP was almost 3 times higher for the top-hat beam.

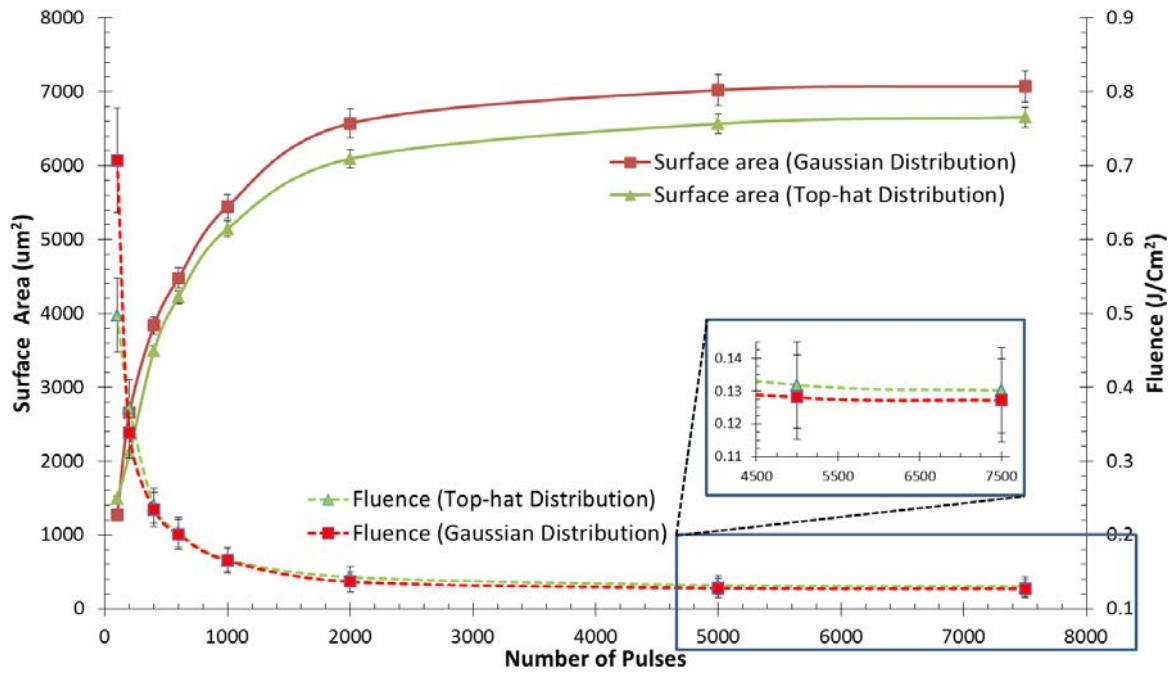


Figure 5.5. Irradiated surface areas inside the holes together with respective effective fluence for Gaussian and top-hat beams

5.4.1.2. Heat Affected Zone (HAZ)

There is no common approach for quantifying HAZ in laser processing. A number of techniques have been applied in laser drilling, e.g. an analysis of general appearance [57] or the grain size changes after processing [58]. In this research the colour shifting around the holes was analysed by scanning their surrounding areas with Alicona G5. 50× objective was used with a lateral resolution of 0.7 μm and HAZ was measured by using the Alicona software. The uncertainty of this method was assessed by employing the type A statistical method and it was 248 μm² with a confidence level of 97%.

The results of the HAZ analysis are provided in Figure 5.6. As expected, HAZ extended with the increase of NoP and this was more evident after drilling with the Gaussian beam. Especially, HAZ increased almost 3 (from 139 to 411 μm^2) and 4.5 (from 472 to 2052 μm^2) times for top-hat and Gaussian distributions, respectively, when NoP increased from 200 to 5000. HAZ at 1000 and 7500 NoP were also compared for both beam shapes and it was 4.6 and 5 times bigger after drilling with the Gaussian beam. The main reason for these significant increases is the “tail” of the Gaussian distribution as shown in Figure 5.7a. In particular, fluence of the tails is lower than the ablation threshold and it is sufficient only to heat the surface surrounding the holes without any ablation. In contrast, fluence of top-hat beams can be tailored at the beam spot as shown in Figure 5.7b and thus can be maintained above the ablation threshold to minimise HAZ. This HAZ decrease can enable laser drilling with higher pulse energies as the negative side effects on the surface integrity and material properties can be reduced considerably.

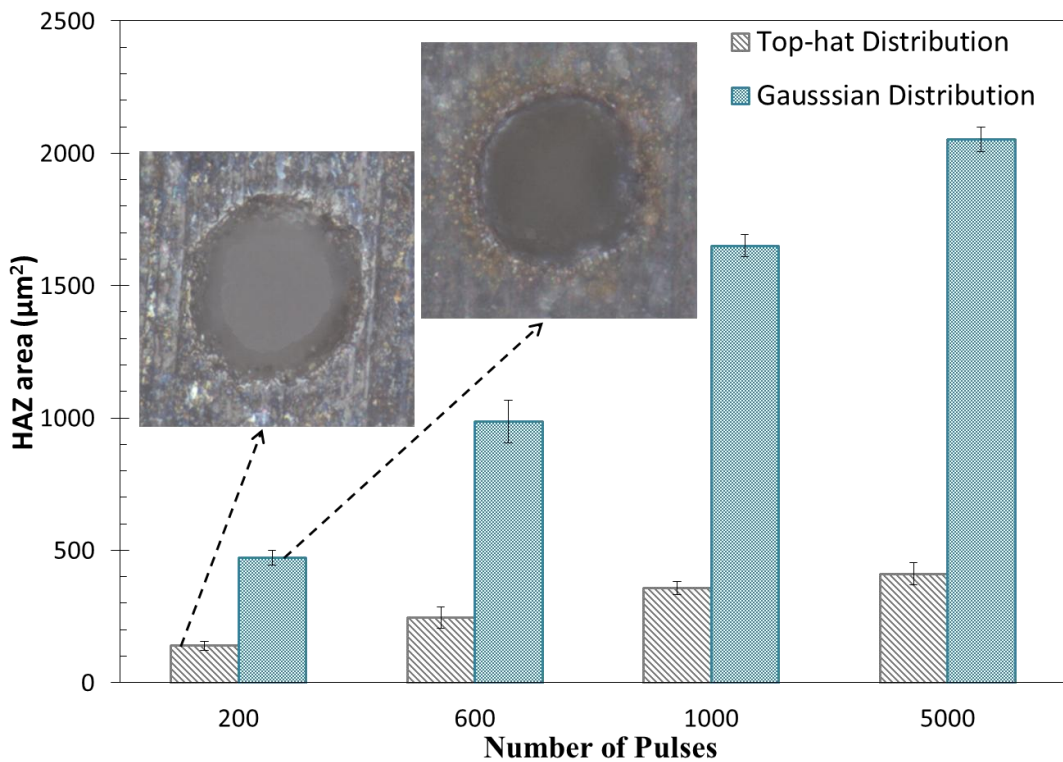


Figure 5.6. HAZ around the holes produced with Gaussian and top-hat beams

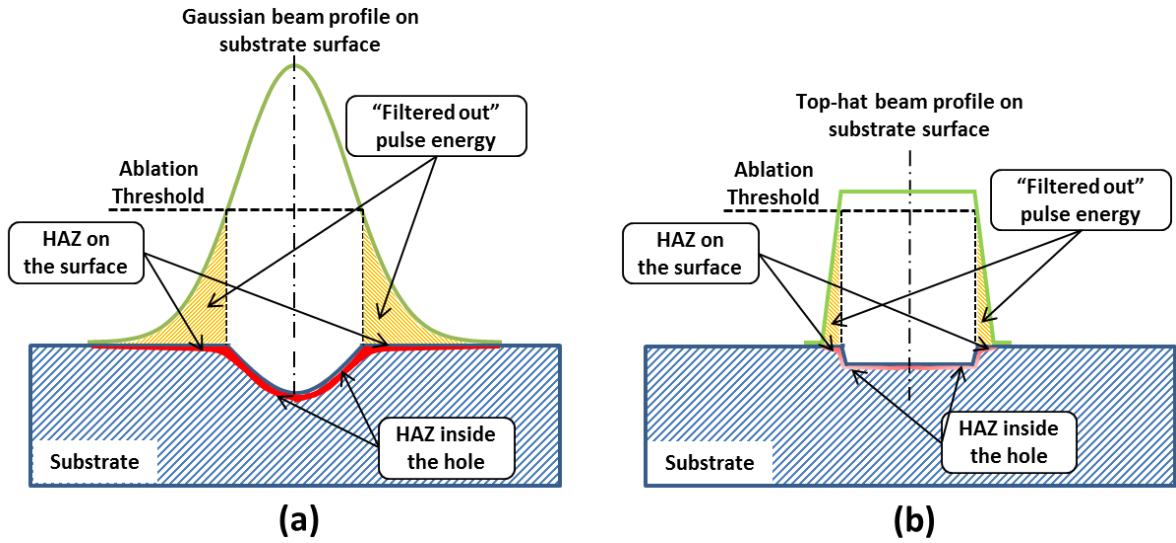


Figure 5.7. The effects of (a) Gaussian and (b) top-hat beams on HAZ and the holes' shape

5.4.1.3. Circularity and cylindricity

The cylindricity of the holes can be evaluated by analysing the holes' cross-sections at different depths. Therefore, the cross-sections at every 10 μm along the hole's depth were extracted from the XCT data set and circles were fitted to the holes' profiles employing the least-squares approach. The holes' diameter decrease after 5000 NoP for both beam shapes is depicted in Figure 5.8. For the top-hat distribution, a decrease of diameters from 43 μm at the hole entrance to 19 μm at depth of 70 μm , the hole bottom, was measured. At the same time, the hole diameter at this depth achieved with the Gaussian beam was 9 μm and stayed nearly unchanged onward. This can be explained with the non-uniform fluence distribution. Based on the Beer-Lambert law, the ablated depth after one pulse is a function of local fluence [59], in particular:

$$Depth = \frac{1}{\alpha} \cdot \ln \frac{F}{F_{th}} \quad (4)$$

where: α is the absorption coefficient; F - fluence and F_{th} - the ablation threshold of material.

When a Gaussian beam is used, the beam irradiation is higher at the centre and respectively

the holes are at the centre, too, and ultimately the pulse trains lead to holes with non-uniform shape in terms of cylindricity. At the same time, the homogeneous energy distribution of the top-hat beam improves uniformity of the holes. This is depicted schematically in Figure 5.7.

Beam shapers can potentially affect the beam circularity and lead to elliptical or irregular hole shapes. Therefore, the holes' circularity at different depths was assessed but there were no irregularities, e.g. the deviations for circularity at depth of 10 μm for both beams were in the same range of 5 μm as shown in Figure 5.8.

Another important morphological parameter of laser-drilled holes is the average taper angle. As shown in Figure 5.3, the taper angle was 2.4° and 8.1° after 400 NoP for the top-hat and Gaussian beams, respectively. However, the taper angle increased only marginally to 8.5° with the increase of NoP in case of the Gaussian beam while the increase was substantial, i.e. to 6.7°, for the top-hat one.

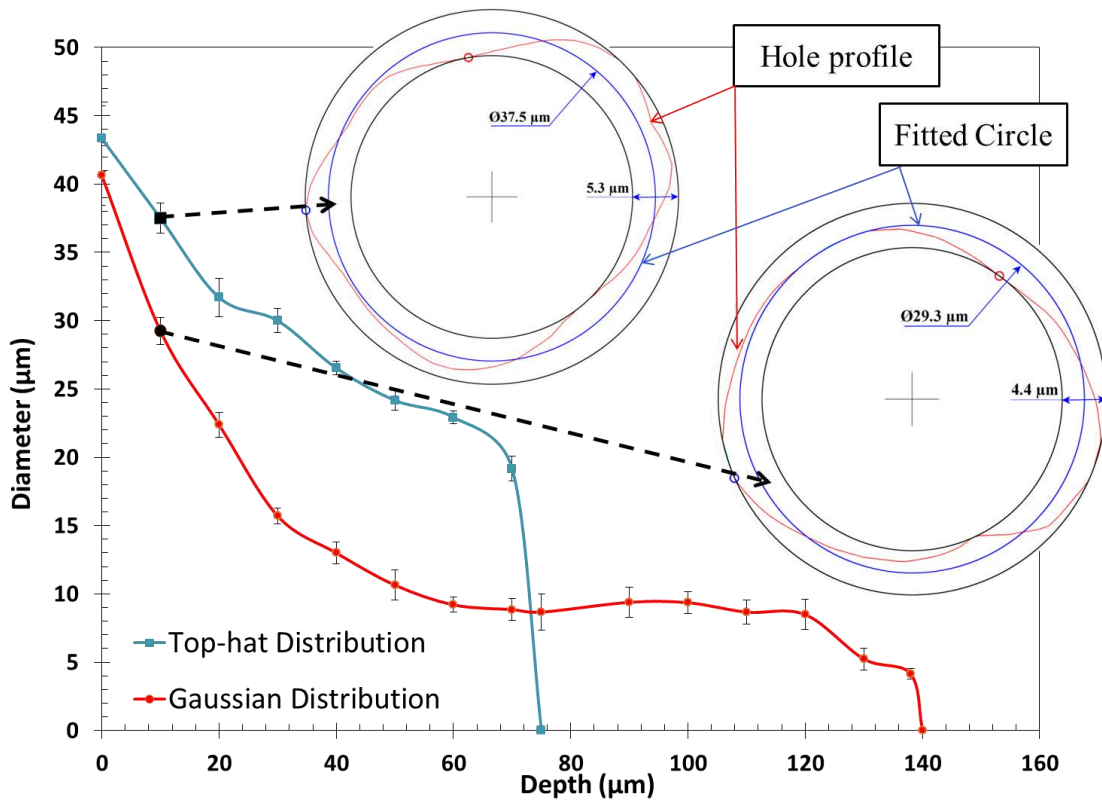


Figure 5.8. The changes of holes' diameters at different depths for the Gaussian and top-hat beams after 5000 NoP

5.4.2. Sensitivity of beam shaper to defocusing

The use a top-hat beam can be advantageous in terms of holes' morphology and HAZ as it was discussed in Section 5.4.1. Nevertheless, the use of beam shapers can make the setting up of the drilling process sensitive to defocusing and so limit their wider application. The effects of beam defocusing on the hole depth after 5000 NoP are depicted in Figure 5.9. While defocussing of $\pm 200 \mu\text{m}$ for both beams did not affect the penetration depth, a defocusing of $-1000 \mu\text{m}$ led to a depth reduction of 81% (from 74 to $13 \mu\text{m}$) and 64% (from 139 to $49 \mu\text{m}$) for the top-hat and the Gaussian beams, respectively. This sharp decrease in the top-hat case reflects the beam profile shifting as shown in the Figure 5.1, e.g. the resulting donut hole shape at Z of $-1000 \mu\text{m}$ shown in Figure 5.9 is in line with the beam shape at this position that might be useful in other applications.

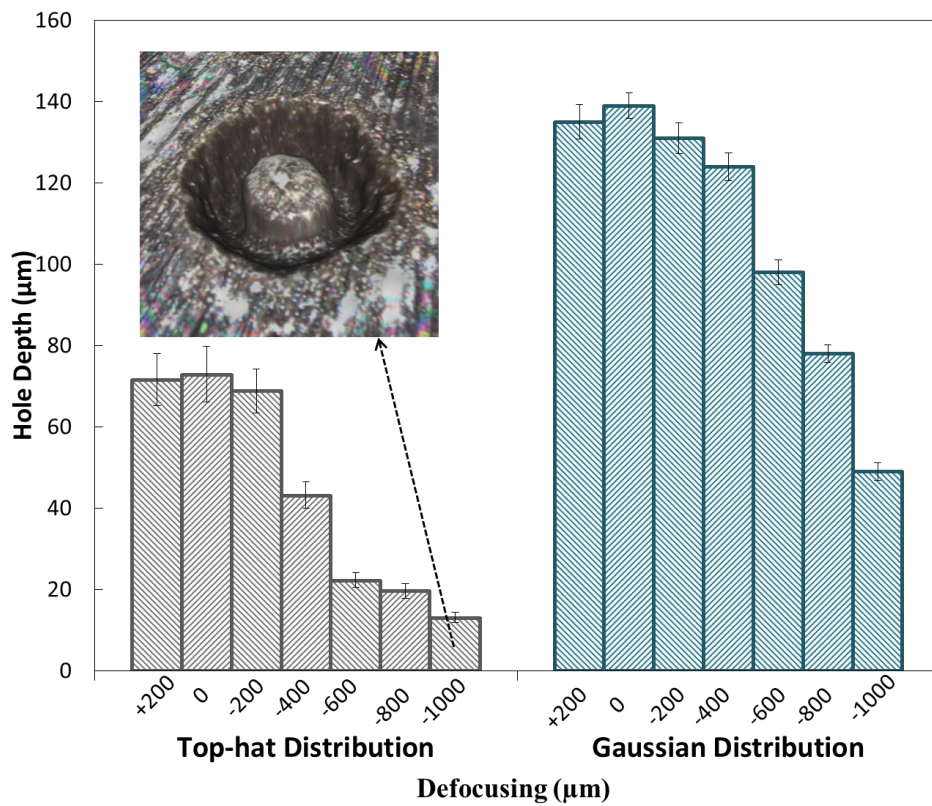


Figure 5.9. Sensitivity of holes' depth after 5000 NoP to defocusing of top-hat and Gaussian beams

5.5. Conclusions

A beam delivery system that integrates Focal- π Shaper was designed and implemented to achieve a top-hat spatial profile and its capabilities for laser micro drilling was investigated and compared with the machining results achievable with a Gaussian beam. The morphology of high aspect ratio holes was investigated employing a high resolution XCT system and the following conclusions were made:

- The penetration depth and aspect ratios achievable with a Gaussian beam are higher but the use of a top-hat beam improves the holes geometrical accuracy, especially the deviations of the holes from cylindricity are less and also the holes are with a lower tapering angle.
- The achievable penetration depth and the respective saturating points for both beam spatial distributions can be explained with the increase of surface area inside the holes during the laser drilling operations that leads to a drop of effective fluence. In particular, due to the lower cylindricity of the holes produced with a Gaussian beam, the equivalent surface area of the holes produced with a top-hat beam can be achieved only at a higher penetration depth.
- The top-hat spatial distribution minimises not only HAZ but also fluence at the beam spot area can be tailored accurately in respect to the ablation threshold. Especially, the negative effect associated with the “tails” of the Gaussian spatial distributions can be minimised. The HAZ decrease offered by the top-hat beams can enable laser drilling with higher pulse energies without impacting the surface integrity.
- It was shown that the field mapping approach based on refractive optics, i.e. Focal- π Shaper, did not affect the holes’ circularity. At the same time, the analysis of the top-hat beam sensitivity to off-focus drilling had shown that the penetration depth would be affected when defocusing exceeded 400 μm .

Acknowledgment

The research reported in this paper was supported by Korea Institute for Advancement of Technology (KIAT), i.e. the project on “Laser Machining of Ceramic Interface Cards for 3D wafer bumps”, and two H2020 Factory of the Future projects, “Modular laser based additive manufacturing platform for large scale industrial applications” (MAESTRO) and “High-Impact Injection Moulding Platform for mass-production of 3D and/or large micro-structured surfaces with Antimicrobial, Self-cleaning, Anti-scratch, Anti-squeak and Aesthetic functionalities” (HIMALAIA). The authors would like to acknowledge the contribution of Martin Corfield and Lars Korner from the University of Nottingham and John Crawshaw from Imperial College London in carrying out the XCT measurements.

References

- [1] W.-S. Chu, C.-S. Kim, H.-T. Lee, J.-O. Choi, J.-I. Park, J.-H. Song, K.-H. Jang, S.-H. Ahn, Hybrid manufacturing in micro/nano scale: A Review, *International Journal of Precision Engineering and Manufacturing-Green Technology*, 1 (2014) 75-92.
- [2] B. Adelman, R. Hellmann, Rapid micro hole laser drilling in ceramic substrates using single mode fiber laser, *Journal of Materials Processing Technology*, 221 (2015) 80-86.
- [3] W.C. Choi, J.Y. Ryu, Fabrication of a guide block for measuring a device with fine pitch area-arrayed solder bumps, *Microsyst Technol*, 18 (2012) 333-339.
- [4] N. Watanabe, M. Suzuki, K. Kawano, M. Eto, M. Aoyagi, Fabrication of a membrane probe card using transparent film for three-dimensional integrated circuit testing, *Jpn. J. Appl. Phys.*, 53 (2014) 06JM06.
- [5] W.C. Choi, J.Y. Ryu, A MEMS guide plate for a high temperature testing of a wafer level packaged die wafer, *Microsyst Technol*, 17 (2011) 143-148.
- [6] H. Huang, L.-M. Yang, J. Liu, Micro-hole drilling and cutting using femtosecond fiber laser, *Optical Engineering*, 53 (2014) 051513.
- [7] Y. Zhang, Y. Wang, J. Zhang, Y. Liu, X. Yang, W. Li, Effects of Laser Repetition Rate and Fluence on Micromachining of TiC Ceramic, *Materials and Manufacturing Processes*, (2015).
- [8] Y. Zhang, Y. Wang, J. Zhang, Y. Liu, X. Yang, Q. Zhang, Micromachining features of TiC ceramic by femtosecond pulsed laser, *Ceram. Int.*, 41 (2015) 6525-6533.
- [9] M. Ghoreishi, O.B. Nakhjavani, Optimisation of effective factors in geometrical specifications of laser percussion drilled holes, *Journal of Materials Processing Technology*, 196 (2008) 303-310.
- [10] M. Ghoreishi, D.K.Y. Low, L. Li, Comparative statistical analysis of hole taper and circularity in laser percussion drilling, *International Journal of Machine Tools and Manufacture*, 42 (2002) 985-995.
- [11] G.K.L. Ng, L. Li, Repeatability characteristics of laser percussion drilling of stainless-steel sheets, *Optics and Lasers in Engineering*, 39 (2003) 25-33.
- [12] S.H. Kim, I.-B. Sohn, S. Jeong, Ablation characteristics of aluminum oxide and nitride ceramics during femtosecond laser micromachining, *Applied Surface Science*, 255 (2009) 9717-9720.
- [13] A. Bharatish, H.N. Narasimha Murthy, B. Anand, C.D. Madhusoodana, G.S. Praveena, M. Krishna, Characterization of hole circularity and heat affected zone in pulsed CO2 laser drilling of alumina ceramics, *Optics & Laser Technology*, 53 (2013) 22-32.
- [14] H. Zhang, J. Di, M. Zhou, Y. Yan, R. Wang, An investigation on the hole quality during picosecond laser helical drilling of stainless steel 304, *Applied Physics a-Materials Science & Processing*, 119 (2015) 745-752.
- [15] C. He, F. Zibner, C. Fornaroli, J. Ryll, J. Holtkamp, A. Gillner, High-precision helical cutting using ultra-short laser pulses, *Physics Procedia*2014, pp. 1066-1072.
- [16] A.H. Khan, S. Celotto, L. Tunna, W. O'Neill, C.J. Sutcliffe, Influence of microsupersonic gas jets on nanosecond laser percussion drilling, *Optics and Lasers in Engineering*, 45 (2007) 709-718.
- [17] J.C. Hsu, W.Y. Lin, Y.J. Chang, C.C. Ho, C.L. Kuo, Continuous-wave laser drilling assisted by intermittent gas jets, *International Journal of Advanced Manufacturing Technology*, 79 (2015) 449-459.

- [18] A. Palya, O.A. Ranjbar, Z. Lin, A.N. Volkov, Effect of the background gas pressure on the effectiveness of laser-induced material removal from deep cavities in irradiated targets, *Applied Physics A*, 124 (2017) 32.
- [19] A. Palya, O.A. Ranjbar, Z. Lin, A.N. Volkov, Kinetic simulations of laser-induced plume expansion into a background gas under conditions of spatial confinement, *Int. J. Heat Mass Transf.*, 132 (2019) 1029-1052.
- [20] V. Nasrollahi, P. Penchev, S. Dimov, L. Korner, R. Leach, K. Kim, Two-Side Laser Processing Method for Producing High Aspect Ratio Microholes, *Journal of Micro and Nano-Manufacturing*, 5 (2017) 041006-041014.
- [21] K. Goya, T. Itoh, A. Seki, K. Watanabe, Efficient deep-hole drilling by a femtosecond, 400 nm second harmonic Ti:Sapphire laser for a fiber optic in-line/pico-liter spectrometer, *Sensors and Actuators B-Chemical*, 210 (2015) 685-691.
- [22] X.C. Wang, H.Y. Zheng, P.L. Chu, J.L. Tan, K.M. Teh, T. Liu, B.C.Y. Ang, G.H. Tay, Femtosecond laser drilling of alumina ceramic substrates, *Applied Physics a-Materials Science & Processing*, 101 (2010) 271-278.
- [23] S. Döring, S. Richter, A. Tünnermann, S. Nolte, Evolution of hole depth and shape in ultrashort pulse deep drilling in silicon, *Applied Physics A: Materials Science and Processing*, 105 (2011) 69-74.
- [24] V. Nasrollahi, P. Penchev, T. Jwad, S. Dimov, K. Kim, C. Im, Drilling of micron-scale high aspect ratio holes with ultra-short pulsed lasers: Critical effects of focusing lenses and fluence on the resulting holes' morphology, *Optics and Lasers in Engineering*, 110 (2018) 315-322.
- [25] C. Föhl, D. Breitling, F. Dausinger, Precise drilling of steel with ultrashort pulsed solid-state lasers, *Proceedings of SPIE - The International Society for Optical Engineering*2002, pp. 271-279.
- [26] H.K. Tönshoff, C. Momma, A. Ostendorf, S. Nolte, G. Kamlage, Microdrilling of metals with ultrashort laser pulses, *Journal of Laser Applications*, 12 (2000) 23-27.
- [27] O.J. Allegre, W. Perrie, K. Bauchert, D. Liu, S.P. Edwardson, G. Dearden, K.G. Watkins, Real-time control of polarisation in ultra-short-pulse laser micro-machining, *Applied Physics A*, 107 (2012) 445-454.
- [28] D.M. Karnakis, J. Fieret, P.T. Rumsby, M.C. Gower, Microhole drilling using reshaped pulsed Gaussian laser beams, *Proceedings of SPIE - The International Society for Optical Engineering*, 4443 (2001) 150-158.
- [29] S. Ahn, D.J. Hwang, H.K. Park, C.P. Grigoropoulos, Femtosecond laser drilling of crystalline and multicrystalline silicon for advanced solar cell fabrication, *Applied Physics A*, 108 (2012) 113-120.
- [30] A. Ruf, P. Berger, F. Dausinger, H. Hügel, Analytical investigations on geometrical influences on laser drilling, *Journal of Physics D: Applied Physics*, 34 (2001) 2918-2925.
- [31] F. He, J. Yu, Y. Tan, W. Chu, C. Zhou, Y. Cheng, K. Sugioka, Tailoring femtosecond 1.5- μm Bessel beams for manufacturing high-aspect-ratio through-silicon vias, *Scientific Reports*, 7 (2017).
- [32] D. M., A. C.B., Bessel and annular beams for materials processing, *Laser & Photonics Reviews*, 6 (2012) 607-621.
- [33] J. Bovatsek, R.S. Patel, High-power, nanosecond-pulse Q-switch laser technology with flattop beam-shaping technique for efficient industrial laser processing, 26th International Congress on Applications of Lasers and Electro-Optics, ICALEO 2007 - Congress Proceedings2007.

- [34] D. Zeng, W.P. Latham, A. Kar, Optical trepanning with a refractive axicon lens system, SPIE Optics + Photonics, SPIE2006, pp. 10.
- [35] D. Zeng, W.P. Latham, A. Kar, Temperature distributions due to annular laser beam heating, Journal of Laser Applications, 17 (2005) 256-262.
- [36] C. Zhang, N.R. Quick, A. Kar, Pitchfork beam shaping for laser microrvia drilling, Journal of Physics D: Applied Physics, 41 (2008) 125105.
- [37] Z. Kuang, J. Li, S. Edwardson, W. Perrie, D. Liu, G. Dearden, Ultrafast laser beam shaping for material processing at imaging plane by geometric masks using a spatial light modulator, Optics and Lasers in Engineering, 70 (2015) 1-5.
- [38] G. Dearden, Z. Kuang, D. Liu, W. Perrie, S.P. Edwardson, K.G. Watkins, Advances in Ultra Short Pulse Laser based Parallel Processing using a Spatial Light Modulator, Physics Procedia, 39 (2012) 650-660.
- [39] N. Sanner, N. Huot, E. Audouard, C. Larat, J.P. Huignard, Direct ultrafast laser microstructuring of materials using programmable beam shaping, Optics and Lasers in Engineering, 45 (2007) 737-741.
- [40] H. Duc Doan, I. Naoki, F. Kazuyoshi, Laser processing by using fluidic laser beam shaper, Int. J. Heat Mass Transf., 64 (2013) 263-268.
- [41] F.M. Dickey, Laser Beam Shaping: Theory and Techniques, Second ed., CRC Press, Boca Raton, FL, 2014.
- [42] N. Bokor, N. Davidson, Anamorphic, adiabatic beam shaping of diffuse light using a tapered reflective tube, Optics Communications, 201 (2002) 243-249.
- [43] K.J. Kanzler, Transformation of a Gaussian laser beam to an Airy pattern for use in focal plane intensity shaping using diffractive optics, International Symposium on Optical Science and Technology, SPIE2001, pp. 8.
- [44] F.M. Dickey, L.S. Weichman, R.N. Shagam, Laser beam shaping techniques, High-Power Laser Ablation, SPIE2000, pp. 11.
- [45] F.M. Dickey, S.C. Holswade, T.E. Lizotte, D.L. Shealy, Laser beam shaping applications, CRC Press2005.
- [46] A. Laskin, N. Šiaulyš, G. Šlekys, V. Laskin, Beam shaping unit for micromachining, SPIE Optical Engineering + Applications, SPIE2013, pp. 18.
- [47] Z. Kuang, W. Perrie, J. Leach, M. Sharp, S.P. Edwardson, M. Padgett, G. Dearden, K.G. Watkins, High throughput diffractive multi-beam femtosecond laser processing using a spatial light modulator, Applied Surface Science, 255 (2008) 2284-2289.
- [48] J.Y. Cheng, C.L. Gu, D.P. Zhang, S.C. Chen, High-speed femtosecond laser beam shaping based on binary holography using a digital micromirror device, Optics Letters, 40 (2015) 4875-4878.
- [49] R.J. Beck, J.P. Parry, W.N. MacPherson, A. Waddie, N.J. Weston, J.D. Shephard, D.P. Hand, Application of cooled spatial light modulator for high power nanosecond laser micromachining, Optics Express, 18 (2010) 17059-17065.
- [50] F. Duerr, H. Thienpont, Refractive laser beam shaping by means of a functional differential equation based design approach, Optics Express, 22 (2014) 8001-8011.
- [51] A. Laskin, V. Laskin, Refractive field mapping beam shaping optics: Important features for a right choice, 29th International Congress on Applications of Lasers and Electro-Optics, ICALEO 2010 - Congress Proceedings2010, pp. 1181-1189.
- [52] A. Laskin, V. Laskin, A. Ostrun, Refractive beam shapers for focused laser beams, SPIE Optical Engineering + Applications, SPIE2016, pp. 12.
- [53] A. Gruner, J. Schille, U. Loeschner, Experimental study on micro hole drilling using ultrashort pulse laser radiation, Physics Procedia2016, pp. 157-166.

- [54] S. Nolte, C. Momma, G. Kamlage, A. Ostendorf, C. Fallnich, F. von Alvensleben, H. Welling, Polarization effects in ultrashort-pulse laser drilling, *Applied Physics A*, 68 (1999) 563-567.
- [55] Recommended alignment procedure for π Shaper 6_6 and Focal- π Shaper 9.
- [56] D. Dergez, M. Schneider, A. Bittner, U. Schmid, Mechanical and electrical properties of DC magnetron sputter deposited amorphous silicon nitride thin films, *Thin Solid Films*, 589 (2015) 227-232.
- [57] K.C. Yung, S.M. Mei, T.M. Yue, A study of the heat-affected zone in the UVPYAG laser drilling of GFRP materials, *Journal of Materials Processing Technology*, 122 (2002) 278-285.
- [58] R. Le Harzic, N. Huot, E. Audouard, C. Jonin, P. Laporte, S. Valette, A. Fraczkiewicz, R. Fortunier, Comparison of heat-affected zones due to nanosecond and femtosecond laser pulses using transmission electronic microscopy, *Applied Physics Letters*, 80 (2002) 3886-3888.
- [59] G.H. Pettit, R. Sauerbrey, Pulsed Ultraviolet-Laser Ablation, *Applied Physics a-Materials Science & Processing*, 56 (1993) 51-63.

CHAPTER 6 : CONTRIBUTIONS, CONCLUSIONS AND FUTURE WORK

6.1. Contributions

1. A new two-side drilling method is proposed, and a pilot two-side laser processing setup was designed. For its implementation the following enabling tools and technologies were developed and validated experimentally:
 - A specially designed laser processing setup that integrates two rotary and three linear mechanical stages together with a modular workpiece holding device to ensure the required motion control, accuracy and repeatability in executing two-side laser processing routines;
 - System level tools for an automated process setting up that allow errors from various sources to be compensated and thus to minimise their impact on achievable accuracy and repeatability in two-side laser processing;
 - A method for an automated correlation of working coordinate systems in two-side laser processing;
 - In-situ, on-machine inspection method for verifying the alignment accuracy achievable with the proposed two-side laser processing method.

It was demonstrated that by adopting the proposed method, micro holes with very good repeatability and dimensional and geometrical accuracy could be produced. The achievable aspect ratios can be more than doubled in comparison with the one-side drilling method while improving the holes' dimensional and geometrical accuracy.

2. The effects of a wide fluence spectrum in percussion drilling with different focal distance lenses were investigated systematically. Especially, the effects on achievable aspect ratios and morphologies of micro holes produced on silicon nitride substrates were analysed. An approach to examine the morphology of high aspect ratio micro holes with a minimum uncertainty was proposed and implemented by employing a high-resolution X-ray tomography (XCT) technology. Based on the obtained results it was possible to quantify the effects of lenses with lower focal distances on achievable aspect ratios, cylindricity and taper angles in drilling micro holes. Also, the limitations associated with the use of lenses with lower focal distances were identified in regards to achievable geometrical accuracy, processing efficiency and flexibility in producing high aspect ratio holes.
3. A beam shaping system based on refractive optics was designed and implemented to perform drilling operations with a top-hat beam. Its capabilities and limitations in laser micro drilling was investigated and compared with the results achievable with a Gaussian beam. The morphology of high aspect ratio holes was investigated employing a high-resolution XCT system and the improvements in terms of cylindricity, taper angle and HAZ were systematically analysed. Also, the impact of using beams with an uniform intensity profile on achievable penetration depths and aspect ratios of micro holes was quantified and the trade-off in comparison to the use of a Gaussian beam were discussed.

6.2. Conclusions

1. A new method for two-side laser processing is proposed. The essential laser processing setup integrates linear and rotary stages and a modular workpiece holding device. The capabilities of a pilot implementation of such laser processing setup in regards to the motion control, accuracy and repeatability were investigated. It was found that the most challenging stage in executing this method was the alignment of the holes produced from two sides. Therefore, a fully automated process setting up routines was designed and implemented that allows errors from various sources to be compensated. It was shown that the achievable alignment accuracy was highly dependent on accuracy and resolution of the stages and sensors. By applying these routines on the implemented multi-axis laser processing setup an alignment accuracy better than 10 μm was attained.
2. The proposed two-side laser drilling method was successfully applied for producing micro holes with very good repeatability and dimensional and geometrical accuracy that was not possible to achieve employing one-side drilling. The achievable aspect ratios were doubled while the holes' morphology, i.e. tapering angle and circularity, was improved substantially.
3. An in-situ, on-machine inspection method for verifying the alignment accuracy achievable with the proposed two-side laser processing method was developed. The required sensors and equipment for executing such inspection routines with their associated measurement uncertainties were analysed. The performance of this inspection approach was evaluated and the expanded uncertainty associated with the adopted procedure and equipment was less than 1 μm with a confidence level of 97%.
4. The effects of a wide fluence spectrum in ultra-short percussion drilling with different focal distance lenses have been analysed experimentally. It was concluded that in

general, a higher fluence led to higher aspect ratio holes. So, the achievable aspect ratio can be increased by carrying out the percussion drilling operations with lower focal distance lenses. For instance, in this research aspect ratios up to 25 was achieved with the maximum pulse energy available, i.e. 9 μJ , by using a 20 mm lens compared with only 8 and 3 for 50 and 100 mm lenses, respectively.

5. Holes with much better cylindricity and lower taper angles can be percussion drilled with smaller focal distance lenses. For example, the taper angle decreased from almost 9° to less than 1° when the lens focal distance was reduced from 100 to 20 mm in the carried out experiments. In addition, lenses with smaller focal distance led to a substantial reduction of resulting cone shape entries with necking.
6. The constrains associated with the use of smaller focal distance lenses were identified that affected the processing flexibility and reliability in general. In particular, it was demonstrated how sensitive such lenses could be to any defocusing and also what would be the impact on penetration depth. For example, when a 20 mm focal distance lens was deployed a relatively small defocusing of only 200 μm led to 85% drop of the penetration depth. In addition, the carried out morphological analysis confirmed that the risks for recast formations inside the holes and holes' bending effects would increase substantially when such lenses are used to produce high aspect ratio holes.
7. A beam delivery system that integrates Focal- π Shaper was designed and implemented to achieve a top-hat spatial beam profile. Capabilities of top-hat micro drilling was investigated and compared with the machining results achievable with a Gaussian beam. It was shown that the penetration depth and aspect ratios achievable with a Gaussian beam were higher. However, the top-hat drilling improves holes geometrical accuracy,

especially the deviations of the holes from cylindricity were less and also the holes were with a lower tapering angle.

8. The achievable penetration depth and the respective saturating points with top-hat and Gaussian beam spatial distributions can be explained with the increase of surface area inside the holes during the laser drilling operations that leads to a drop of effective fluence. In particular, due to the lower cylindricity of the holes produced with a Gaussian beam, the equivalent surface area of the holes produced with a top-hat beam can be achieved only at a higher penetration depth.
9. The use of top-hat spatial distribution reduces energy intensity at the beam spot area and thus the processing fluence can be tailored accurately in respect to the ablation threshold. Especially, the negative effect associated with the “tails” of the Gaussian spatial distributions can be minimised. The HAZ decrease offered by the top-hat beams can enable laser drilling with higher pulse energies without impacting the surface integrity.
10. The designed beam delivery system that incorporates a beam shaping sub-system based on refractive optics, i.e. Focal- π Shaper, did not affect the holes’ circularity. However, there are some constraints associated with this field mapping method for beam shaping. For instance, any misalignment of the beam shaper leads to undesirable beam intensity profiles at the focal plane. So, the installation and alignment of the beam shaping sub-systems should be performed with great care. The analysis of the micro holes drilled with a top-hat beam had shown that their penetration depths were more sensitive to defocusing compared to drilling with a normal Gaussian distribution.

6.3. Future Research

1. The application area of the proposed two side drilling method can be broadened by extending these capabilities for multi-axis laser processing of not parallel surfaces, e.g. for drilling intersecting holes and micro channels inside components for fluid flow and heat exchange applications. This will demand a new automatic setting up procedures to be developed that will require much more complex compensational functions to be defined and experimentally validated.
2. An automatic in-process metrology procedure with enabling tools and equipment for establishing a close-loop two-side and multi-axis laser processing in general can be developed based on the inspection routes implemented and validated in this research. Especially, such tools should provide the required level of holes and structures alignment with an acceptable uncertainty.
3. The use of different focal distance lenses and beam shapers with other drilling strategies i.e. helical or trepanning approaches, should be investigated, too. Such research should be focused not only on improvements that these optical elements can bring but also on their limitations in regards to the respective fields of view and sensitivity to defocusing of beam paths that integrate them.
4. An analytic model for predicting the saturation point in laser micro drilling operations can be developed based on experimental findings in this research that the main reason for the decrease of penetration rate is the increase of the holes' surface area. Thus, an analytical model can be developed that takes into account the effective fluence and beam spatial profiles.
5. Pulse energies and/or beam polarisation from pulse to pulse can be tailored and controlled in real time which can improve holes' quality and processing efficiency.

Developing such dynamic control approaches requires a proper understanding of dominant regimes in different stages of the drilling process and thus to be able to synchronise pulse repetition rates with the varying polarisation, e.g. with the use of motorised wave plates.